SEARCHING FOR NEW PHYSICS IN THE b-QUARK'S AND HIGGS' SECTORS VIA KINEMATIC AND ANGULAR DISTRIBUTIONS

A dissertation
presented in partial fulfillment of requirements
for the degree of Doctor of Philosophy
in the Department of Physics and Astronomy
The University of Mississippi

by

Shanmuka Tumkur Shivashankara

August 2017

UMISS-HEP-2017-03

ABSTRACT

The kinematic and angular distributions are calculated for the decay $\Lambda_b \to \Lambda_c \ell \bar{\nu}_\ell$. Deviations from the standard model are expected given the apparent lepton flavor violation in the process $\bar{B} \to D^{(*)+} \tau^- \bar{\nu}_\tau$. Including these measured deviations from the SM, the upper and lower bounds for $R_{\Lambda_b} = \dfrac{\mathscr{B}(\Lambda_b \to \Lambda_c \tau \bar{\nu}_\tau)}{\mathscr{B}(\Lambda_b \to \Lambda_c \ell \bar{\nu}_\ell)}$ are calculated along with other observables for a variety of new physics Lorentz structures. Distributions are also calculated for $H \to W^- W^{+*}(\text{or } H^{+*}) \to \tau^- \bar{\nu}_\tau \tau^+ \nu_\tau$ via Type II and leptophilic 2HDM's. Although, the Higgs was found at the LHC in 2012, the question remains whether it is of the SM variety. A MadGraph simulation is performed confirming the dihedral distribution calculation given the experimentally determined uncertainties in the Higgs' couplings. The density matrix method and helicity formalism technique are employed for deriving these distributions.

DEDICATION

This dissertation is dedicated to my father and mother.

ACKNOWLEDGEMENTS

I am grateful for the generous financial support from the University of Mississippi and the National Science Foundation (Grant No. NSF PHY-1414345) that allowed me to focus on my coursework and research. Special thanks to the committee members for their service and comments on my dissertation. Many thanks to Dr. Bhubanjyoti Bhattacharya, Dr. David London, and Wanwei Wu for their collaboration on recent research projects. Lastly, a heartfelt thanks to my advisors Dr. Luca Bombelli and Dr. Alakabha Datta for their kind guidance, patience, and support without which this dissertation would not have been possible.

TABLE OF CONTENTS

LIST OF TABLES

LIST OF FIGURES

CHAPTER 1: MOTIVATION

1.1 Introduction

This dissertation pertains to applying decay distribution techniques in the b-quark and Higgs sectors to identify potential signatures for new physics. The first part of the dissertation covers decay distributions. Decay distribution techniques herein consist of the density matrix method and the helicity formalism. The second and third parts of the dissertation are the applications of these techniques to decays in the b-quark sector and the Higgs sector in light of possible new physics. In the b-quark sector, B meson decays and a Λ_b decay are covered in light of the $R(D^{(*)})$ and R_K puzzles. A pertinent subtopic is lepton flavor non-universality. In the Higgs sector, a charged Higgs, $H^{\pm}$, is sought after in the decay $H \to W^- W^{+*}(\text{or } H^{+*}) \to \tau^- \bar{\nu}_\tau \tau^+ \nu_\tau$.

The density matrix method and helicity formalism techniques are demonstrated in the context of the decays $H \to W^{+*}(\to \tau^+ \nu_\tau) W^-(\to \tau^- \bar{\nu}_\tau)$ and $\bar{B} \to D^{*+} \tau^- \bar{\nu}_\tau$, respectively. These techniques are extremely useful for sequential decay processes. Although the calculated distributions are ultimately just formulas, much care in accounting is required given the multiple decay channels between the initial and final states. Chapter 2 covers these techniques.

The relevant hadronic B decays investigated have a pair of final state leptons plus a final state meson. The final state pair of leptons belong to one of the three generations of leptons. With respect to the standard model (SM), experimentalists have found a discrepancy in the ratio of decay rates of B mesons between different generations of final state leptons. When the final state meson is a D or D^* meson, a combined 4σ discrepancy occurs with respect to the standard model[1, 2]. This is known by the name $R(D^{(*)})$ puzzle. When the final state meson is a K^+ meson, the discrepancy is 2.6σ with respect to the standard model [3]. This is known as the R_K puzzle. Given the similarity of these B meson decays to a particular Λ_b decay, i.e. $\Lambda_b \to \Lambda_c(\to \Lambda_s \pi^+)\ W^{-*}(\to \tau^- \bar{\nu}_\tau)$, the latter is expected to carry the same anomaly. These anomalies may be explained by significant new physics effects in the second and third generation of leptons, i.e. lepton flavor non-universality. These puzzles along with the expected anomaly in a Λ_b decay are covered in chapters 3 and 4 with lepton flavor non-universality being a possible resolution. Lorentz structures are used for the new physics effects and couplings (or interaction strengths) are constrained given the experimental data of the $R(D^{(*)})$ puzzle. For the b-quark sector, two papers have been completed [4, 5].

The next investigation is in the Higgs' sector. There are multiple non-composite spin-$\frac{1}{2}$ (fermions) and spin-1 particles (e.g. a photon). Yet, the Higgs boson is the only known non-composite spin-0 particle. As of now, no principle prevents other Higgs-like particles from existing. Discovering such particles would not only be new physics beyond the standard model, but explain the gulf between the Planck and electroweak scale amongst other things. Although the Higgs has been discovered in various decay processes, the Higgs couplings have a sizable uncertainty allowing room for new physics effects. In chapter 5, an investigation is made into the existence of a charged Higgs. The Type II and Leptophilic two-Higgs-doublet models [88, 103] with the SM decay $H \to W^{+*}(\to \tau^+ \nu_\tau) W^-(\to \tau^- \bar{\nu}_\tau)$ are analyzed for signatures indicating the existence of a charged Higgs.

1.2 General Remarks

From the macroscopic scale down to the microscopic scale, fundamental forces govern the dynamics of physical phenomena. The four known fundamental forces in nature consist of the gravitational, weak, electromagnetic and strong forces. In space gravity keeps our planets in orbit about the sun while explaining the range of a projectile on earth. The weak force explains the source of heat from the sun, namely fusing protons and neutrons. Electromagnetism consists of all electrical and magnetic phenomena such as electronic circuits and the orbit of an electron about a nucleus. The strong force holds together an atom's nucleus.

Unlike gravity, the other three forces can thus far be very well explained with a quantum field theory. The specific form of this theory has the name standard model (SM). This model's elemen-

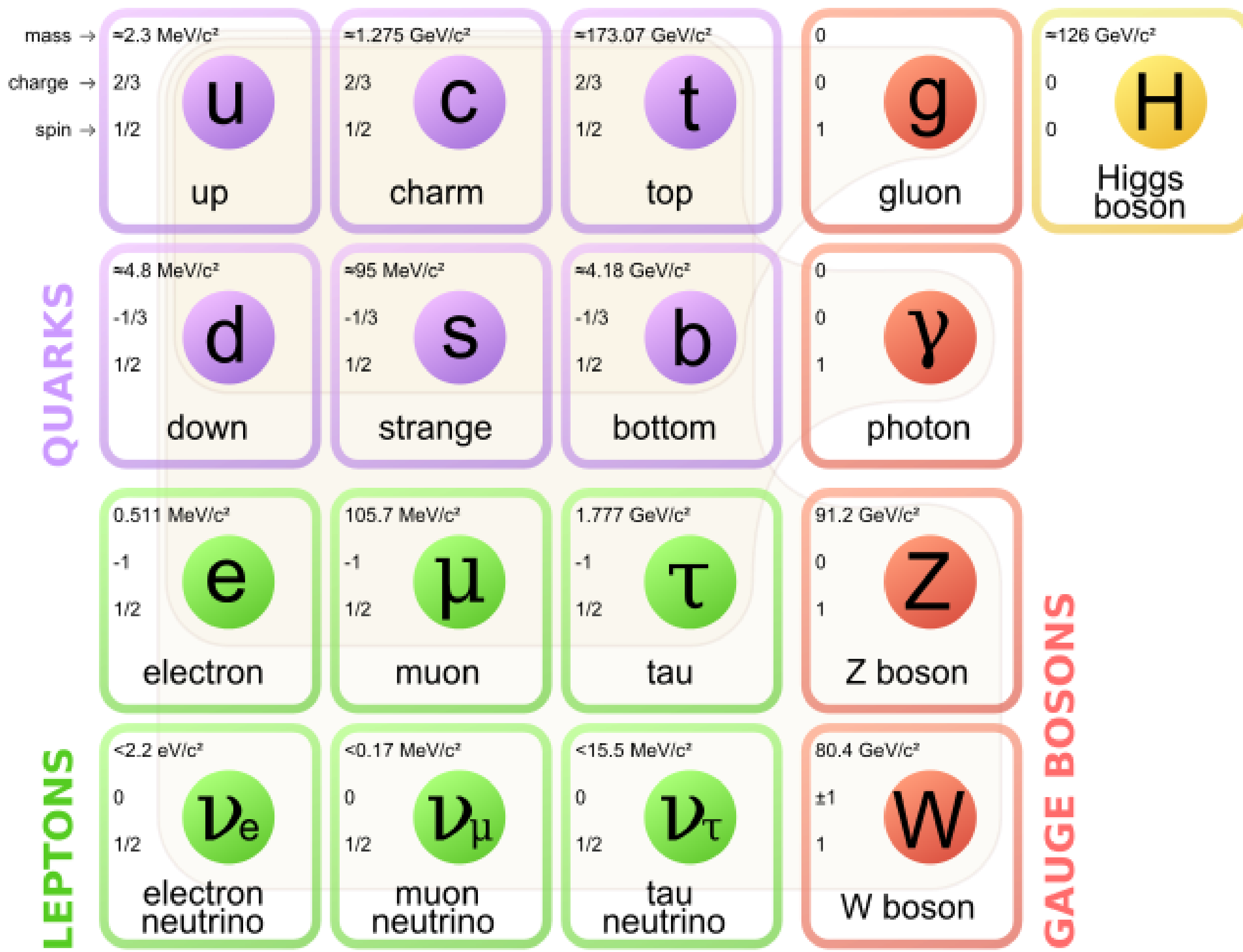

Figure 1: Standard Model of elementary particles. Source: `https://en.wikipedia.org/wiki/Standard_Model`

tary particles are fermions, gauge bosons, and a Higgs boson. Roughly speaking, visible matter is made up of fermions with the gauge bosons serving as their force carriers. Figure 1 depicts the SM particles along with their properties of mass, charge, and spin. Leptons and quarks are fermions, i.e. half-integral spin particles. Bosons are integral spin particles. Two up and one antidown quark can make a proton or hydrogen nucleus via gluons, the force carriers. The Higgs boson explains why some of the particles have mass via a process known as symmetry breaking, where nature chooses a vacuum energy.

However successful, the SM is not complete. The particles making up SM are only about five percent of the visible universe[1]. Since right handed neutrinos are not observed, the neutrinos within the model are assumed massless. This means one may not boost to a reference frame where a right handed neutrino becomes a left handed neutrino. One can think of handedness as pertaining to a particle's *screwlike* motion or spin projected onto momentum. Yet, neutrino flavor oscillations imply neutrinos must have mass. Also, SM does not explain the gulf between the Planck (10^{19} GeV) and electroweak (10^2 GeV) scales, otherwise known as the hierarchy problem. A resolution to the hierarchy problem and an explanation of the failure to detect right handed neutrinos may require supersymmetry, which includes two-Higgs-doublet models (2HDM's). Type II and leptophilic 2HDM's are explored in this dissertation in the context of the decay channel $H \to W^{+*}(\to \tau^+ \nu_\tau) W^-(\to \tau^- \bar{\nu}_\tau)$. As mentioned above, flavor physics is another area of interest for finding physics beyond SM. The quark-flavor channels $b \to c$ and $b \to s$ are pursued herein via B mesons. Material from past and current papers are used in this disseration [4, 5, 6]

[1]The remaining amount consists of dark matter and dark energy. Dark simply means *hidden*. Dark matter keeps a galaxy intact while dark energy explains the accelerating expansion of the universe.

CHAPTER 2: HELICITY DISTRIBUTIONS

2.1 Introduction

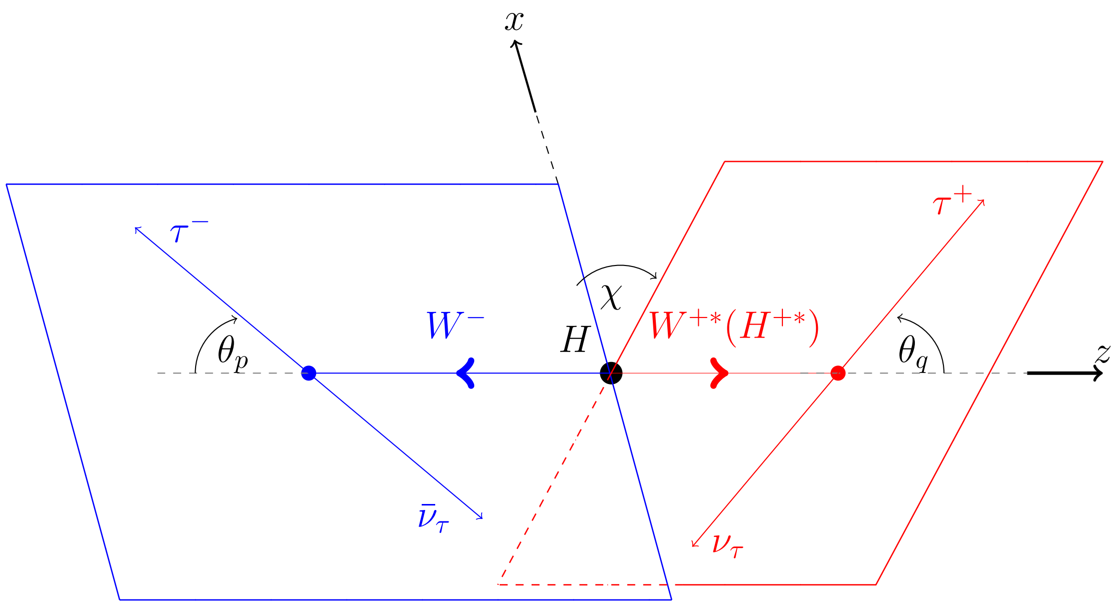

Figure 2: Four body decay of H: $H \to W^{+*}(or\ H^{+*}), W^- \to (\tau^+, \nu_\tau), (\tau^-, \bar{\nu}_\tau)$. θ_q and θ_p are the decay angles in the center of momentum frame of τ^+ and ν_τ and the rest frame of W^-, respectively. χ is the dihedral angle between the decay planes.

Consider the decay process in Figure 2. A Higgs, H, decays to a pair of bosons, either $W^{+*}W^-$ or $H^{+*}W^-$. Both bosons then decay to a pair of leptons. Sequential decay processes such as this one can be handled quite compactly via the density matrix method. Exploiting Lorentz invariants, the calculation is simplified by rotating and boosting to the rest frame of the decaying particle.

The method relies on writing decay amplitudes for each part of the sequential decay process and summing over possible helicities. Helicity is the particle's spin projected onto its direction of motion. For massless particles or in the relativistic regime, helicity is conserved and indicates the particle's chirality, i.e. handedness. Massless fermions and antifermions are left-handed and right-handed, respectively. An elementary example is a negative pion decaying into either a negative muon or electron with an anti-neutrino. The initial helicity is zero since the pion has a spin of zero. Given that the decay is back to back in the rest frame of the pion, there is no orbital angular momentum. It follows that spin (or the total angular momentum) and helicity are conserved. Since the mass of the electron is 1/200 the mass of the muon, production of electrons would favor left-handedness but that choice would violate conservation of total angular momentum. Hence, helicity suppression occurs, and the negative pion decay extremely favors negative muons over electrons. Furthermore, it is helicity that guides the sequential decay process.

Before giving the outline for the density matrix method, an explanation of polarization is required. Given the polarization-spin correspondence, the three polarizations of the on-shell W^- boson correspond to three helicities. This is one more than for a photon since the photon has the Coulomb gauge as a constraint. Also, the off-shell W^{+*} boson will have four polarizations where the fourth pertains to time. The new physics particle H^+ has a helicity of zero. The resulting probability amplitudes will have pure and mixed helicities/polarizations. Some terms can give CP violation. Ignoring H^+, the SM process $H \to W^{+*}(\to \tau^+\nu_\tau)W^-(\to \tau^-\bar{\nu}_\tau)$ of Figure 2 has the following four-fold distribution prescription.

2.2 Density Matrix Method

W^- and W^{+*} are on-shell and off-shell W bosons, respectively. The positive z-axis points in the direction of W^+'s momentum. θ_p is the polar angle of τ^- in W^-'s rest frame. Since W^{+*} is off-shell, θ_q is the polar angle of τ^+ in the center of mass frame of τ^+ and ν_τ. χ is the dihedral angle between the decay planes of $W^- \to \tau^-\bar{\nu}_\tau$ and $W^{+*} \to \tau^+\nu_\tau$. The four-fold distribution can be calculated below by the density matrix method, including the lepton mass. Spins, helicities, polarization vectors, and four momenta are defined as follows.

- Spins of bosons: $s_H = 0, \quad s_{W^+} = 0, 1, \quad s_{W^-} = 1$

- Helicities of bosons: $\lambda_H = \lambda_{W^+} - \lambda_{W^-} = 0, \quad \lambda_{W^+} = 0, \pm 1, t, \quad \lambda_{W^-} = 0, \pm 1$
- Lepton helicities: $\lambda_\ell = \pm\frac{1}{2},\ \ell = \tau^+, \tau^-$
- Four-momenta of W^{+*}, W^-: $q,\, p$
- Polarization vectors
  of W^{+*} boson: $\varepsilon_1^\mu(\pm 1) = \frac{1}{\sqrt{2}}(0; \mp 1, -i, 0), \quad \varepsilon_1^\mu(0) = \frac{1}{\sqrt{q^2}}(|\vec{q}\,|; 0, 0, q_0),$

$$\varepsilon_1^\mu(t) = \frac{1}{\sqrt{q^2}}(q_0; 0, 0, |\vec{q}\,|),$$

- Polarization vectors
  of W^- boson: $\varepsilon_2^\mu(\pm 1) = \frac{1}{\sqrt{2}}(0; \pm 1, -i, 0), \quad \varepsilon_2^\mu(0) = \frac{1}{M_W}(|\vec{q}\,|; 0, 0, -p_0)$

The four-fold angular distribution is

$$\frac{d\Gamma\Big(H \to W^{+*}(\to \tau^+ \nu_\tau) W^-(\to \tau^- \bar{\nu}_\tau)\Big)}{dq^2 d(\cos\theta_q) d(\cos\theta_p) d\chi} \tag{1}$$

$$= \frac{Br_{W\tau\nu_\tau}}{(2\pi)^4} \frac{(1-\frac{m^2}{q^2})|\vec{q}|}{2^5 M_H^2} \sum_{\lambda_{W^-}, \lambda_{W^+}, \lambda'_{W^-}, \lambda'_{W^+}, s_{W^+}, s'_{W^+}} D^{\lambda_{W^-}, \lambda_{W^+}, \lambda'_{W^-}, \lambda'_{W^+}}_{s_{W^+}, s'_{W^+}}$$

The Hermetian density matrix is

$$\begin{aligned} D^{\lambda_{W^-}, \lambda_{W^+}, \lambda'_{W^-}, \lambda'_{W^+}}_{s_{W^+}, s'_{W^+}} &= \sum_{\lambda_{\tau^-}, \lambda_{\bar{\nu}_\tau}, \lambda_{\tau^+}, \lambda_{\nu_\tau}} M^{\lambda_{W^-}, \lambda_{W^+}, s_{W^+}}_{\lambda_{\tau^-}, \lambda_{\bar{\nu}_\tau}, \lambda_{\tau^+}, \lambda_{\nu_\tau}} [M^{\lambda'_{W^-}, \lambda'_{W^+}, s'_{W^+}}_{\lambda_{\tau^-}, \lambda_{\bar{\nu}_\tau}, \lambda_{\tau^+}, \lambda_{\nu_\tau}}]^\dagger, \text{where} \\ M^{\lambda_{W^-}, \lambda_{W^+}, s_{W^+}}_{\lambda_{\tau^-}, \lambda_{\bar{\nu}_\tau}, \lambda_{\tau^+}, \lambda_{\nu_\tau}} &= (-1 + \frac{q^2}{M_W^2})^{1 - s_{W^+}} A_{\lambda_{W^+} \lambda_{W^-}} B^{\lambda_{W^+}}_{\lambda_{\tau^+}, \lambda_{\nu_\tau}} C^{\lambda_{W^-}}_{\lambda_{\tau^-}, \lambda_{\bar{\nu}_\tau}} \end{aligned}$$

A, B, and C are the decay amplitudes of H, W^-, and W^{+*}, respectively, and are written as follows. $(1+\gamma_5 \not{n})$ is the spin or helicity projection operator.

$$A_{\lambda_{W^+}\lambda_{W^-}} = igM_W\ \varepsilon_1^{\mu *}(\lambda_{W^+})\varepsilon_2^{\nu *}(\lambda_{W^-})\, g_{\mu\nu} \tag{2a}$$

$$B^{\lambda_{W^+}}_{\lambda_{\tau^+},\lambda_{\nu_\tau}} = \frac{-ig}{2\sqrt{2}}\ \bar{u}(p_1,\lambda_{\nu_\tau})\frac{i\not{\varepsilon}_1(\lambda_{W^+})}{(q^2-M_W^2+iM_W\Gamma_W)}(1-\gamma_5)v(p_2,\lambda_{\tau^+}) \tag{2b}$$

$$C^{\lambda_{W^-}}_{\lambda_{\tau^-},\lambda_{\bar{\nu}_\tau}} = \frac{-ig}{2\sqrt{2}}\ \bar{u}(p_3,\lambda_{\tau^-})\frac{i\not{\varepsilon}_2(\lambda_{W^-})}{M_W\Gamma_W}(1-\gamma_5)v(p_4,\lambda_{\bar{\nu}_\tau}). \tag{2c}$$

2.3 Helicity Formalism

Now consider the B meson decay in Figure 3. Ignoring the subsequent D^* decay, the three-fold distribution of the decay rate is expressed below by the helicity formalism. The prescription follows the treatment in [7].

The three-fold angular distribution is

$$\frac{d\Gamma\left(\bar{B}\to D^{*+}\tau^-\bar{\nu}_\tau\right)}{dq^2 d(\cos\theta_\ell)d\chi}$$

$$= \frac{1}{(2\pi)^4}|V_{bc}|^2\frac{1}{2^6 M_B^2}(1-\frac{m_\ell^2}{q^2})|\vec{q}|\ L_{\mu\nu}H^{\mu\nu}.$$

$L_{\mu\nu}$ and $H^{\mu\nu}$ are the leptonic and hadronic tensors, respectively. $H^{\mu\nu}$ is written in terms of a general second rank tensor $T^{D^*}_{\mu\alpha}$.

$$H_{\mu\nu} = \sum_{\text{helicities}} < D^*, p_2|j_\mu|\bar{B}, p_1 >< D^*, p_2|j_\nu|\bar{B}, p_1 >^*$$

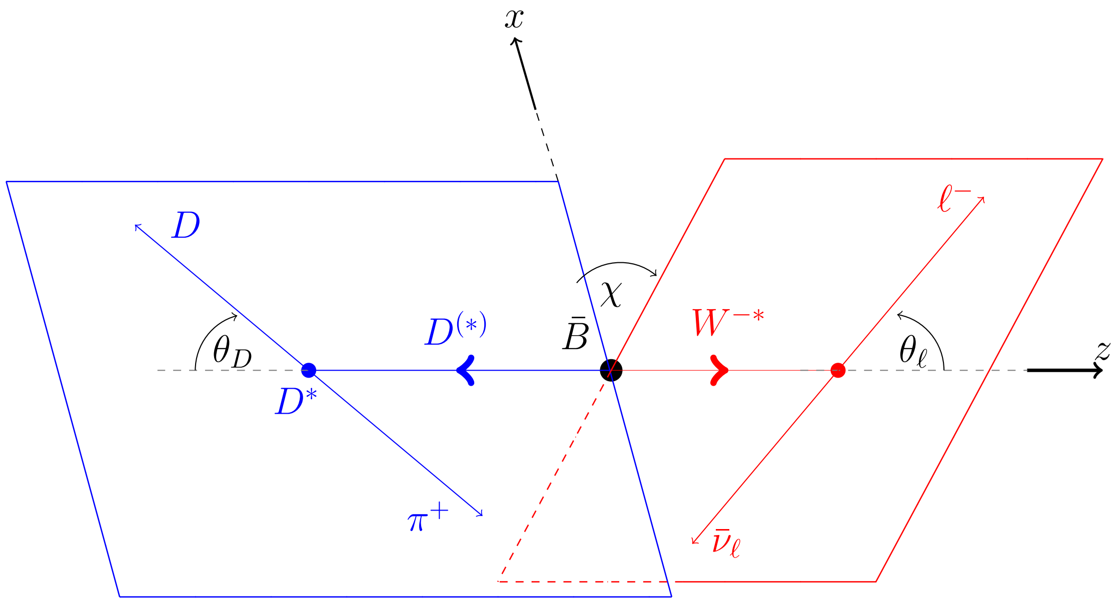

Figure 3: Four body decay of a B meson: $\bar{B} \to D^{(*)}(\to D\pi^+)\ W^{-*}(\to \ell^- \bar{\nu}_\ell)$. θ_D and θ_ℓ are the decay angles in the rest frame of D and the center of momentum frame of ℓ^- and $\bar{\nu}_\ell$, respectively. χ is the dihedral angle between the decay planes.

$$= \quad T^{D^*}_{\mu\alpha}(T^{D^*}_{\nu\beta})^* \, (-g^{\alpha\beta} + \frac{p_2^\alpha p_2^\beta}{M_2^2}),$$

where

$$T^{D^*}_{\mu\alpha} = \quad F_1^A g_{\mu\alpha} + F_2^A p_{1\mu} p_{1\alpha} + F_3^A q_\mu p_{1\alpha} + iF^V \varepsilon_{\mu\alpha\rho\sigma} p_1^\rho p_2^\sigma.$$

$\varepsilon_{\mu\alpha\rho\sigma}$ is the Levi-Civita antisymmetric tensor. $F^A_{1,2,3}$ and F^V are the form factors. q_μ is the momentum of W^{-*}.

$L_{\mu\nu}$ is written in terms of Wigner d-functions as

$$L_{\mu\nu} \quad = \quad \sum_{\lambda_\ell, m, m', J, J'} |h_{\lambda_\ell, \lambda_{\ell'} = \frac{1}{2}}|^2 e^{i(m-m')\chi} d^J_{m, \lambda_\ell - \frac{1}{2}}(\theta_\ell) d^{J'}_{m', \lambda_\ell - \frac{1}{2}}(\theta_\ell) \varepsilon^*_\mu(m) \varepsilon_\nu(m').$$

$\lambda_{\ell'} = \dfrac{1}{2}$ since the anti-neutrino,$\bar{\nu}_\ell$, is right-handed. $\varepsilon(\cdot)$ is the polarization vector of W^{-*}. $J = 0, 1$

and $m = 0\pm$ represent the spin and helicities, respectively of W^{-*}.

$h_{\lambda_\ell,\lambda_{\ell'}=\frac{1}{2}}$ is the decay amplitude for W^{-*} in the dilepton center of momentum frame. $|h_{\lambda_\ell,\lambda_{\ell'}=\frac{1}{2}}|^2$ denotes the spin-flip ($\lambda_\ell = \frac{1}{2}$) and spin non-flip ($\lambda_\ell = -\frac{1}{2}$) helicity amplitudes. d-functions rotate the dilepton decay with respect to the W^{-*} trajectory in the B rest frame (see Figure 3), giving the final orientation of the dilepton decay in the dilepton center of momentum frame. Hence, the leptonic decay angle θ_ℓ is in the dilepton center of momentum frame.

CHAPTER 3: LEPTON FLAVOR NON-UNIVERSALITY

3.1 Introduction

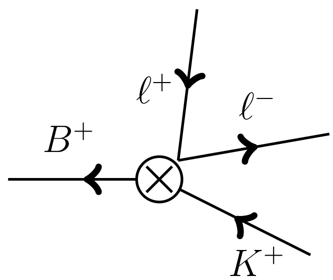

Figure 4: Feynman diagram for the three body decay of a B^+ meson: $B^+ \to K^+ \ell^- \ell^+$. The circle with an X represents both the box and penguin channels.

To date, the standard model (SM) has been extremely successful in describing experimental data. There are, however, a few measurements that are in disagreement with the predictions of the SM. For example, the LHCb Collaboration recently measured the ratio of decay rates for $B^+ \to K^+ \ell^+ \ell^-$ ($\ell = e, \mu$) in the dilepton invariant mass-squared range $1\ \text{GeV}^2 \leq q^2 \leq 6\ \text{GeV}^2$ [8] (see Figure 4). They found

$$R_K \equiv \frac{\mathscr{B}(B^+ \to K^+ \mu^+ \mu^-)}{\mathscr{B}(B^+ \to K^+ e^+ e^-)} = 0.745^{+0.090}_{-0.074}\ (\text{stat}) \pm 0.036\ (\text{syst})\ , \tag{3}$$

which is a 2.6σ difference from the SM prediction of $R_K = 1 \pm O(10^{-4})$ [3]. Notice that the ratio R_K drops the uncertainties associated with the CKM matrix elements while the uncertainties associated with the hadronic form factors are reduced. Combining R_K with other anomalies associated with $b \to s$ transitions, e.g. $B_s \to \phi \mu^+ \mu^-$, yields a 4-5σ discrepancy with respect to the SM [9].

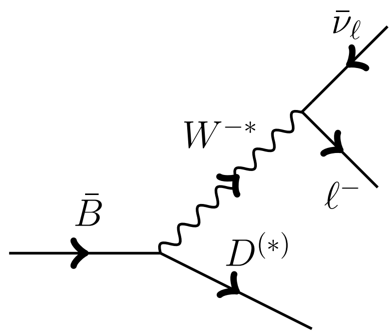

Figure 5: Feynman Diagram for the three body decay of a B meson: $\bar{B} \to D^{(*)}\, W^{-*}(\to \ell^- \bar{\nu}_\ell)$.

Another example is the process $\bar{B} \to D^{(*)}\, W^{-*}(\to \ell^- \bar{\nu}_\ell)$ (see Figure 5). The Heavy-Flavor Averaging Group has evaluated the averages of $R(D)$ and $R(D^*)$ [1]:

$$\begin{aligned} R(D) &\equiv \frac{\mathscr{B}(\bar{B} \to D^+ \tau^- \bar{\nu}_\tau)}{\mathscr{B}(\bar{B} \to D^+ \ell^- \bar{\nu}_\ell)} = 0.397 \pm 0.040 \pm 0.028 \,, \\ R(D^*) &\equiv \frac{\mathscr{B}(\bar{B} \to D^{*+} \tau^- \bar{\nu}_\tau)}{\mathscr{B}(\bar{B} \to D^{*+} \ell^- \bar{\nu}_\ell)} = 0.316 \pm 0.016 \pm 0.010 \,, \end{aligned} \tag{4}$$

where $\ell = e, \mu$. The SM predictions are $R(D) = 0.305 \pm 0.012$ and $R(D^*) = 0.252 \pm 0.004$ [10]. Hence, the $R(D)$ and $R(D^*)$ experimental averages deviate from the SM by 1.9σ and 3.3σ, respectively. (A combined analysis of $R(D)$ and $R(D^*)$, including correlations, gives a 4σ deviation from the SM [1, 2].) These two measurements of lepton flavor non-universality, respectively referred to as the R_K and $R(D^{(*)})$ puzzles, may be providing a hint of the new physics (NP) believed to exist beyond the SM. Recent reviews of the anomalies in R_K and R_{D^*} may be found in Refs. [11].

Recently, the ratio R_{K^*} has also been measured by the LHCb Collaboration and shows a similar tension with respect to the standard model as R_K [12]. The process is $B^0 \to K^* \ell^+ \ell^-$, i.e. a neutral B meson decay.

$$R_{K^*}^{\rm expt} = \begin{cases} 0.660^{+0.110}_{-0.070}\,({\rm stat}) \pm 0.024\,({\rm syst})\,, & 0.045 \le q^2 \le 1.1\ {\rm GeV}^2\,, \quad ({\rm low\ q}^2) \\ 0.685^{+0.113}_{-0.069}\,({\rm stat}) \pm 0.047\,({\rm syst})\,, & 1.1 \le q^2 \le 6.0\ {\rm GeV}^2\,, \quad ({\rm central\ q}^2)\,. \end{cases} \tag{5}$$

The ratios differ from the standard model by 2.2-2.4σ at low q^2 and 2.4-2.5σ at central q^2. This further hints at b anomalies pointing towards new physics. Refs. [13] and [14] try reconciling the R_K and R_{K^*} puzzles.

In addition, note that the three-body decay $B^0 \to K^* \mu^+ \mu^-$ by itself offers a large number of observables in the kinematic and angular distributions of the final-state particles, and it has been argued that some of these distributions are less affected by hadronic uncertainties [15]. Interestingly, the measurement of one of these observables shows a deviation from the SM prediction [16]. However, the situation is not clear whether this anomaly is truly a first sign of new physics. There are unknown hadronic uncertainties that must be taken into account before one can draw this conclusion [17, 18, 19].

3.2 GGL

To search for an explanation of R_K, in Ref. [20] Hiller and Schmaltz perform a model-independent analysis of $b \to s\ell^+\ell^-$. They consider NP operators of the form $(\bar{s}\mathscr{O}b)(\bar{\ell}\mathscr{O}'\ell)$, where $\mathscr{O}$ and $\mathscr{O}'$ span all Lorentz structures. They find that the only NP operator that can reproduce the experimental value of R_K is $(\bar{s}\gamma_\mu P_L b)(\bar{\ell}\gamma^\mu P_L \ell)$. This is consistent with the NP explanations for the $B \to K^{(*)}\mu^+\mu^-$ angular distributions measured by LHCb [18].

Typically, lepton-flavour non-universality implies LFV [4], but not always [21]. In Ref. [22], Glashow, Guadagnoli and Lane (GGL) note that lepton flavor non-universality is necessarily associated with lepton flavor violation (LFV). With this in mind, they assume that the NP couples preferentially to the third generation, giving rise to the operator

$$G(\bar{b}'_L \gamma_\mu b'_L)(\bar{\tau}'_L \gamma^\mu \tau'_L) \ , \tag{6}$$

where $G = O(1)/\Lambda^2_{NP}\lambda_\ell G_F$, and the primed fields are the fermion eigenstates in the gauge basis. The gauge eigenstates are related to the physical mass eigenstates by unitary transformations involving U_L^d and U_L^ℓ:

$$d'_{L3} \equiv b'_L = \sum_{i=1}^{3} U^d_{L3i} d_i \ , \quad \ell'_{L3} \equiv \tau'_L = \sum_{i=1}^{3} U^\ell_{L3i} \ell_i \ . \tag{7}$$

With this, Eq. (6) generates an NP operator that contributes to $\bar{b} \to \bar{s}\mu^+\mu^-$:

$$G \left[U^d_{L33} U^{d*}_{L32} |U^\ell_{L32}|^2 (\bar{b}_L \gamma_\mu s_L)(\bar{\mu}_L \gamma^\mu \mu_L) + h.c. \right] . \tag{8}$$

Because the coefficient of this operator involves elements of the mixing matrices, which are unknown, one cannot make a precise evaluation of the effect of this operator on $\mathscr{B}(B^+ \to K^+\mu^+\mu^-)$, and hence on R_K. Still, GGL note that the hierarchy of the elements of Cabibbo-Kobayashi-Maskawa quark mixing matrix, along with the apparent preference of the NP for muons over electrons, suggests that $|U^{d,\ell}_{L33}| \simeq 1$ and $|U^{d,\ell}_{L31}|^2 << |U^{d,\ell}_{L32}|^2 << 1$. Furthermore, there are limits on some ratios of magnitudes of matrix elements. Taken together, GGL find that the observed value of R_K can be accommodated with the addition of the NP operator in Eq. (8).

In any case, GGL's main point is not so much to offer Eq. (6) as an explanation of R_K, but rather to stress that the NP responsible for the lepton flavor non-universality will generally also lead to an enhancement of the rates for lepton-flavor-violating processes such as $B \to K\mu e, K\mu\tau$ and $B_s \to \mu e, \mu\tau$. In the case of Eq. (6), it is clear how LFV arises. This operator is written in terms of the fermion fields in the gauge basis and does not respect lepton-flavor universality. In transforming to the mass basis, the GIM mechanism [23] is broken, and processes with LFV are generated.

In fact, this behavior is quite general. In writing down effective Lagrangians, it is usually only required that the operators respect $SU(3)_C \times U(1)_{em}$ gauge invariance. However, it was argued in Refs. [20, 24] that if the scale of NP is much larger than the weak scale, the operators generated (when one integrates out the heavy NP degrees of freedom) must be invariant under the full $SU(3)_C \times SU(2)_L \times U(1)_Y$ gauge group. In the same vein, the operators should be written in terms of the fermion fields in the gauge basis – after all, above the weak scale, the mass eigenstates do not (yet) exist. If these operators break lepton universality, lepton-flavor-violating interactions will appear at low energy when one transforms to the mass basis. (Note, however, that in explicit models one can avoid lepton flavor non-universality and lepton flavor violation through the imposition of additional symmetries. One such example can be found in Ref. [25].)

There have been a number of analyses, both model-independent and model-dependent, examining explanations of the R_K puzzle. (Sometimes the data from the $B \to K^{(*)}\mu^+\mu^-$ angular distributions were also included.) In all cases, the low-energy operators were written in terms of mass eigenstates, and lepton-flavor-violating operators were not included. However, as argued above, such operators will appear when lepton universality is broken. Now, the model-independent analyses [18, 20, 24, 26] will be little changed by the inclusion of such operators. However, considerations of such lepton-flavor-violating interactions would be useful in the context of model-dependent analyses. Leptoquarks [20, 27] and R-parity-violating SUSY [28] have been proposed as possible solutions to the R_K puzzle. In both cases, it would be interesting to examine the predictions for the lepton-flavor-violating processes.

Coming back to the GGL operator of Eq. (6), it too must be made invariant under $SU(3)_C \times SU(2)_L \times U(1)_Y$. There are two consequences. First, the left-handed fermion fields must be replaced by $SU(2)_L$ doublets: $b'_L \to Q'_L$ and $\tau'_L \to L'_L$, where $Q' \equiv (t', b')^T$ and $L' \equiv (\nu'_\tau, \tau')^T$. Second, there are two NP operators that are invariant under $SU(2)_L$ and contain Eq. (6):

$$\begin{aligned} \mathcal{O}^{(1)}_{NP} &= G_1 (\bar{Q}'_L \gamma_\mu Q'_L)(\bar{L}'_L \gamma^\mu L'_L) , \\ \mathcal{O}^{(2)}_{NP} &= G_2 (\bar{Q}'_L \gamma_\mu \sigma^I Q'_L)(\bar{L}'_L \gamma^\mu \sigma^I L'_L) , \end{aligned} \tag{9}$$

where G_1 and G_2 are both $O(1)/\Lambda^2_{NP}$ (but not equal to one another), and σ^I are the Pauli matrices (the generators of $SU(2)$). Using the identity

$$\sigma^I_{ij}\sigma^I_{kl} = 2\delta_{il}\delta_{kj} - \delta_{ij}\delta_{kl} , \tag{10}$$

where i, j are $SU(2)_L$ indices, the second operator can be written as

$$\mathscr{O}_{NP}^{(2)} = G_2 \left[2(\bar{Q}_L'^i \gamma_\mu Q_L'^j)(\bar{L}_L'^j \gamma^\mu L_L'^i) - (\bar{Q}_L' \gamma_\mu Q_L')(\bar{L}_L' \gamma^\mu L_L') \right] . \tag{11}$$

The two operators correspond to different types of underlying NP. Specifically, $\mathscr{O}_{NP}^{(1)}$ contains only neutral-current (NC) interactions, while $\mathscr{O}_{NP}^{(2)}$ contains both neutral-current and charged-current (CC) interactions. $\mathscr{O}_{NP}^{(2)}$ therefore offers the potential to simultaneously explain both the R_K and $R(D^{(*)})$ puzzles, and one may examine the effects of including this NP operator.

Writing $\mathscr{O}_{NP}^{(2)}$ explicitly in terms of the up-type and down-type fields, there are four NC operators and one CC operator:

$$\mathscr{O}_{NP}^{(2)} = O_{tt\nu_\tau\nu_\tau} + O_{bb\tau\tau} + O_{tt\tau\tau} + O_{bb\nu_\tau\nu_\tau} + O_{tb\tau\nu_\tau} \ , \tag{12}$$

with

$$\begin{aligned}
O_{tt\nu_\tau\nu_\tau} &= G_2(\bar{t}_L' \gamma_\mu t_L')(\bar{\nu}_{\tau_L}' \gamma^\mu \nu_{\tau_L}') \ , \\
O_{bb\tau\tau} &= G_2(\bar{b}_L' \gamma_\mu b_L')(\bar{\tau}_L' \gamma^\mu \tau_L') \ , \\
O_{tt\tau\tau} &= -G_2(\bar{t}_L' \gamma_\mu t_L')(\bar{\tau}_L' \gamma^\mu \tau_L') \ , \\
O_{bb\nu_\tau\nu_\tau} &= -G_2(\bar{b}_L' \gamma_\mu b_L')(\bar{\nu}_{\tau L}' \gamma^\mu \nu_{\tau L}') \ , \\
O_{tb\tau\nu_\tau} &= 2G_2(\bar{t}_L' \gamma_\mu b_L')(\bar{\tau}_L' \gamma^\mu \nu_{\tau L}').
\end{aligned} \tag{13}$$

If both $\mathscr{O}_{NP}^{(1)}$ and $\mathscr{O}_{NP}^{(2)}$ are present then the NC interactions receive contributions from both NP operators.

Above, notice that the NC part of $\mathscr{O}_{NP}^{(2)}$ contains $O_{bb\tau\tau}$, which is the GGL operator of Eq. (6). In transforming to the mass basis, the GGL piece therefore contributes to $\bar{b} \to \bar{s}$ transitions through the quark-level decays $\bar{b} \to \bar{s}\ell^+\ell^-$ and $\bar{b} \to \bar{s}\ell^+\ell'^-$. These generate the meson-level decays $B \to K^{(*)}\mu^+\mu^-, B \to K^{(*)}\mu^\pm e^\mp, B \to K^{(*)}\mu^\pm\tau^\mp, B_s \to \mu^+\mu^-, B^0 \to X_s\mu^+\mu^-, B_s^0 \to \mu^+\mu^-\gamma$, etc. (Many of these decays are discussed by GGL.) The largest effects will be an enhancement of the SM contribution to $\bar{b} \to \bar{s}\tau^+\tau^-$, and the generation of the lepton-flavor-violating decays $\bar{b} \to \bar{s}\tau^\pm\mu^\mp$[31]. Thus far, LFV has been only observed in neutrino oscillations. Ref. [32] relates possible LFV in B decays to the CP phase δ in neutrino oscillations.

3.3 R_K

Let us begin by discussing the effect of $\mathcal{O}_{NP}^{(2)}$ on R_K. The amplitude for $\bar{b} \to \bar{s}\ell_i^+\ell_i^-$ ($\ell_1 = e, \ell_2 = \mu$) can be expressed as

$$A_{\ell_i} \;=\; A^{\rm SM}\left(1 + V_L^{bs\ell_i}\right) \;, \quad V_L^{bs\ell_i} \;=\; \frac{\kappa}{C_9}\frac{U^d_{L33}U^{d*}_{L32}}{V_{tb}V^*_{ts}}|U^\ell_{L3i}|^2 \;, \quad \kappa \;=\; \frac{4\pi}{\alpha_{\rm EM}}\frac{g_2^2}{g^2}\frac{M_W^2}{\Lambda^2_{\rm NP}} \;. \tag{14}$$

Here $A^{\rm SM}$ is the lepton-flavor-universal (SM) contribution, the V_{ij} are Cabibbo-Kobayashi-Maskawa (CKM) matrix elements, C_9 is a Wilson coefficient, and $G_2 = g_2^2/\Lambda^2_{\rm NP}$. Neglecting the masses of the leptons one arrives at the following result:

$$\begin{aligned} R_K \;&=\; \frac{1 + 2\,{\rm Re}[V_L^{bs\mu}] + |V_L^{bs\mu}|^2}{1 + 2\,{\rm Re}[V_L^{bse}] + |V_L^{bse}|^2} \\ &\approx\; 1 + \frac{8\pi}{C_9\alpha_{\rm EM}}\frac{g_2^2}{g^2}\frac{M_W^2}{\Lambda^2_{\rm NP}}\frac{U^d_{L32}|U^\ell_{L32}|^2}{\lambda^2} \;, \end{aligned} \tag{15}$$

where λ is the sine of the Cabibbo angle. The usual hierarchy of CKM matrix elements is assumed and all CP-violating phases are ignored. The 5σ limit on R_K from LHCb then implies

$$-2\times 10^{-4} \lesssim \frac{1}{C_9}\frac{g_2^2}{g^2}\frac{M_W^2}{\Lambda^2_{\rm NP}}\frac{U^d_{L32}|U^\ell_{L32}|^2}{\lambda^2} \lesssim 7\times 10^{-5} \;. \tag{16}$$

It is clear that the LHCb measurement [8] constrains the magnitudes of the down-type and lepton mixing-matrix elements. However, a further set of constraints will be obtained below.

In addition to the decays produced by the GGL operator, one now also has the quark-level decay $\bar{b} \to \bar{s}\nu\bar{\nu}$ that contributes to $B \to K^{(*)}\nu\bar{\nu}$. The amplitude for $\bar{b} \to \bar{s}\nu_i\bar{\nu}_j$ can be expressed as

$$A_{ij} \;=\; C_{ij}(\bar{b}_L\gamma_\mu s_L)(\bar{\nu}_{iL}\gamma^\mu\nu_{jL}) \;. \tag{17}$$

The SM contributes only to terms diagonal in neutrino flavor ($i = j$), while the NP operator also gives rise to off-diagonal terms that violate lepton flavor ($i \neq j$). Then

$$C_{ij} \;=\; \kappa_{\rm SM}\left(\delta_{ij} - \frac{\kappa}{C_L^{\rm SM}}\frac{U^d_{L33}U^{d*}_{L32}}{V_{tb}V^*_{ts}}U^{*\nu}_{L3i}U^{\nu}_{L3j}\right) , \tag{18}$$

where

$$\kappa_{\rm SM} \;=\; \frac{\sqrt{2}G_F\alpha_{\rm EM}}{\pi}V_{tb}V^*_{ts}C_L^{\rm SM} . \tag{19}$$

In the above, $C_L^{\rm SM}$ is a Wilson coefficient [19]. The square of the amplitude for the process is thus proportional to

$$\sum_{i,j}|C_{ij}|^2 \;=\; 3|\kappa_{\rm SM}|^2\left(1 - \frac{2\kappa}{3}{\rm Re}\,[x] + \frac{\kappa^2}{3}|x|^2\right) , \tag{20}$$

where $x = \left(U^d_{L33}U^{d*}_{L32}\right) / \left(V_{tb}V^*_{ts}\right)$.

Ignore all CP-violating phases, so that x is real. Taking $|U^d_{L33}| \sim 1$, then $x \sim U^d_{L32}/\lambda^2$. The decay rate for $B \to K^{(*)}\nu\bar{\nu}$ is given by

$$\Gamma \;=\; \Gamma_{\rm SM}\left(1 - \frac{2\kappa U^d_{L32}}{3\lambda^2} + \frac{(\kappa U^d_{L32})^2}{3\lambda^4}\right) . \tag{21}$$

The SM decay rate can be expressed as follows:

$$\Gamma_{\rm SM} \;=\; \frac{m_B|\kappa_{\rm SM}|^2}{64\pi^3}\int_0^{q^2|_{\rm max}}\rho_{K^{(*)}}(q^2)dq^2 , \tag{22}$$

where q represents the sum of four momenta of the neutrino and the antineutrino, and $\rho_{K^{(*)}}$ is the appropriate $B \to K^{(*)}$ transition form factor. (Note that neutrinos are treated as massless particles.) Thus the NP term simply modifies the SM rate for $B \to K\nu\bar{\nu}$ by an overall numerical factor.

One can use the above result to get an estimate of how large the NP couplings and mixing matrix elements can be. A precise calculation of the SM branching ratio for $B^+ \to K^+ \nu\bar{\nu}$ was performed in Ref. [19]. It was found that

$$\mathscr{B}(B^+ \to K^+ \nu\bar{\nu})_{\rm SM} = (4.20 \pm 0.33 \pm 0.15) \times 10^{-6} \ . \tag{23}$$

The strongest experimental bounds from the BaBar Collaboration [30] at present set an upper limit of 3.7×10^{-5} at the 90% confidence level. Thus there is still room for the measured decay rate to be larger than the SM prediction. Taking $C_L^{\rm SM} \approx -6.13$ [19], it follows $\kappa \simeq -281(g_2/g)^2(M_W/\Lambda_{\rm NP})^2$. A factor of five enhancement in the decay rate due to the NP operator $\mathscr{O}_{NP}^{(2)}$ would then imply

$$-1.6 \times 10^{-2} \lesssim \frac{g_2^2}{g^2}\frac{M_W^2}{\Lambda_{\rm NP}^2}\frac{U_{L32}^d}{\lambda^2} \lesssim 9.3 \times 10^{-3} \ . \tag{24}$$

If $\Lambda_{\rm NP} \simeq 10 M_W$ then $(g_2^2/g^2)(U_{L32}^d/\lambda^2)$ must be $O(1)$. In this case, a NP coupling of the same order as that of the SM will still allow a reasonably large value for U_{L32}^d. For example, if $g/2 \lesssim g_2 \lesssim g$, one can have $\lambda \gtrsim U_{L32}^d \gtrsim \lambda^2$. In addition, combine Eqs. (16) and (24). Since C_9 is an $O(1)$ number, this implies that an $O(10^{-1})$ value for $|U_{L32}^l|$ is still allowed. A more precise measurement of both R_K and $B^+ \to K^+ \nu\bar{\nu}$ will put stricter bounds on both the down-type and lepton mixing-matrix elements.

Finally, the neutral-current part of $\mathscr{O}_{NP}^{(2)}$ also contributes to the decays $t \to c\ell^+\ell^-$, $t \to c\ell^+\ell'^-$ and $t \to c\nu\bar{\nu}$. The branching ratios for these decays are negligible in the SM, so any observation would be a clear sign of NP. For decays to charged leptons, the most promising is $t \to c\tau^+\tau^-$. In the mass basis, the contributing NP operator is

$$G\left[U_{L32}^{u*} U_{L33}^{u} \, |U_{L33}^{\ell}|^2 \, (\bar{c}_L \gamma^\mu t_L)(\bar{\tau}_L \gamma_\mu \tau_L) + h.c.\right] \ , \tag{25}$$

which gives a partial width of

$$\frac{g_2^4 |U_{L32}^u|^2 \, |U_{L33}^u|^2 \, |U_{L33}^{\ell}|^4}{16 \Lambda_{NP}^4} \frac{m_t^5}{48\pi^3} \ . \tag{26}$$

Taking $g_2 \sim g$, $|U^u_{L33}| \simeq |U^\ell_{L33}| \simeq 1$, $|U^u_{L32}| \simeq \lambda$, and $\Lambda_{NP} = 800$ GeV, this gives

$$\Gamma(t \to c\tau^+\tau^-) = 1 \times 10^{-7} \text{ GeV} . \tag{27}$$

The full width of the t quark is 2 GeV, so this corresponds to a branching ratio of 5×10^{-8}. This is much larger than the SM branching ratio ($O(10^{-16})$), but is still tiny. The branching ratio for $t \to c\nu\bar{\nu}$ takes the same value, while those for all other $t \to c\ell^+\ell^-$ and $t \to c\ell^+\ell'^-$ decays are considerably smaller. Thus, while the branching ratios for these decays can be enormously enhanced compared to the SM, they are still probably unmeasurable. (This point is also noted in Ref. [20].)

Another process involving t quarks that could potentially reveal the presence of NP with LFV is $pp \to t\bar{t}$, followed by the radiation of a $\tau^\pm\mu^\mp$ pair. At the LHC with a 13 TeV center-of-mass energy, gluon fusion dominates the production of $t\bar{t}$ pairs. MadGraph 5 [33] has been used to calculate the cross section for $gg \to t\bar{t}\tau^\pm\mu^\mp$, taking $g_2 \sim g$. The result is $\sigma_{t\bar{t}\tau\mu} \approx 0.4|U^\ell_{L32}|^2$ fb. By contrast, the SM cross section for $t\bar{t}$ pair production is $\sigma_{t\bar{t}} \approx 450$ pb, so that $\sigma_{t\bar{t}\tau\mu}/\sigma_{t\bar{t}} \approx 10^{-6}|U^\ell_{L32}|^2$, which is extremely small. With a luminosity of 100 fb^{-1} /year at the 13 TeV LHC [34], one may therefore expect about 40 events/year for $gg \to t\bar{t}\tau^\pm\mu^\mp$ if $|U^\ell_{L32}| \sim 1$, or about two events/year if $|U^\ell_{L32}| \sim \lambda$. Thus, even though the final-state signal is striking, $pp \to t\bar{t}\tau^\pm\mu^\mp$ is probably unobservable.

3.4 $R(D^{(*)})$

Turning to the charged-current interactions, these contribute to both b and t semileptonic decays. Even with the enhancement from NP, the decay $t \to b\tau\bar{\nu}_\tau$ will still be difficult to observe, as it is swamped by the two-body decay $t \to bW$. On the other hand, the decay $b \to c\tau\bar{\nu}_i$ ($i = \tau, \mu, e$) is particularly interesting, since it contributes to the decay $\bar{B} \to D^{(*)+}\tau^-\bar{\nu}_\tau$ and the $R(D^{(*)})$ puzzle [Eq. (4)], and provides a source of lepton flavor non-universality in such decays.

In the SM, the effective Hamiltonian for the quark-level transition $b \to c\tau\bar{\nu}_\tau$ is

$$\mathscr{H}_{eff} = \frac{4G_F V_{cb}}{\sqrt{2}} (\bar{c}_L \gamma_\mu b_L)(\bar{\tau}_L \gamma^\mu \nu_{\tau L}) + h.c. \,. \tag{28}$$

Now, if $\mathscr{O}_{NP}^{(2)}$ is also present, in addition to $\tau\bar{\nu}_\tau$ in the final state, the NP operator also produces $\tau\bar{\nu}_\mu$ and $\tau\bar{\nu}_e$. However, as the final-state neutrino is not observed, one must sum over the neutrino species. That is, the squared-amplitude for $b \to c\tau^-\bar{\nu}_i$ can be written as

$$|A|^2 = \sum_{i=\tau,\mu,e} |A_i|^2 \,, \tag{29}$$

with

$$A_i \;=\; \frac{4G_F V_{cb}}{\sqrt{2}} \left[\delta_{i\tau} + V_L^{cb\tau\nu_i}\right] \;,\quad V_L^{cb\tau\nu_i} = 4\,\frac{g_2^2}{g^2}\frac{M_W^2}{\Lambda_{NP}^2}\frac{U_{L33}^{d} U_{L32}^{u} U_{L33}^{\ell} U_{L3i}^{\nu}}{V_{cb}} \,. \tag{30}$$

As was done above, it is written $G_2 \equiv g_2^2/\Lambda_{NP}^2$ and used $G_F/\sqrt{2} = g^2/8M_W^2$. One then has

$$|A|^2 = |A|^2_{SM} \left[1 + 2\,\mathrm{Re}(V_L^{cb\tau\nu_\tau}) + |V_L^{cb\tau}|^2\right] \,, \tag{31}$$

where

$$|V_L^{cb\tau}|^2 \equiv \sum_i |V_L^{cb\tau\nu_i}|^2 = \left|4\,\frac{g_2^2}{g^2}\frac{M_W^2}{\Lambda_{NP}^2}\frac{U_{L33}^{d} U_{L32}^{u} U_{L33}^{\ell}}{V_{cb}}\right|^2 \,. \tag{32}$$

(Here the fact that $\sum_i |U_{L3i}^{\nu}|^2 = 1$ is used.) The addition of the NP operator thus has the effect of modifying the SM prediction for $\Gamma(b \to c\tau\bar{\nu}_i)$ by an overall factor that is lepton flavor non-universal. In fact, if the elements of the charged-lepton mixing matrix obey the hierarchy suggested by GGL, namely $|U_{L33}^{\ell}| \simeq 1$ and $|U_{L31}^{\ell}|^2 << |U_{L32}^{\ell}|^2 << 1$, then $b \to c\tau\bar{\nu}_i$ is affected by the NP, but $b \to c\mu\bar{\nu}_i$ and $b \to ce\bar{\nu}_i$ are basically unchanged from the SM.

The simple prediction then follows.

$$\left[\frac{R(D)}{R(D^*)}\right]_{exp} \;=\; \left[\frac{R(D)}{R(D^*)}\right]_{SM} \,. \tag{33}$$

Using Eq. (4), it is seen that

$$\left[\frac{R(D)}{R(D^*)}\right]_{exp} = 1.26 \pm 0.17 \ , \quad \left[\frac{R(D)}{R(D^*)}\right]_{SM} = 1.21 \pm 0.05 \ . \tag{34}$$

So this model is consistent with experiment, but a careful measurement of the double ratio can rule it out. The double ratio in the SM is also likely to have less uncertainty from hadronic form factors. Furthermore, all angular asymmetries, such as the D^* polarization, forward-backward asymmetries, and the azimuthal angle asymmetries including the triple products, will show no deviation from the SM as these asymmetries probe non-SM operator structures.

If the ratios $R(D^{(*)})$ are defined with respect to the $B \to D^{(*)}\mu\nu$ decay mode, one can also write

$$\left[\frac{R(D^*)_{exp}}{R(D^*)_{SM}}\right] = \left[\frac{R(D)_{exp}}{R(D)_{SM}}\right] = \frac{\left[1 + 2\,\mathrm{Re}(V_L^{cb\tau\nu_\tau}) + |V_L^{cb\tau}|^2\right]}{\left[1 + 2\,\mathrm{Re}(V_L^{cb\mu\nu_\mu}) + |V_L^{cb\mu}|^2\right]} \ . \tag{35}$$

Again assuming a hierarchy in the mixing matrix, to leading order one has

$$\left[\frac{R(D^*)_{exp}}{R(D^*)_{SM}}\right] = \left[\frac{R(D)_{exp}}{R(D)_{SM}}\right] \approx \left[1 + 8\frac{g_2^2}{g^2}\frac{M_W^2}{\Lambda^2}\frac{U_{L32}^u}{V_{cb}}\right] \ . \tag{36}$$

Averaging $[R(D^*)_{exp}/R(D^*)_{SM}]$ and $[R(D)_{exp}/R(D)_{SM}]$, one gets

$$8\frac{g_2^2}{g^2}\frac{M_W^2}{\Lambda^2}\frac{U_{L32}^u}{V_{cb}} \approx 0.3 \ . \tag{37}$$

Taking $g/2 \lesssim g_2 \lesssim g$ and $\Lambda \sim 10M_W$, this gives $0.6 \gtrsim U_{L32}^u \gtrsim \lambda$.

There have been numerous analyses examining NP explanations of the $R(D^{(*)})$ measurements [35, 36]. Above, in the context of R_K, it has been noted that, assuming the scale of NP is much larger than the weak scale, all NP operators must be invariant under the full $SU(3)_C \times SU(2)_L \times U(1)_Y$ gauge group. This same argument applies also to NP proposed to explain $R(D^{(*)})$. Such considerations were applied to the semileptonic $b \to c$ transitions in Ref. [37], but they could have important implication for the various NP explanations of the $R(D^{(*)})$ puzzle.

Recent literature provides other avenues of investigating these possible flavor anomalies. Z' models with FCNC's at tree-level imply lepton-flavour non-universal couplings [38]. Ref. [39] considers RGE's from above the electroweak scale down to 1 GeV obtaining LFU breaking and LFV effects in B-decays. Other papers considering radiative corrections can be found in Ref. [40]. R-parity violating supersymmetric effects are probed in $R(D^{(*)})$ with sensitivity to the slepton exchange coupling, but herein, $R(D^{(*)})$ does not reach the lower limit of the 95% confidence level experimental average of BaBar, Belle, and LHCb [41]. Ref. [42] decreases the discrepancies between inclusive and exclusive determinations of V_{ub} and V_{cb} along with the tension between the SM and experimental values of R_K and $R(D^{(*)})$ with a triplet of massive vector bosons under $SU(2)_L$ coupled to third generation fermions. Composite Higgs models with leptoquarks are used to explain the R_K anomaly [43]. R_K and $R(D^{(*)})$ anomalies are correlated to $B \to K^{(*)}\nu\bar{\nu}$ using gauge invariant dim-6 operators [44]. Leptoquark scenarios [45] are ubiquitous in the literature. Vector-like fermions have been pursued [46]. Testing lepton universality is possible in tau neutrino scattering [110]. Finally, Ref. [47] uses the LFV in $\mathscr{B}(h \to \tau\mu)$ through a scalar operator to predict R_K while a calculation of the charged-lepton mixing matrices has also been done[49].

3.5 Conclusion for Lepton Flavor Non-Universality in R_K and $R(D^{(*)})$

To sum up, the recent measurement of $R_K \equiv \mathscr{B}(B^+ \to K^+\mu^+\mu^-)/\mathscr{B}(B^+ \to K^+e^+e^-)$ by the LHCb Collaboration differs from the SM prediction of $R_K = 1$ by 2.6σ. And the Heavy-Flavor Averaging Group has averaged the ratios $R(D^{(*)}) \equiv \mathscr{B}(\bar{B} \to D^{(*)+}\tau^-\bar{\nu}_\tau)/\ \mathscr{B}(\bar{B} \to D^{(*)+}\ell^-\bar{\nu}_\ell)$ ($\ell = e,\mu$), finding discrepancies with the SM of 1.9σ ($R(D)$) and 3.3σ ($R(D^*)$). The R_K and $R(D^{(*)})$ puzzles exhibit lepton flavor non-universality, and therefore hint at new physics (NP).

Recently, Glashow, Guadagnoli and Lane (GGL) [22] proposed an explanation of the R_K puzzle. They assume that the NP couples preferentially to the third generation, and generates the neutral-current operator $(\bar{b}'_L\gamma_\mu b'_L)(\bar{\tau}'_L\gamma^\mu\tau'_L)$, where the primed fields denote states in the gauge basis. When one transforms to the mass basis, one obtains operators that give rise to decays that violate lepton universality (and lepton flavor conservation).

It is known that, assuming the scale of NP is much larger than the weak scale, all NP operators must be made invariant under the full $SU(3)_C \times SU(2)_L \times U(1)_Y$ gauge group. We find that when this is applied to the GGL operator, there are two types of fully gauge-invariant NP operators that are possible. And one of these contains both neutral-current and charged-current interactions. While GGL has shown that the neutral-current piece of this NP operator can explain the R_K puzzle, another possibility is that the charged-current piece can simultaneously explain the $R(D^{(*)})$ puzzle. This model makes a prediction for the double ratio $R(D)/R(D^*)$, so that it can be ruled out with a more precise measurement of this quantity.

CHAPTER 4: IMPLICATIONS FOR Λ_b DECAY

4.1 Introduction

A major part of particle physics research is focused on finding physics beyond the standard model (SM). In the flavor sector a key property of the SM gauge interactions is that they are lepton flavor universal. Evidence for violation of this property would be a clear sign of new physics (NP) beyond the SM. In the search for NP, the second and third generation quarks and leptons are quite special because they are heavier and are expected to be relatively more sensitive to NP. As an example, in certain versions of the two Higgs doublet models (2HDM) the couplings of the new Higgs bosons are proportional to the masses and so NP effects are more pronounced for the heavier generations. Moreover, the constraints on new physics, especially involving the third generation leptons and quarks, are somewhat weaker allowing for larger new physics effects.

From BaBar [50, 51], Belle [52], and LHCb [53], the averages as evaluated by the Heavy-Flavor Averaging Group are [1]:

$$
\begin{aligned}
R(D) &\equiv \frac{\mathscr{B}(\bar{B} \to D^+\tau^-\bar{\nu}_\tau)}{\mathscr{B}(\bar{B} \to D^+\ell^-\bar{\nu}_\ell)} = 0.397 \pm 0.040 \pm 0.028 \,, \\
R(D^*) &\equiv \frac{\mathscr{B}(\bar{B} \to D^{*+}\tau^-\bar{\nu}_\tau)}{\mathscr{B}(\bar{B} \to D^{*+}\ell^-\bar{\nu}_\ell)} = 0.316 \pm 0.016 \pm 0.010 \,,
\end{aligned} \tag{38}
$$

where $\ell = e, \mu$. The SM predictions are $R(D) = 0.305 \pm 0.012$ and $R(D^*) = 0.252 \pm 0.004$ [10]. Hence, the $R(D)$ and $R(D^*)$ experimental averages deviate from the SM by 1.9σ and 3.3σ, respectively. (A combined analysis of $R(D)$ and $R(D^*)$, including correlations, gives a 4σ deviation from the SM [1, 2].) This measurement of lepton flavor non-universality, referred to as the $R(D^{(*)})$ puzzles, may be providing a hint of the new physics (NP) believed to exist beyond the SM. There have been numerous analyses examining NP explanations of the $R(D^{(*)})$ measurements [4, 35, 36, 54].

The underlying quark level transition $b \to c\tau^- \bar{\nu}_\tau$ can be probed in both B and Λ_b decays [48]. Note that in the presence of lepton non-universality the flavor of the neutrino does not have to match the flavor of the charged lepton [4]. Moreover the NP can affect all the lepton flavors. The main assumption here is that the NP effect is largest for the τ sector and for simplicity one may neglect the smaller NP effects in the μ and e leptons. The Λ_b being a spin 1/2 baryon has a complex angular distribution for its decay products. As in B decays, several observables are constructed from the angular distribution of the Λ_b decay which can be used to find evidence of NP and to probe the structure of NP.

The decay $\Lambda_b \to \Lambda_c \tau \bar{\nu}_\tau$ has not been measured experimentally though it might be possible to observe this decay at the LHCb. Λ_b baryons make up 20% of the b-hadrons produced at the LHC and are comparable in number to the production of B_u and B_d mesons, but significantly higher than B_s mesons [55]. The full angular distribution of this decay is experimentally challenging and thus, for the sake of phenomenology, the focus is on the rate as well as the q^2 differential distribution for this decay. Using constraints on the new physics couplings obtained by using Eq. (38) predictions are made for the effects of these couplings in $\Lambda_b \to \Lambda_c \tau \bar{\nu}_\tau$ decay. Recently, in Ref. [56] this decay was discussed in the standard model and with new physics in Ref. [57]. Note that both the Belle [58] and the BaBar [59] experiments have scanned close to the $\Lambda_b \bar{\Lambda}_b$ threshold.

The main uncertainty in the $\Lambda_b \to \Lambda_c \tau \bar{\nu}_\tau$ decays are the hadronic form factors for the $\Lambda_b \to \Lambda_c$ transition. These form factors can also be studied systematically in a heavy m_b and m_c expansion [60]. However, unlike the B system the heavy baryon form factors have not been extensively studied. Therefore ratios are constructed where the form factor uncertainties will mostly cancel leaving behind a smaller uncertainty for the theoretical predictions. Then an investigation is done to see if the NP effects are large enough to produce observable deviations from the SM predictions.

The topic is organized in the following manner. The effective Lagrangian is introduced to parametrize the NP operators. The formalism of the decay process is described and the relevant observables are introduced. Results and conclusions are presented.

4.2 Formalism

In the presence of NP, the effective Hamiltonian for the quark-level transition $b \to c l^- \bar{\nu}_l$ can be written in the form [61]

$$
\begin{aligned}
\mathscr{H}_{eff} &= \frac{G_F V_{cb}}{\sqrt{2}} \Big\{ \Big[\bar{c}\gamma_\mu(1-\gamma_5)b + g_L \bar{c}\gamma_\mu(1-\gamma_5)b + g_R \bar{c}\gamma_\mu(1+\gamma_5)b \Big] \bar{l}\gamma^\mu(1-\gamma_5)\nu_l \\
&\quad + \Big[g_S \bar{c}b + g_P \bar{c}\gamma_5 b \Big] \bar{l}(1-\gamma_5)\nu_l + h.c \Big\}. \qquad (39)
\end{aligned}
$$

where $G_F = 1.1663787 \times 10^{-5}$ GeV^{-2} is the Fermi coupling constant, V_{cb} is the Cabibbo-Koboyashi-Maskawa (CKM) matrix element and use $\sigma_{\mu\nu} = i[\gamma_\mu, \gamma_\nu]/2$ later. The neutrinos are assumed to be always left chiral and to introduce non-universality. The NP couplings are in general different for different lepton flavors. The NP effect is assumed to occur mainly through the τ lepton while tensor operators are not included in the analysis [62]. Further, no relation shall be assumed between $b \to u l^- \bar{\nu}_l$ and $b \to c l^- \bar{\nu}_l$ transitions and hence do not include constraints from $B \to \tau\nu_\tau$. The SM effective Hamiltonian corresponds to $g_L = g_R = g_S = g_P = 0$.

In Ref.[54] the NP is parameterized in terms of the couplings g_S, g_P, $g_V = g_R + g_L$ and $g_A = g_R - g_L$ while in this work g_V and g_A have been traded for $g_{L,R}$ to align our analysis closer to realistic models [4]. The couplings $g_{L,R,P}$ contribute to $R(D^*)$ while $g_{L,R,S}$ contribute to $R(D)$. One NP coupling shall be considered at a time, incorporating constraints on these couplings from $R(D^{(*)})$.

4.2.1 Decay Process

The process under consideration is

$$\Lambda_b(p_{\Lambda_b}) \to \tau^-(p_1) + \bar{\nu}_\tau(p_2) + \Lambda_c(p_{\Lambda_c})$$

In the SM the amplitude for this process is

$$M_{SM} = \frac{G_F V_{cb}}{\sqrt{2}} L^\mu H_\mu, \tag{40}$$

where the leptonic and hadronic currents are,

$$\begin{aligned} L^\mu &= \bar{u}_\tau(p_1)\gamma^\mu(1-\gamma_5)v_{\nu_\tau}(p_2), \\ H_\mu &= \langle\Lambda_c|\bar{c}\gamma_\mu(1-\gamma_5)b|\Lambda_b\rangle. \end{aligned} \tag{41}$$

The hadronic current is expressed in terms of six form factors,

$$\begin{aligned} \langle\Lambda_c|\bar{c}\gamma_\mu b|\Lambda_b\rangle &= \bar{u}_{\Lambda_c}(f_1\gamma_\mu + if_2\sigma_{\mu\nu}q^\nu + f_3 q_\mu)u_{\Lambda_b}, \\ \langle\Lambda_c|\bar{c}\gamma_\mu\gamma_5 b||\Lambda_b\rangle &= \bar{u}_{\Lambda_c}(g_1\gamma_\mu\gamma_5 + ig_2\sigma_{\mu\nu}q^\nu\gamma_5 + g_3 q_\mu\gamma_5)u_{\Lambda_b}. \end{aligned} \tag{42}$$

Here $q = p_{\Lambda_b} - p_{\Lambda_c}$ is the momentum transfer and the form factors are functions of q^2. When considering NP operators one may use the following relations obtained by using the equations of motion.

$$\begin{aligned} \langle\Lambda_c|\bar{c}b|\Lambda_b\rangle &= \bar{u}_{\Lambda_c}(f_1\frac{\not{q}}{m_b-m_c} + f_3\frac{q^2}{m_b-m_c})u_{\Lambda_b}, \\ \langle\Lambda_c|\bar{c}\gamma_5 b|\Lambda_b\rangle &= \bar{u}_{\Lambda_c}(-g_1\frac{\not{q}\gamma_5}{m_b+m_c} - g_3\frac{q^2\gamma_5}{m_b+m_c})u_{\Lambda_b}. \end{aligned} \tag{43}$$

Define the following ratio.

$$R_{\Lambda_b} = \frac{\mathscr{B}(\Lambda_b \to \Lambda_c\tau\bar{\nu}_\tau)}{\mathscr{B}(\Lambda_b \to \Lambda_c\ell\bar{\nu}_\ell)} \tag{44}$$

Here ℓ represents μ or e. Also, define the ratio of differential distributions as

$$B_{\Lambda_b}(q^2) = \frac{\frac{d\Gamma[\Lambda_b\to\Lambda_c\tau\bar{\nu}_\tau]}{dq^2}}{\frac{d\Gamma[\Lambda_b\to\Lambda_c\ell\bar{\nu}_\ell]}{dq^2}}. \tag{45}$$

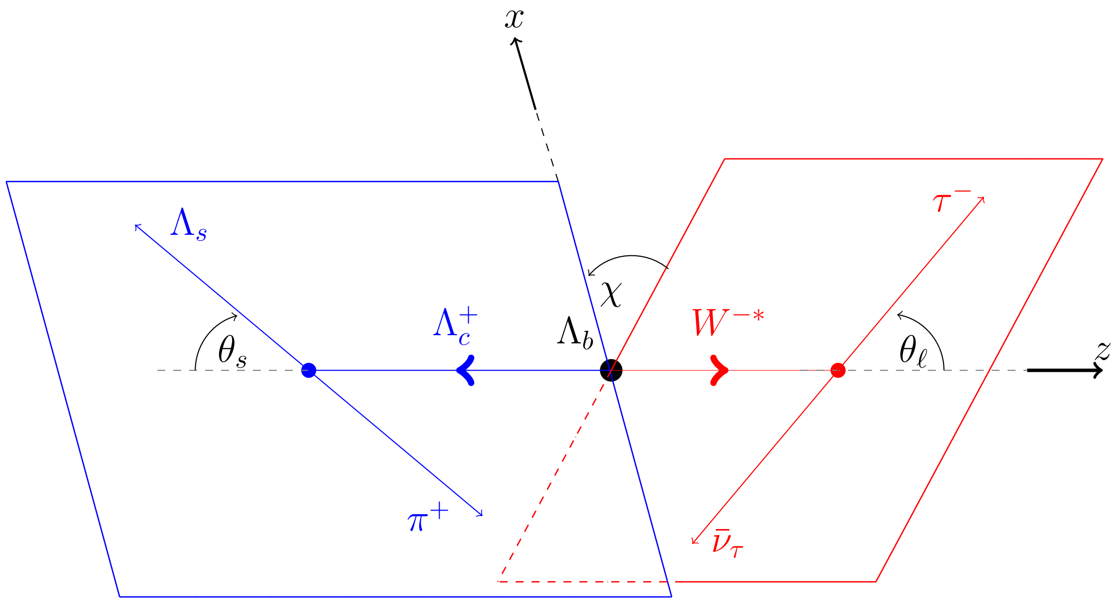

Figure 6: Four body decay of Λ_b: $\Lambda_b \to (\Lambda_s \pi^+)\Lambda_c^+ \ (\tau^- \bar{\nu}_\tau)W^{-*}$. θ_s and θ_ℓ are the decay angles in the rest frame of Λ_c and the center of momentum frame of τ^- and $\bar{\nu}_\tau$, respectively. χ is the dihedral angle between the decay planes.

The results will show that these observables are not very sensitive to variations in the hadronic form factors.

4.2.2 Helicity Amplitudes and the Full Angular Distribution

The decay $\Lambda_b \to \Lambda_c \tau \bar{\nu}_\tau$ proceeds via $\Lambda_b \to \Lambda_c W^*$(off-shell W) followed by $W^* \to \tau \bar{\nu}_\tau$. The full decay process is $\Lambda_b \to \Lambda_c(\to \Lambda_s \pi) W^*(\to \tau \bar{\nu}_\tau)$ (see Figure 6). Following [63] one can analyze the decay in terms of helicity amplitudes which are given by

$$H_{\lambda_2 \lambda_W} = M_\mu(\lambda_2)\varepsilon^{*\mu}(\lambda_W), \tag{46}$$

where λ_2, λ_W are the polarizations of the daughter baryon and the W-boson, respectively and M_μ is the hadronic current for $\Lambda_b \to \Lambda_c$ transition. The helicity amplitudes can be expressed in terms of form factors and the NP couplings.

$$H_{\lambda_{\Lambda_c}, \lambda_w} = H^V_{\lambda_{\Lambda_c}, \lambda_w} - H^A_{\lambda_{\Lambda_c}, \lambda_w},$$

$$
\begin{aligned}
H^V_{\frac{1}{2}0} &= (1+g_L+g_R)\frac{\sqrt{Q_-}}{\sqrt{q^2}}\Big((M_1+M_2)f_1-q^2f_2\Big),\\
H^A_{\frac{1}{2}0} &= (1+g_L-g_R)\frac{\sqrt{Q_+}}{\sqrt{q^2}}\Big((M_1-M_2)g_1+q^2g_2\Big),\\
H^V_{\frac{1}{2}1} &= (1+g_L+g_R)\sqrt{2Q_-}\Big(f_1-(M_1+M_2)f_2\Big),\\
H^A_{\frac{1}{2}1} &= (1+g_L-g_R)\sqrt{2Q_+}\Big(g_1+(M_1-M_2)g_2\Big),\\
H^V_{\frac{1}{2}t} &= (1+g_L+g_R)\frac{\sqrt{Q_+}}{\sqrt{q^2}}\Big((M_1-M_2)f_1+q^2f_3\Big),\\
H^A_{\frac{1}{2}t} &= (1+g_L-g_R)\frac{\sqrt{Q_-}}{\sqrt{q^2}}\Big((M_1+M_2)g_1-q^2g_3\Big),
\end{aligned} \tag{47}
$$

where $Q_\pm = (M_1 \pm M_2)^2 - q^2$. In the maximum recoil limit, $q^2 \to 0$, the longitudinal and scalar helicity amplitudes dominate. At minimum recoil, $q^2 \to q_{max}$ or $Q_- \to 0$, the axial transverse helicity amplitude is proportional to the axial longitudinal helicity amplitude. In other words, an s-wave dominates at the phase boundaries of $q = 0$ and $q = q_{max}$ [63].

Also,

$$
\begin{aligned}
H^V_{\lambda_{\Lambda_c},\lambda_w} &= H^V_{-\lambda_{\Lambda_c},-\lambda_w},\\
H^A_{\lambda_{\Lambda_c},\lambda_w} &= -H^A_{-\lambda_{\Lambda_c},-\lambda_w}.
\end{aligned} \tag{48}
$$

The scalar and pseudo-scalar helicities associated with the new physics scalar and pseudo-scalar interactions are

$$
\begin{aligned}
H^{SP}{}_{1/2,0} &= H^P{}_{1/2,0} + H^S{}_{1/2,0},\\
H^S{}_{1/2,0} &= g_S\frac{\sqrt{Q_+}}{m_b-m_c}\Big((M_1-M_2)f_1+q^2f_3\Big),\\
H^P{}_{1/2,0} &= -g_P\frac{\sqrt{Q_-}}{m_b+m_c}\Big((M_1+M_2)g_1-q^2g_3\Big).
\end{aligned} \tag{49}
$$

The parity related amplitudes are,

$$
\begin{aligned}
{H^S}_{\lambda_{\Lambda_c},\lambda_{NP}} &= {H^S}_{-\lambda_{\Lambda_c},-\lambda_{NP}}, \\
{H^P}_{\lambda_{\Lambda_c},\lambda_{NP}} &= -{H^P}_{-\lambda_{\Lambda_c},-\lambda_{NP}}.
\end{aligned} \tag{50}
$$

With the W boson momentum defining the positive z-axis for the decay process ($\Lambda_b \to \Lambda_c \tau^- \nu_\tau$), the twofold angular distribution[2] can be written as

$$
\begin{aligned}
\frac{d\Gamma(\Lambda_b \to \Lambda_c \tau^- \nu_\tau)}{dq^2 d(\cos\theta_l)} &= \frac{{G_F}^2 |V_{cb}|^2 q^2 |\mathbf{p}_{\Lambda_c}|}{512\pi^3 {M_1}^2} \left(1 - \frac{{m_l}^2}{q^2}\right)^2 \Big[A_1^{SM} + \frac{{m_l}^2}{q^2} A_2^{SM} + 2A_3^{NP} \\
&\quad + \frac{4m_l}{\sqrt{q^2}} A_4^{Int}\Big]
\end{aligned} \tag{51}
$$

where,

$$
\begin{aligned}
A_1^{SM} &= 2\sin^2\theta_l(|H_{1/2,0}|^2 + |H_{-1/2,0}|^2) + (1-\cos\theta_l)^2 |H_{1/2,1}|^2 \\
&\quad + (1+\cos\theta_l)^2 |H_{-1/2,-1}|^2, \\
A_2^{SM} &= 2\cos^2\theta_l(|H_{1/2,0}|^2 + |H_{-1/2,0}|^2) + \sin^2\theta_l(|H_{1/2,1}|^2 + |H_{-1/2,-1}|^2) \\
&\quad + 2(|H_{1/2,t}|^2 + |H_{-1/2,t}|^2) - 4\cos\theta_l Re[(H_{1/2,t}\ (H_{1/2,0})^* + H_{-1/2,t}\ (H_{-1/2,0})^*)], \\
A_3^{NP} &= |{H^{SP}}_{1/2,0}|^2 + |{H^{SP}}_{-1/2,0}|^2, \\
A_4^{Int} &= -\cos\theta_l Re[(H_{1/2,0}\ ({H^{SP}}_{1/2,0})^* + H_{-1/2,0}\ ({H^{SP}}_{-1/2,0})^*)] \\
&\quad + Re[(H_{1/2,t}\ ({H^{SP}}_{1/2,0})^* + H_{-1/2,t}\ ({H^{SP}}_{-1/2,0})^*)].
\end{aligned} \tag{52}
$$

${A_1}^{SM}$, ${A_2}^{SM}$, ${A_3}^{NP}$, and ${A_4}^{Int}$ are the standard model non-spin-flip, standard model spin-flip, new physics, and interference terms, respectively apart from g_L and g_R. Note ${A_1}^{SM}$, ${A_2}^{SM}$ have the same structure as the SM contributions but the helicity amplitudes in these quantities include the new physics contributions from $g_{L,R}$. θ_l is the angle of the lepton in the W rest frame with respect to

[2]In 1.1, a general derivation is provided including tensor interactions.

the W momentum.

The leptonic forward-backward asymmetry is

$$
\begin{aligned}
AFB(q^2) &= \frac{\int_0^1 \frac{d\Gamma}{dq^2 d\cos\theta_l} d\cos\theta_l - \int_{-1}^0 \frac{d\Gamma}{dq^2 d\cos\theta_l} d\cos\theta_l}{\int_0^1 \frac{d\Gamma}{dq^2 d\cos\theta_l} d\cos\theta_l + \int_{-1}^0 \frac{d\Gamma}{dq^2 d\cos\theta_l} d\cos\theta_l} \\
&= -\frac{3}{4}\frac{H_P + \frac{2{m_l}^2}{q^2} H_{SL} + \frac{2m_l}{\sqrt{q^2}} H_{L+SP}}{H_{U+L} + \frac{3}{2} H_{SP} + \frac{{m_l}^2}{2q^2}(H_{U+L} + 3H_S) + \frac{3m_l}{\sqrt{q^2}} H_{S+SP}},
\end{aligned}
\tag{53}
$$

where

$$
\begin{aligned}
H_P &= |H_{1/2,1}|^2 - |H_{-1/2,-1}|^2, \\
H_{SL} &= Re[(H_{1/2,t}\ (H_{1/2,0})^* + H_{-1/2,t}\ (H_{-1/2,0})^*)], \\
H_{L+SP} &= Re[(H_{1/2,0}\ ({H^{SP}}_{1/2,0})^* + H_{-1/2,0}\ ({H^{SP}}_{-1/2,0})^*)], \\
H_{U+L} &= |H_{1/2,1}|^2 + |H_{-1/2,-1}|^2 + |H_{1/2,0}|^2 + |H_{-1/2,0}|^2, \\
H_{SP} &= |{H^{SP}}_{1/2,0}|^2 + |{H^{SP}}_{-1/2,0}|^2, \\
H_S &= |H_{1/2,t}|^2 + |H_{-1/2,t}|^2, \\
H_{S+SP} &= Re[(H_{1/2,t}\ ({H^{SP}}_{1/2,0})^* + H_{-1/2,t}\ ({H^{SP}}_{-1/2,0})^*)].
\end{aligned}
\tag{54}
$$

After integrating out $\cos\theta_l$, the kinematic differential distribution occurs.

$$
\begin{aligned}
\frac{d\Gamma(\Lambda_b \to \Lambda_c \tau^- \nu_\tau)}{dq^2} &= \frac{{G_F}^2 |V_{cb}|^2 q^2 |\mathbf{p}_{\Lambda_c}|}{192\pi^3 {M_1}^2} \left(1 - \frac{{m_l}^2}{q^2}\right)^2 \left[B_1^{SM} + \frac{{m_l}^2}{2q^2} B_2^{SM} + \frac{3}{2} B_3^{NP} \right. \\
&\quad \left. + \frac{3m_l}{\sqrt{q^2}} B_4^{Int}\right]
\end{aligned}
\tag{55}
$$

where,

$$
\begin{aligned}
B_1^{SM} &= |H_{1/2,0}|^2 + |H_{-1/2,0}|^2 + |H_{1/2,1}|^2 + |H_{-1/2,-1}|^2, \\
B_2^{SM} &= |H_{1/2,0}|^2 + |H_{-1/2,0}|^2 + |H_{1/2,1}|^2 + |H_{-1/2,-1}|^2 \\
&\quad +3(|H_{1/2,t}|^2 + |H_{-1/2,t}|^2), \\
B_3^{NP} &= |H^{SP}_{1/2,0}|^2 + |H^{SP}_{-1/2,0}|^2, \\
B_4^{Int} &= Re[(H_{1/2,t}\ ({H^{SP}}_{1/2,0})^* + H_{-1/2,t}\ ({H^{SP}}_{-1/2,0})^*)]. \qquad (56)
\end{aligned}
$$

${B_1}^{SM}$, ${B_2}^{SM}$, ${B_3}^{NP}$, and ${B_4}^{Int}$ are the standard model non-spin-flip, standard model spin-flip, new physics, and interference terms, respectively apart from g_L and g_R. Again, ${B_1}^{SM}$, ${B_2}^{SM}$ have the same structure as the SM contributions but the helicity amplitudes in these quantities include the new physics contributions from $g_{L,R}$. The $g_{S,P}$ operators generate new terms in the angular distribution.

The angular distribution for the four body decay process $\left(\Lambda_b \to (\Lambda_s, \pi^+)\Lambda_c \tau^- \nu_\tau\right)$ can be written as below where α is the asymmetry parameter for the process $\Lambda_c \to \Lambda_s \pi^+$. θ_l is again the same leptonic angle. θ_s is the angle of Λ_s in the Λ_c rest frame with respect to the Λ_c momentum. χ is the dihedral angle between the decay planes of (τ^-, ν_τ) and (Λ_s, π^+) (see Figure 6).

$$
\begin{aligned}
\frac{d\Gamma(\Lambda_b \to (\Lambda_s, \pi^+)\Lambda_c \tau^- \nu_\tau)}{dq^2 d(\cos\theta_l) d\chi d(\cos\theta_s)} &= \frac{{G_F}^2 |V_{cb}|^2 q^2 |\mathbf{p}_{\Lambda_c}|}{2^7 (2\pi)^4 {M_1}^2} \left(1 - \frac{{m_l}^2}{q^2}\right)^2 \Big[C_1^{SM} + \frac{{m_l}^2}{q^2} C_2^{SM} + 2C_3^{NP} \\
&\quad + \frac{4m_l}{\sqrt{q^2}} C_4^{Int}\Big]\ B_{\Lambda_c \Lambda_s \pi^+} \qquad (57)
\end{aligned}
$$

where $B_{\Lambda_c\Lambda_s\pi^+}$ is the branching ratio for the process $\Lambda_c \to \Lambda_s\pi^+$ and

$$\begin{aligned}
C_1^{SM} &= 2\sin^2\theta_l\Big((1+\alpha\cos\theta_s)|H_{1/2,0}|^2+(1-\alpha\cos\theta_s)|H_{-1/2,0}|^2\Big)\\
&+(1+\cos\theta_l)^2(1-\alpha\cos\theta_s)|H_{-1/2,-1}|^2+(1-\cos\theta_l)^2(1+\alpha\cos\theta_s)|H_{1/2,1}|^2\\
&-\frac{4\alpha}{\sqrt{2}}\sin\theta_l\sin\theta_s\cos\chi\Big((1+\cos\theta_l)Re[H_{1/2,0}\ (H_{-1/2,-1})^*]\\
&\qquad\qquad +(1-\cos\theta_l)Re[H_{-1/2,0}\ (H_{1/2,1})^*]\Big)\\
&-\frac{4\alpha}{\sqrt{2}}\sin\theta_l\sin\theta_s\sin\chi\Big((1+\cos\theta_l)Im[H_{1/2,0}\ (H_{-1/2,-1})^*]\\
&\qquad\qquad -(1-\cos\theta_l)Im[H_{-1/2,0}\ (H_{1/2,1})^*]\Big).
\end{aligned}$$

$$\begin{aligned}
C_2^{SM} &= 2\cos^2\theta_l\Big((1+\alpha\cos\theta_s)|H_{1/2,0}|^2+(1-\alpha\cos\theta_s)|H_{-1/2,0}|^2\Big)\\
&+\sin^2\theta_l\Big((1+\alpha\cos\theta_s)|H_{1/2,1}|^2+(1-\alpha\cos\theta_s)|H_{-1/2,-1}|^2\Big)\\
&+\frac{2\alpha}{\sqrt{2}}\sin 2\theta_l\sin\theta_s\cos\chi\Big(Re[H_{1/2,0}\ (H_{-1/2,-1})^*]-Re[H_{-1/2,0}\ (H_{1/2,1})^*]\Big)\\
&+\frac{2\alpha}{\sqrt{2}}\sin 2\theta_l\sin\theta_s\sin\chi\Big(Im[H_{1/2,0}\ (H_{-1/2,-1})^*]+Im[H_{-1/2,0}\ (H_{1/2,1})^*]\Big)\\
&-4\cos\theta_l\Big((1+\alpha\cos\theta_s)Re[H_{1/2,t}\ (H_{1/2,0})^*]+(1-\alpha\cos\theta_s)Re[H_{-1/2,t}\ (H_{-1/2,0})^*]\Big)\\
&-\frac{4\alpha}{\sqrt{2}}\sin\theta_l\sin\theta_s\cos\chi\Big(Re[H_{1/2,t}\ (H_{-1/2,-1})^*]-Re[H_{-1/2,t}\ (H_{1/2,1})^*]\Big)\\
&-\frac{4\alpha}{\sqrt{2}}\sin\theta_l\sin\theta_s\sin\chi\Big(Im[H_{1/2,t}\ (H_{-1/2,-1})^*]+Im[H_{-1/2,t}\ (H_{1/2,1})^*]\Big)\\
&+2\Big((1+\alpha\cos\theta_s)|H_{1/2,t}|^2+(1-\alpha\cos\theta_s)|H_{-1/2,t}|^2\Big).
\end{aligned}$$

$$C_3^{NP} = (1+\alpha\cos\theta_s)|{H^{SP}}_{1/2,0}|^2+(1-\alpha\cos\theta_s)|{H^{SP}}_{-1/2,0}|^2,$$

$$\begin{aligned}
C_4^{Int} &= -\cos\theta_l\Big((1+\alpha\cos\theta_s)Re[H_{1/2,0}\ ({H^{SP}}_{1/2,0})^*]\\
&+(1-\alpha\cos\theta_s)Re[H_{-1/2,0}\ ({H^{SP}}_{-1/2,0})^*]\Big)\\
&+(1+\alpha\cos\theta_s)Re[H_{1/2,t}\ ({H^{SP}}_{1/2,0})^*]
\end{aligned}$$

$$
\begin{aligned}
&+(1-\alpha\cos\theta_s)Re[H_{-1/2,t}\ (H^{SP}{}_{-1/2,0})^*] \\
&+\frac{\alpha\ \sin\theta_l\sin\theta_s\cos\chi}{\sqrt{2}}\Big(Re[H_{-1/2,-1}\ (H^{SP}{}_{1/2,0})^*]-Re[H_{1/2,1}\ (H^{SP}{}_{-1/2,0})^*]\Big) \\
&+\frac{\alpha\ \sin\theta_l\sin\theta_s\sin\chi}{\sqrt{2}}\Big(Im[H_{-1/2,-1}\ (H^{SP}{}_{1/2,0})^*]-Im[H_{1/2,1}\ (H^{SP}{}_{-1/2,0})^*]\Big). \quad (58)
\end{aligned}
$$

${C_1}^{SM}$, ${C_2}^{SM}$, ${C_3}^{NP}$, and ${C_4}^{Int}$ are the standard model non-spin-flip, standard model spin-flip, new physics, and interference terms, respectively apart from g_L and g_R. ${C_1}^{SM}$ and ${C_2}^{SM}$ have the same structure as the SM contributions but the helicity amplitudes in these quantities include the new physics contributions from $g_{L,R}$. Several additional observables can be constructed from the angular distributions, such as polarization asymmetries and CP violating triple product asymmetries [64] which can be sensitive probes of new physics. T-odd asymmetries, which are based on triple product correlations, are vanishing due to the SM and is a promising way for searching NP in $\Lambda_b \to \Lambda_c \tau \bar{\nu}_\tau$ [65]. Note that the standard model portion of the twofold and fourfold distributions above, Eq. 51 and Eq. (84b), are the same as in a recent paper [56] apart from a minus sign in C_2^{SM} above. [3]

4.3 Numerical Results

4.3.1 New Physics Couplings

The constraints on the NP couplings from $R(D^{(*)})$ are first presented. The couplings g_S only contributes to $R(D)$, g_P only contributes to $R(D^*)$ while $g_{L,R}$ contributes to both $R(D)$ and $R(D^*)$. The details of the calculations for Figure 7 can be found in Refs. [36, 54]. Disentangling NP scalar and vector interactions in $b \to c(u)\tau\nu$ is done in Refs. [66, 67] through polarization of the final particles τ and D^* as well as decays $\Lambda_b \to \Lambda_c \tau \bar{\nu}_\tau$ and $\bar{B} \to X_c \tau^- \bar{\nu}_\tau$.

[3] In [56] Eq. (51), the minus sign is required in front of $\sin 2\theta$ on the second line in the spin-flip term as can be seen by the $d-matrix$ elements.

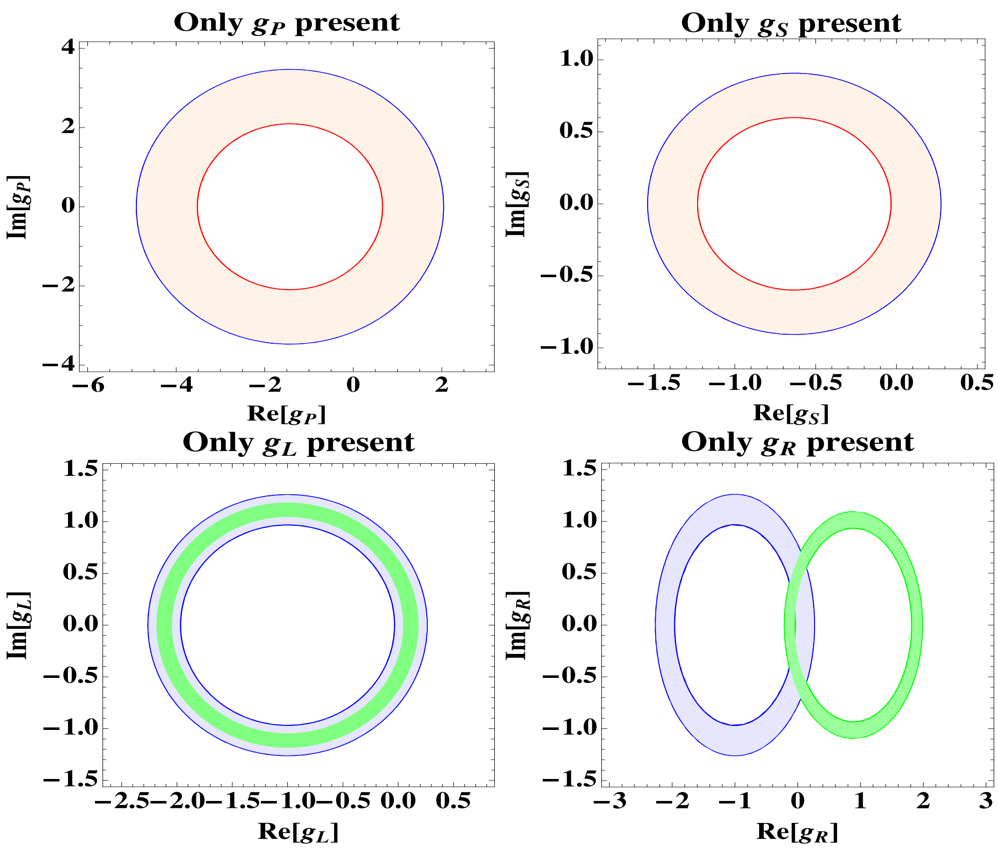

Figure 7: The figures show the constraints on the NP couplings taken one at a time at the 95% CL limit [36, 54]. When the couplings contribute to both $R(D)$ and $R(D^*)$ the green contour indicates constraint from $R(D^*)$ and blue from $R(D)$.

4.3.2 Form Factors

One of the main inputs in our calculations are the form factors. As first principle, lattice calculations of the form factors are not yet available. The form factors used here are from QCD sum rules, which is a well known approach to compute non-perturbative effects like form factors for systems with both light and heavy quarks[68, 69].

In Ref. [69], various parametrizations of the form factors are used. They are shown below ($t = q^2$).

continuum model	κ	$F_1^V(t) = f_1$	$F_2^V(t)(\text{GeV}^{-1}) = f_2$
rectangular	1	$6.66/(20.27 - t)$	$-0.21/(15.15 - t)$
rectangular	2	$8.13/(22.50 - t)$	$-0.22/(13.63 - t)$
triangular	3	$13.74/(26.68 - t)$	$-0.41/(18.65 - t)$
triangular	4	$16.17/(29.12 - t)$	$-0.45/(19.04 - t)$

Table 1: Various choices of Form Factors.

The form factors satisfy the heavy quark effective theory relations in the $m_b \to \infty$ limit[4].

$$f_1 = g_1 \quad f_2 = g_2 \quad f_3 = g_3 = f_2. \tag{59}$$

A recent paper includes lattice QCD tensor form factors [62].

4.3.3 Graphs and Results

The masses of the particles are $m_{\Lambda_b} = 5.6195$ GeV, $m_\tau = 1.77682$ GeV, $m_\mu = 0.10565837$ GeV, $m_{\lambda_{\Lambda_c}} = 2.28646$ GeV, $m_b = 4.18$ GeV, $m_c = 1.275$ GeV and $V_{cb} = 0.0414$ [80].

In the following the results are presented for $R_{\Lambda_b}, \frac{d\Gamma}{dq^2}$ and $B_{\Lambda_b}(q^2)$. For the first and third observables different models of the form factors given in Table1 are used. For the differential distribution $\frac{d\Gamma}{dq^2}$ the average result over the form factors is presented.

The prediction herein for R_{Λ_b} in the SM is shown in Table 2, for the various choices of the form factors in Table 1. The results are compared with other calculations of this quantity by other groups

[4] In [5], it was incorrectly written that $f_3 = g_3 = 0$

continuum model	1	2	3	4	Average	Ref. [56]	Ref. [57]	Ref. [70]
$R_{\Lambda_b}(SM)$	0.31	0.29	0.28	0.28	$0.29 \pm .02$	0.29	0.31	$0.34 \pm .01$

Table 2: Values of R_{Λ_b} in the SM

using different form factors. Herein, the average value for R_{Λ_b} in the SM is $R_{\Lambda_b,SM} = 0.29 \pm .02$. This agrees very well with values for this quantity obtained in Ref. [56] which uses a covariant confined quark model for the form factors, Ref. [57] which uses the form factor model in Ref. [71], and Ref. [70] which uses the lattice QCD. This confirms our earlier assertion that the ratio R_{Λ_b} is largely free from form factor uncertainties making it an excellent probe to find new physics.

Results may now be interpreted. From the structure of Eq. (55) we can make some general observations. Start with the case where only g_L is present. In this case the NP has the same structure as the SM and the SM amplitude gets modified by the factor $(1+g_L)$ [4]. Hence, if only g_L is present then

$$R_{\Lambda_b} = R^{SM}_{\Lambda_b} |1+g_L|^2. \tag{60}$$

Therefore in this case $R_{\Lambda_b} \geq R^{SM}_{\Lambda_b}$ and one finds the range of R_{Λ_b} to be $0.40 - 0.27$. The shape of the differential distribution $\frac{d\Gamma}{dq^2}$ is the same as the SM. In the left-side figures of Figure 8 the plots are shown for $R_{\Lambda_b}, \frac{d\Gamma}{dq^2}$ and $B_{\Lambda_b}(q^2)$ when only g_L is present. Then consider the case when only g_R is present. If only g_R is present then from Eq. (86),

$$\begin{aligned} H^V_{\lambda_{\Lambda_c},\lambda_w} &= (1+g_R)\left[H^V_{\lambda_{\Lambda_c},\lambda_w}\right]_{SM}, \\ H^A_{\lambda_{\Lambda_c},\lambda_w} &= (1-g_R)\left[H^A_{\lambda_{\Lambda_c},\lambda_w}\right]_{SM}. \end{aligned} \tag{61}$$

In this case no clear relation between R_{Λ_b} and $R^{SM}_{\Lambda_b}$ can be obtained. However, for the allowed g_R couplings R_{Λ_b} is greater than the SM value and is in the range $0.42 - 0.30$. The shape of the differential distribution $\frac{d\Gamma}{dq^2}$ is the same as the SM. In the right-side figures of Figure 8 the plots are shown for $R_{\Lambda_b}, \frac{d\Gamma}{dq^2}$ and $B_{\Lambda_b}(q^2)$ when only g_R is present.

Now consider the case when only $g_{S,P}$ are present. Using Eq. (55) and Eq. (88) one can write,

$$\begin{aligned} R_{\Lambda_b} &= R^{SM}_{\Lambda_b} + |g_P|^2 A_P + 2Re(g_P) B_P, \\ R_{\Lambda_b} &= R^{SM}_{\Lambda_b} + |g_S|^2 A_S + 2Re(g_S) B_S. \end{aligned} \tag{62}$$

The quantities $A_{S,P}$ and $B_{S,P}$ depend on masses and form factors and they are positive. Hence for $Re(g_P) \geq 0$ or $Re(g_S) \geq 0$, R_{Λ_b} is always greater than or equal to $R^{SM}_{\Lambda_b}$. But, for $Re(g_P) < 0$ or $Re(g_S) < 0$, R_{Λ_b} can be less than the SM value. However, given the constraints on $g_{S,P}$ one can make R_{Λ_b} only slightly less than the SM value. One finds R_{Λ_b} is in the range $0.34 - 0.28$ when only g_S is present and in the range $0.39 - 0.31$ when only g_P is present. 13 TeV LHC data rules out a pseudoscalar, A, explaining $R(D^{(*)})$ and $(g-2)_\mu$ by a FCNC $t \to A\ c$ [72]

In Figure 9 we show the plots for R_{Λ_b},$\frac{d\Gamma}{dq^2}$ and $B_{\Lambda_b}(q^2)$ when only g_P is present. The shape of the differential distribution $\frac{d\Gamma}{dq^2}$ can be different from the SM. In Figure 10 the plots are shown for R_{Λ_b},$\frac{d\Gamma}{dq^2}$ and $B_{\Lambda_b}(q^2)$ when only g_S is present. In this case also the shape of the differential distribution $\frac{d\Gamma}{dq^2}$ can be different from the SM. In Table 3 the minimum and maximum values for the averaged R_{Λ_b} are given with the corresponding NP couplings.

NP	$R_{\Lambda_b,min}$	$R_{\Lambda_b,max}$
Only g_L	0.27, $g_L = -0.0214\ i$	0.40, $g_L = 0.182\ i$
Only g_R	0.30, $g_R = -0.0386 + 0.166\ i$	0.42, $g_R = 0.0472 - 0.692\ i$
Only g_S	0.28, $g_S = -0.0352$	0.34, $g_S = .270$
Only g_P	0.31, $g_P = 0.684$	0.39, $g_P = -4.882$

Table 3: Minimum and Maximum values for the averaged R_{Λ_b}.

There has been recent work following our paper using leptoquarks [45]. A one TeV scalar LQ transforming as ($\mathbf{3}$, $\mathbf{1}$,-$\frac{1}{3}$) under the SM gauge group may address the R_K, $R(D^{(*)})$, and $(g-2)_\mu$ anomalies [73]. One vector LQ transforming as ($\mathbf{3}$, $\mathbf{3}$,$\frac{2}{3}$) under the SM gauge group may address R_K, $R(D^{(*)})$, and the angular observable P_5' in $\bar{B} \to \bar{K}^* \mu^+ \mu^-$ [74]. $\Lambda_b \to \Lambda_c \tau \bar{\nu}_\tau$ has been considered in the literature since it has the same quark transition as $\bar{B} \to D^{*+} \tau^- \bar{\nu}_\tau$. The two scenarios of using a scalar LQ or vector LQ give similar enhancements for the ratio $R_{\lambda_{\Lambda_c}}$ and the branching fraction $B(\Lambda_b \to \Lambda_c \tau \bar{\nu}_\tau)$ [75]. Also for the latter Λ_b decay, these two scenarios coincide nearly with the SM predictions of lepton forward-backward asymmetry and longitudinal polarizations of λ_{Λ_c} and τ. Li et al. [75] conclude it is difficult to distinguish between these two scenarios in $\Lambda_b \to \Lambda_c \tau \bar{\nu}_\tau$.

Another pursuit in the recent literature has been τ identification. τ identification and detection systematics are largely canceled by introducing the observable $R^{\tau}_{D^{(*)}} = \dfrac{R(D^{(*)})}{\mathscr{B}(B^- \to \tau^- \bar{\nu}_\tau)}$. According to BaBar and Belle, notwithstanding the uncertainty in the parameter V_{ub}, the new observables are consistent with the SM [76]. With a more precise measurement of V_{ub}, these new observables can further constrain the NP scalar and vector parameter space for $R(D^{(*)})$ and $\mathscr{B}(B^- \to \tau^- \bar{\nu}_\tau)$ [77]. Finally, Ref. [78] extends the work herein on the NP implications for $\Lambda_b \to \Lambda_c \ell \bar{\nu}_\ell$ by performing a combined analysis of the latter and $\Lambda_b \to p \ell \bar{\nu}_\ell$ and including the anomaly $R^{\ell}_{\pi} = \dfrac{\tau_{B^0}}{\tau_{B^-}} \dfrac{\mathscr{B}(B^- \to \tau^- \bar{\nu}_\tau)}{\mathscr{B}(B^0 \to \pi^+ \ell^- \bar{\nu}_\ell)}$. The latter ratio has more than a 2σ discrepancy with respect to the standard model.

4.4 Conclusion of Lepton Flavor Non-Universality for Λ_b Decay

The SM and NP predictions are calculated for the decay $\Lambda_b \to \Lambda_c \tau \bar{\nu}_\tau$. Motivation to study this decay comes from the recent hints of lepton flavor non-universality observed by the BaBar Collaboration [50, 51], Belle [52], and LHCb [53] in $R(D^{(*)}) \equiv \frac{\mathscr{B}(\bar{B} \to D^{(*)+} \tau^- \bar{\nu}_\tau)}{\mathscr{B}(\bar{B} \to D^{(*)+} \ell^- \bar{\nu}_\ell)}$ $(\ell = e, \mu)$. A general parametrization of the NP operators has been used while the new physics couplings were fixed from the experimental measurements of $R(D)$ and $R(D^*)$. Then predictions followed for R_{Λ_b} (Eq. (44)), $\frac{d\Gamma}{dq^2}$, and $B_{\Lambda_b}(q^2)$ (Eq. (45)) for the various NP couplings taken one at a time. It has been found that $g_{L,R}$ couplings gave predictions larger than the SM values for all the three observables. Also, the g_P couplings produce larger effects than the g_S couplings. Lastly, the general formula for the various angular distributions in the presence of NP operators has been given.

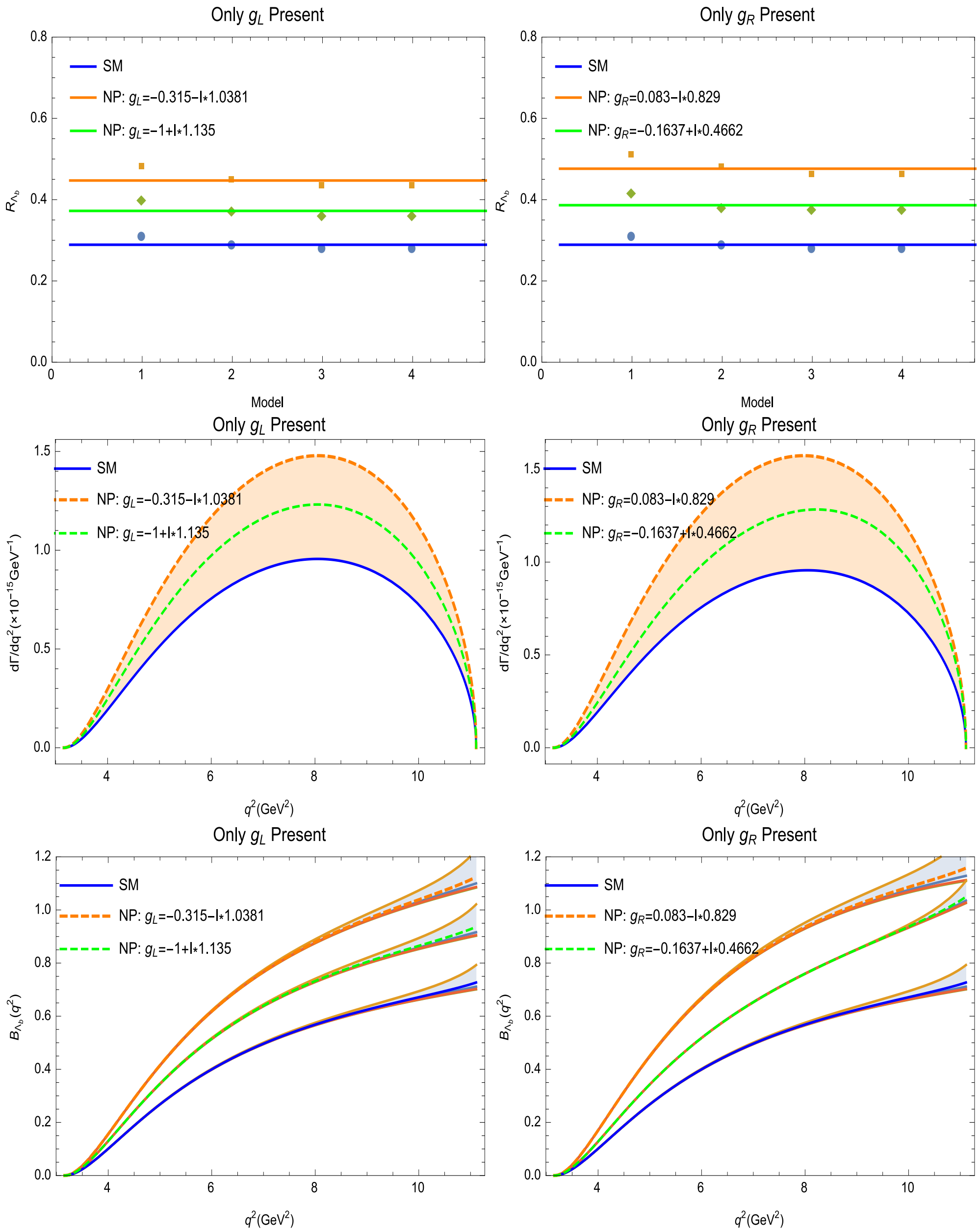

Figure 8: The graphs on the left-side (right-side) show the compared results between the standard model and new physics with only g_L (g_R) present. The top and bottom row of graphs depict $R_{\Lambda_b} = \frac{\mathscr{B}(\Lambda_b \to \Lambda_c \tau \bar{\nu}_\tau)}{\mathscr{B}(\Lambda_b \to \Lambda_c \ell \bar{\nu}_\ell)}$ and the ratio of differential distributions $B_{\Lambda_b}(q^2) = \frac{\frac{d\Gamma}{dq^2}(\Lambda_b \to \Lambda_c \tau \bar{\nu}_\tau)}{\frac{d\Gamma}{dq^2}(\Lambda_b \to \Lambda_c \ell \bar{\nu}_\ell)}$ as a function of q^2, respectively for the various form factors in Table 1. The middle graphs depict the average differential decay rate with respect to q^2 for the process $\Lambda_b \to \Lambda_c \tau \bar{\nu}_\tau$. Some representative values of the couplings have been chosen.

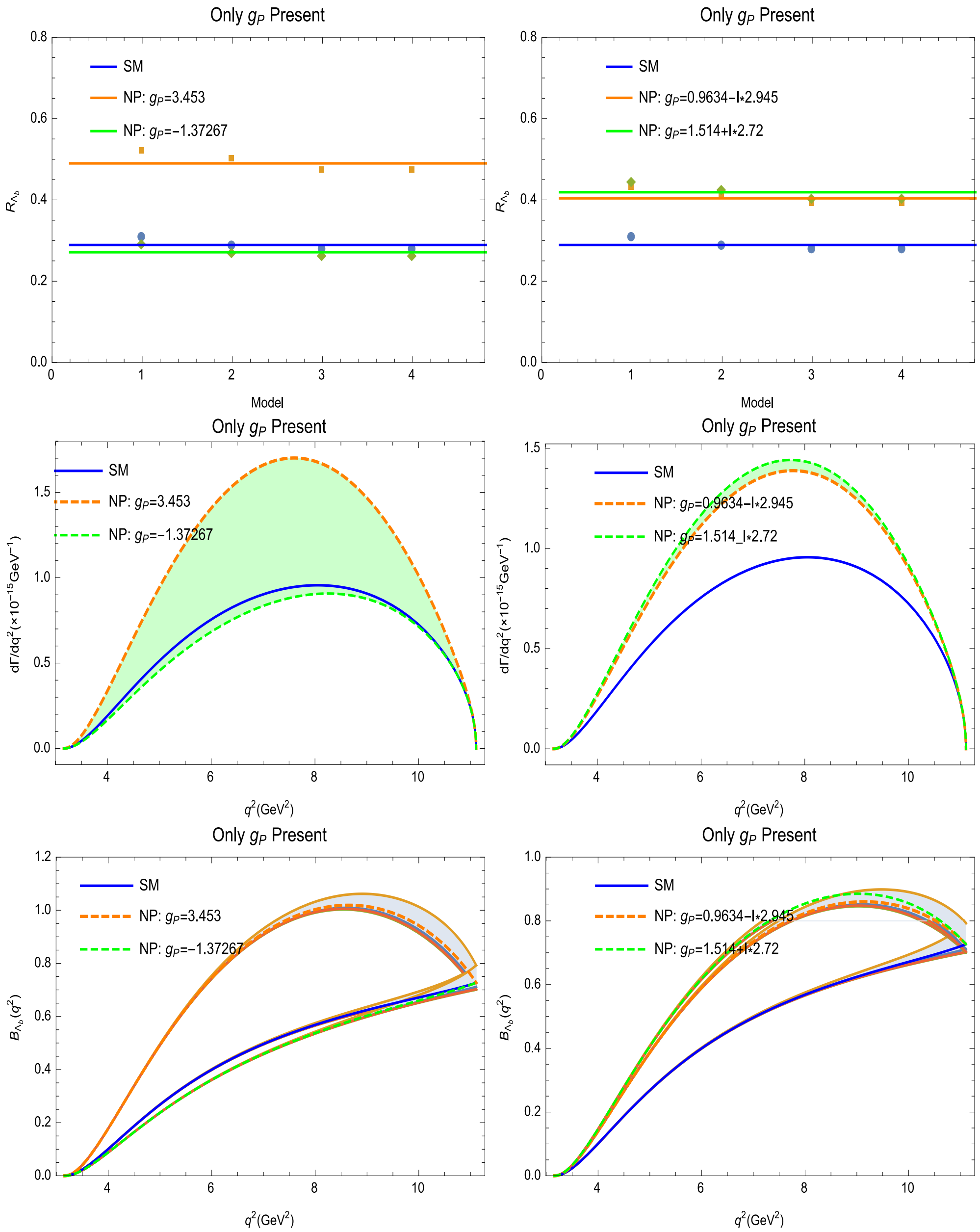

Figure 9: The figures show the compared results between the standard model and new physics with only g_P present. The top and bottom row of graphs depict $R_{\Lambda_b} = \frac{\mathscr{B}(\Lambda_b\to\Lambda_c\tau\bar{\nu}_\tau)}{\mathscr{B}(\Lambda_b\to\Lambda_c\ell\bar{\nu}_\ell)}$ and the ratio of differential distributions $B_{\Lambda_b}(q^2) = \frac{\frac{d\Gamma}{dq^2}(\Lambda_b\to\Lambda_c\tau\bar{\nu}_\tau)}{\frac{d\Gamma}{dq^2}(\Lambda_b\to\Lambda_c\ell\bar{\nu}_\ell)}$ as a function of q^2, respectively for the various form factors in Table 1. The middle graphs depict the average differential decay rate with respect to q^2 for the process $\Lambda_b \to \Lambda_c\tau\bar{\nu}_\tau$. Some representative values of the couplings have been chosen.

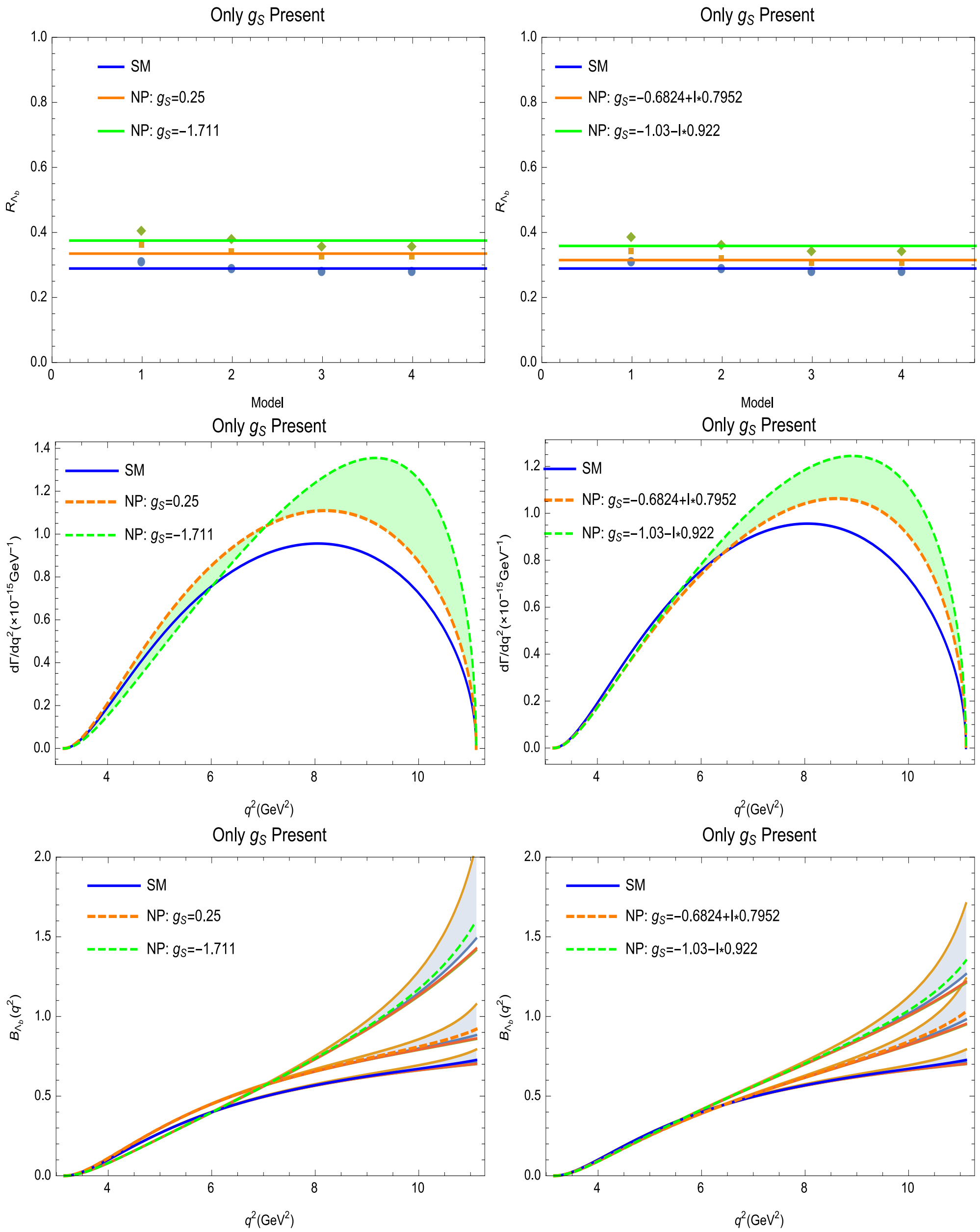

Figure 10: The figures show the compared results between the standard model and new physics with only g_S present. The top and bottom row of graphs depict $R_{\Lambda_b} = \frac{\mathscr{B}(\Lambda_b\to\Lambda_c\tau\bar{\nu}_\tau)}{\mathscr{B}(\Lambda_b\to\Lambda_c\ell\bar{\nu}_\ell)}$ and the ratio of differential distributions $B_{\Lambda_b}(q^2) = \frac{\frac{d\Gamma}{dq^2}(\Lambda_b\to\Lambda_c\tau\bar{\nu}_\tau)}{\frac{d\Gamma}{dq^2}(\Lambda_b\to\Lambda_c\ell\bar{\nu}_\ell)}$ as a function of q^2, respectively for the various form factors in Table 1. The middle graphs depict the average differential decay rate with respect to q^2 for the process $\Lambda_b \to \Lambda_c\tau\bar{\nu}_\tau$. Some representative values of the couplings have been chosen.

CHAPTER 5: SEARCHING FOR A CHARGED HIGGS

5.1 Introduction

In 2012 ATLAS and CMS discovered the standard model Higgs boson in ZZ^* and $\gamma\gamma$ final states [79]. This discovery corroborates spontaneous symmetry breaking and the generation of mass for the fermions and weak bosons. Yet, there is no principle forbidding other Higgs-like scalars. Additional Higgs-like scalars appear in many extensions of the standard model (SM) such as supersymmetry that requires at least two Higgs doublets. Herein, the focus is on a charged Higgs, $H^{\pm}$, from the two Higgs Doublet Model (2HDM) of the Type II and leptophilic (L2HDM) variety.

There is a lower limit of 80 GeV for the charged Higgs mass at 95 % CL [80] coming from LEP searches in $e^+e^- \to H^+H^-$. Older limits give charged Higgs mass greater than 92 GeV at 95 % CL [81]. Note that one can also put limits on the charged Higgs mass from the $B \to X_s\gamma$ measurement [82], but in principle there can be additional contributions to this decay in which case the limits do not apply. Also if the charged Higgs has suppressed coupling to quarks then this charged Higgs mass limit is weakened.

In the era of LHC there have been searches for the charged Higgs which can be turned into exclusion regions for the parameters of a specific model. At ATLAS, in top quark-pair production, the likelihood of a charged Higgs has been constrained in the mode $t \to b(\tau^+\nu_\tau)H^+$ to $\mathscr{B}(t \to bH^+) \times \mathscr{B}(H^+ \to \tau^+\nu_\tau) < 1\%$ for 80 GeV$< M_{H^\pm} <$ 160 GeV while the standard model is in agreement with the data [83]. For this search, most of tanβ values above one are ruled out in the latter mass range under different scenarios of MSSM. In a vector-boson fusion produced $H^{\pm}$, the direct decay $H^{\pm} \to W^{\pm}Z$ is not observed for 200 GeV$< M_{H^\pm} <$ 1000 GeV [84]. The latter charged Higgs mass range has also been searched in associated top quark production without yielding promising results [85]. Recent results from CMS have also set similar upper limits on a charged Higgs branching ratios and production cross sections [86].

In this work the main focus is the effect of a charged Higgs in the decay $H \to W^-W^+(\text{or } H^+) \to$ 4 leptons. At the standard model value of about 125 GeV, the mode $H \to W^-W^+$ provides the second highest branching ratio among standard model Higgs decays, though missing transverse momentum of the neutrinos and controlling for the background are challenges in the leptonic decays of $W\pm$ and $H^\pm$. The four-fold distribution for the above process is provided via two-Higgs-doublet models (2HDM's) of the leptophilic (L2HDM) and Type II variety. Assume the mass of the charged Higgs to be greater than the W boson mass. To be specific, W^- and W^+ are assumed on-shell and off-shell, respectively and so channels H^-W^+ and H^-H^+ are not included in the process. The other case where W^+ and W^- are assumed on-shell and off-shell, respectively, can be treated in a similar manner.

The 2HDM models are an extension of the standard model Higgs doublet, and include the standard model Higgs along with an usually heavier CP even version plus a CP odd scalar and two charged Higgs. To avoid a flavor changing neutral current (FCNC) from the Higgs sector a discrete symmetry is imposed which then leads to various types of 2HDM models. One of the popular 2HDM is the type II model which cannot be completely fermiophobic (unlike Type I), does not have FCNC's (unlike Type III and triplet Higgs models) [87], and has the Yukawa couplings of the Minimal Supersymmetric standard model (MSSM). Others have provided thorough reviews of 2HDM's [88, 89, 90].

The sections are ordered as follows. In section 5.2, for the standard model process $H \to W^-(\to \tau^-\bar{\nu}_\tau)W^+(\to \tau^+\nu_\tau)$, an alternative calculation of the general four-fold distribution with respect to the literature is given via expansion by helicity amplitudes. Others have given formulas for this decay or a similar decay via the helicity formalism (see [91, 92, 93]), but either ignore mass or new physics terms. Section 5.3 provides general remarks about the Type II 2HDM and L2HDM. In section 5.3.3, the charged Higgs is added to the decay process via the 2HDM [5]. Plots of kinematic

[5] The situation here is similar to B decays to a pair of vector mesons with scalar backgrounds [94].

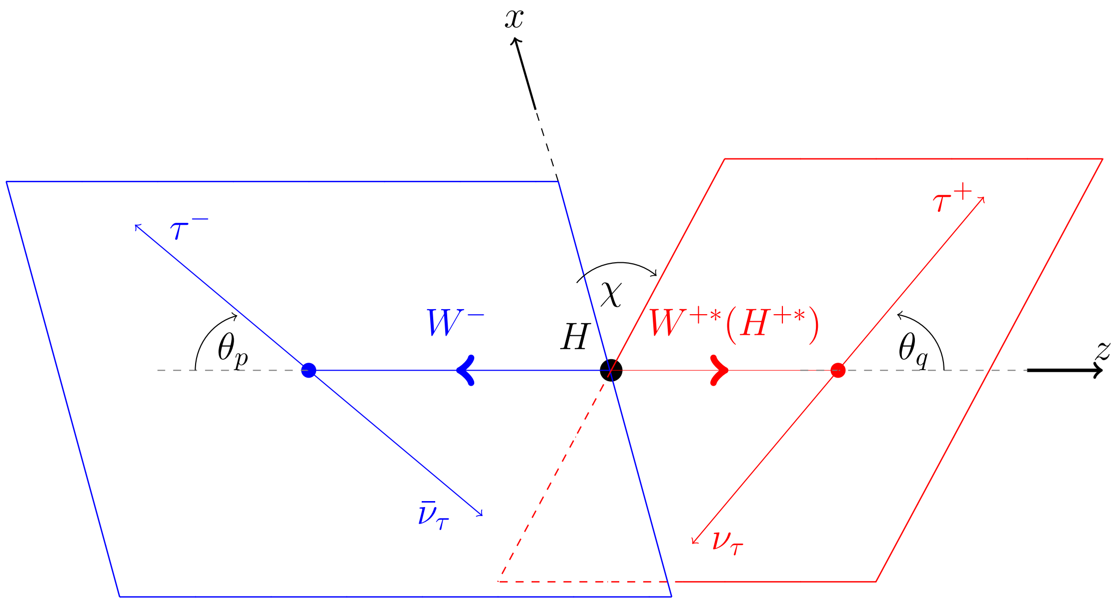

Figure 11: Four body decay of H: $H \to W^{+*}(or\ H^{+*}), W^- \to (\tau^+, \nu_\tau), (\tau^-, \bar{\nu}_\tau)$. θ_q and θ_p are the decay angles in the center of momentum frame of τ^+ and ν_τ and the rest frame of W^-, respectively. χ is the dihedral angle between the decay planes. In section 5.3.3, the charged Higgs, H^+, is added.

and dihedral distributions are provided for various possible masses for the charged Higgs. Lastly, a MadGraph 5 simulation is performed of the dihedral distribution.

5.2 Standard Model Decay

The process $H \to W^{+*}(\to \tau^+\nu_\tau)W^-(\to \tau^-\bar{\nu}_\tau)$ is illustrated in Figure 11. W^- and W^{+*} are on-shell and off-shell W bosons, respectively. The positive z-axis points in the direction of W^+'s momentum. θ_p is the polar angle of τ^- in W^-'s rest frame. Since W^{+*} is off-shell, θ_q is the polar angle of τ^+ in the center of mass frame of τ^+ and ν_τ. χ is the dihedral angle between the decay planes of $W^- \to \tau^-\bar{\nu}_\tau$ and $W^{+*} \to \tau^+\nu_\tau$. The four-fold distribution is calculated below by the density matrix method, including the lepton mass. In $H \to ZZ^* \to \ell_1\ell_2\ell_3\ell_4$, leptonic mass effects are not as pronounced as in $H \to W^{+*}(\to \tau^+\nu_\tau)W^-(\to \tau^-\bar{\nu}_\tau)$ [93]. Helicities, polarization vectors, and four momenta are defined as follows.

- Helicities of bosons: $\quad \lambda_H = \lambda_{W^+} - \lambda_{W^-} = 0, \quad \lambda_{W^+} = 0, \pm 1, t, \quad \lambda_{W^-} = 0, \pm 1$

- Lepton helicities: $\lambda_\ell = \pm\frac{1}{2},\ \ell = \tau^+, \tau^-$

- Four-momenta of W^{+*}, W^-: q, p

- Polarization vectors
  of W^{+*} boson: $\varepsilon_1^\mu(\pm 1) = \frac{1}{\sqrt{2}}(0; \mp 1, -i, 0)$, $\varepsilon_1^\mu(0) = \frac{1}{\sqrt{q^2}}(|\vec{q}\,|; 0, 0, q_0)$,

  $$\varepsilon_1^\mu(t) = \frac{1}{\sqrt{q^2}}(q_0; 0, 0, |\vec{q}\,|),$$

- Polarization vectors
  of W^- boson: $\varepsilon_2^\mu(\pm 1) = \frac{1}{\sqrt{2}}(0; \pm 1, -i, 0)$, $\varepsilon_2^\mu(0) = \frac{1}{M_W}(|\vec{q}\,|; 0, 0, -p_0)$

The four-fold angular distribution is

$$\frac{d\Gamma\Big(H \to W^{+*}(\to \tau^+ \nu_\tau) W^-(\to \tau^- \bar{\nu}_\tau)\Big)}{dq^2 d(\cos\theta_q) d(\cos\theta_p) d\chi} \tag{63}$$

$$= \frac{Br_{W\tau\nu_\tau}}{(2\pi)^4} \frac{(1-\frac{m^2}{q^2})|\vec{q}|}{2^5 M_H^2} \sum_{\lambda_{\tau^-},\lambda_{\tau^+}} \Big| \sum_{s_{W^+},\ \lambda_{W^\pm}} (-1+\frac{q^2}{M_W^2})^{1-s_{W^+}}\ A_{\lambda_{W^+}\lambda_{W^-}} B^{\lambda_{W^+}}_{\lambda_{\tau^+},\lambda_{\nu_\tau}} C^{\lambda_{W^-}}_{\lambda_{\tau^-},\lambda_{\bar{\nu}_\tau}} \Big|^2.$$

$Br_{W\tau\nu_\tau}$ is the $W^- \to \tau^- \bar{\nu}_\tau$ branching ratio. Integrating with respect to χ and $\cos\theta_p$ reduces Eq. (63) into the three-body decay $H \to \tau^+ \nu_\tau W^-$. When $s_{W^+} = 0$, the time helicity, $\lambda_{W^+} = t$, occurs. For the latter case, $-1 + \frac{q^2}{M_W^2}$ appears in Eq. (63) [93]. When $s_{W^+} = 1$, $\lambda_{W^+} = 0, \pm$.

The partial amplitudes are written as follows.

$$A_{\lambda_{W^+}\lambda_{W^-}} = igM_W\ \varepsilon_1^{\mu*}(\lambda_{W^+}) \varepsilon_2^{\nu*}(\lambda_{W^-})\, g_{\mu\nu} \tag{64a}$$

$$B^{\lambda_{W^+}}_{\lambda_{\tau^+},\lambda_{\nu_\tau}} = \frac{-ig}{2\sqrt{2}}\ \bar{u}(p_1, \lambda_{\nu_\tau}) \frac{i\not{\varepsilon}_1(\lambda_{W^+})}{(q^2 - M_W^2 + iM_W\Gamma_W)} (1-\gamma_5) v(p_2, \lambda_{\tau^+}) \tag{64b}$$

$$C^{\lambda_{W^-}}_{\lambda_{\tau^-},\lambda_{\bar{\nu}_\tau}} = \frac{-ig}{2\sqrt{2}}\ \bar{u}(p_3, \lambda_{\tau^-}) \frac{i\not{\varepsilon}_2(\lambda_{W^-})}{M_W\Gamma_W} (1-\gamma_5) v(p_4, \lambda_{\bar{\nu}_\tau}). \tag{64c}$$

$A_{\lambda_{W^+}\lambda_{W^-}}$, $B^{\lambda_{W^+}}_{\lambda_{\tau^+},\lambda_{\nu_\tau}}$, and $C^{\lambda_{W^-}}_{\lambda_{\tau^-},\lambda_{\bar{\nu}_\tau}}$ above are the amplitudes for $H \to W^{+*}W^-$, $W^{+*} \to \tau^+\nu_\tau$, and $W^- \to \tau^-\bar{\nu}_\tau$, respectively. The leptonic amplitudes (Eqs. 64b and 64c) are written in Appendix 2.1. The general four-fold distribution is provided in Appendix 2.2. Therein, NP terms such as triple products and parity violating terms are included.

If desired $A^{\lambda_{W^-}\lambda_{W^+}}$ might be defined in the transversity basis as

$$A_L = A^{0,0}, \quad A_\parallel = \frac{A^{+,+} + A^{-,-}}{\sqrt{2}}, \quad A_\perp = \frac{A^{+,+} - A^{-,-}}{\sqrt{2}}, \quad A_t = A^{0,t}.$$

Herein, this redefinition is not used. Normalized with respect to igM_W, the helicity amplitudes are written as

$$A_{t0} = \frac{M_H|\vec{q}|}{\sqrt{q^2}M_W}, \quad A_{00} = \frac{q \cdot p}{\sqrt{q^2}M_W}, \quad A_{++} = A_{--} = 1.$$

Notice the HWW vertex may be generalized to include both CP even and CP odd terms [91, 92] as follows,

$$V^{\mu\nu}_{HWW} \quad = \quad igM_W g^{\mu\nu} \to igM_W(a_1 g^{\mu\nu} + a_2 P^\mu P^\nu + i a_3 \varepsilon^{\mu\nu\alpha\beta} q_{1\alpha} q_{2\beta}), \qquad (65)$$

where a_3 represents the CP odd triple product term [95]. HWW is only CP even if $a_3 = 0$. Although an admixture may be possible, pure CP odd is disfavored [96]. The standard model occurs for $a_1 = 1, a_2 = a_3 = 0$.

Dropping NP terms, the SM four-fold distribution may written from Eq. (105). It consists of non-spin flip and spin flip terms. For massless leptons, the spin flip terms, the terms with leptonic mass, become identically zero. After integrating Eq. (105) over the angles, the SM differential distributions below are obtained.

The dihedral distribution is

$$\frac{d\Gamma^{SM}}{dq^2 d\chi} = f(q^2)\,(\gamma_1 + \gamma_2), \qquad (66a)$$

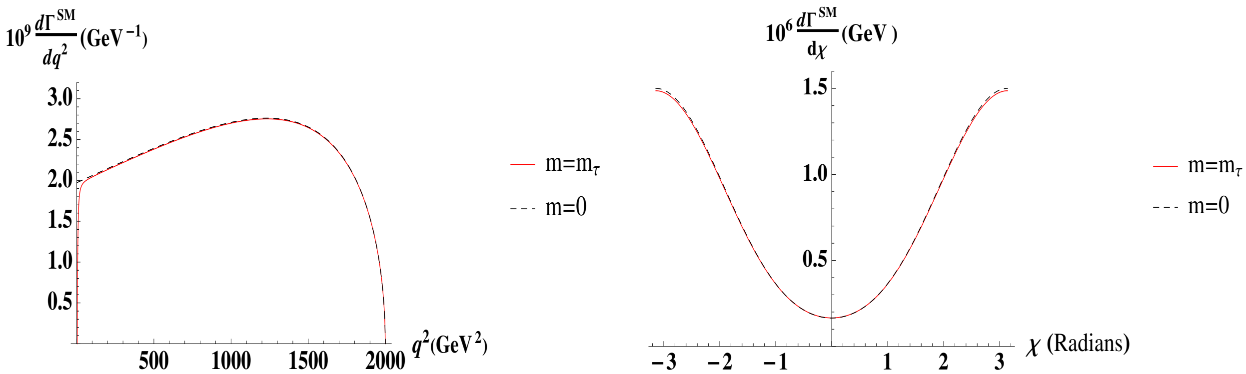

Figure 12: The above two plots show the kinematic and dihedral distributions for the SM process $H \to W^{+*}(\to \tau^+ \nu_\tau)W^-(\to \tau^- \bar{\nu}_\tau)$. The black dashed curve is for massless leptons and the red curve is for $m = m_\tau$.

where

$$
\begin{aligned}
\gamma_1 &= 6|A_{t0}|^2\, F_s^2\, \varepsilon_q\left(\frac{\varepsilon_p}{2}+1\right), \\
\gamma_2 &= 4|A_{00}|^2\left(\frac{\varepsilon_p}{2}+\frac{\varepsilon_p\varepsilon_q}{4}+\frac{\varepsilon_q}{2}+1\right) \\
&\quad +4|A_{--}|^2\left(\frac{\varepsilon_p}{2}+\frac{\varepsilon_p\varepsilon_q}{4}+\frac{\varepsilon_q}{2}+1\right) \\
&\quad +4|A_{++}|^2\left(\frac{\varepsilon_p}{2}+\frac{\varepsilon_p\varepsilon_q}{4}+\frac{\varepsilon_q}{2}+1\right) \\
&\quad -\frac{9}{16}\pi^2\,\mathrm{Re}\left[\mathrm{A}_{--}\mathrm{A}_{00}^*\right]\cos\chi \\
&\quad -\frac{9}{16}\pi^2\,\mathrm{Re}\left[\mathrm{A}_{++}\mathrm{A}_{00}^*\right]\cos\chi \\
&\quad +2\mathrm{Re}\left[\mathrm{A}_{++}\mathrm{A}_{--}^*\right]\cos 2\chi\,\left(1-\varepsilon_\mathrm{p}-\varepsilon_\mathrm{q}+\varepsilon_\mathrm{p}\varepsilon_\mathrm{q}\right).
\end{aligned} \tag{66b}
$$

See Eq. (106) in Appendix 2.2 for definitions of $f(q^2), \varepsilon, \varepsilon_q, F_s$.

The kinematic differential distribution is

$$
\frac{d\Gamma^{SM}}{dq^2} = 8\pi f(q^2)\,(\beta_1+\beta_2), \tag{67a}
$$

where

$$\begin{aligned}
\beta_1 &= \frac{3}{2}|A_{t0}|^2\, F_s^2\, \varepsilon_q\Big(\frac{\varepsilon_p}{2}+1\Big), \\
\beta_2 &= |A_{00}|^2\Big(\frac{\varepsilon_p}{2}+\frac{\varepsilon_p\varepsilon_q}{4}+\frac{\varepsilon_q}{2}+1\Big) \\
&\quad +|A_{--}|^2\Big(\frac{\varepsilon_p}{2}+\frac{\varepsilon_p\varepsilon_q}{4}+\frac{\varepsilon_q}{2}+1\Big) \\
&\quad +|A_{++}|^2\Big(\frac{\varepsilon_p}{2}+\frac{\varepsilon_p\varepsilon_q}{4}+\frac{\varepsilon_q}{2}+1\Big). \qquad (67b)
\end{aligned}$$

Figure 12 shows the kinematic and dihedral distributions for a massless τ and τ's mass. The curves are the same except for about $q^2 < 100$ GeV^2 and $\chi = \pm\pi$. Apart from the scale, the dihedral distribution is interpreted as number of events versus the dihedral angle in the Higgs rest frame. Therefore, the events peak at $\chi = \pm\pi$, which is when τ^+ and τ^- may be back to back. The events are minimized at $\chi = 0$.

5.3 Type II 2HDM and L2HDM

5.3.1 Type II 2HDM

In the Type II 2HDM model, Φ_1 and Φ_2 designate the two Higgs doublets. One doublet couples to leptons and down-type quarks whereas the other doublet couples to up-type quarks. Acquiring a vev, ($\upsilon_{1,2}$), the doublets are written as

$$\Phi_1 = \begin{pmatrix} \Phi_1^+ \\ \dfrac{h_1+\upsilon_1+ig_1}{\sqrt{2}} \end{pmatrix};\ \Phi_2 = \begin{pmatrix} \Phi_2^+ \\ \dfrac{h_2+\upsilon_2+ig_2}{\sqrt{2}} \end{pmatrix}. \qquad (68)$$

The Type II 2HDM Lagrangian is $\mathscr{L}^{\Phi}$ = $\mathscr{L}_{kin}$ - $\mathscr{L}_Y^{leptons}$ - V. The kinetic Lagrangian, Yukawa Lagrangian, and potential are

$$\mathscr{L}_{kin} = (D_\mu\Phi_1)^+(D^\mu\Phi_1)+(D_\mu\Phi_2)^+(D^\mu\Phi_2),$$

$$-\mathscr{L}_Y = \eta_{ij}^{E,0}\ \bar{\ell}_{iL}^0\Phi_1 E_{jR}^0+\eta_{ij}^{D,0}\ Q_{iL}^0\Phi_1 D_{jR}^0+\xi_{ij}^{U,0}\ \bar{Q}_{iL}^0\tilde{\Phi}_2 U_{jR}^0+h.c.$$

$$\begin{aligned} V &= -\mu_1^2\ |\Phi_1|^2-\mu_2^2\ |\Phi_2|^2-\mu_3^2\ Re(\Phi_1^+\Phi_2)+\lambda_1\ |\Phi_1|^4+\lambda_2\ |\Phi_2|^4 \\ &\quad +\lambda_3\ ([Re(\Phi_1^+\Phi_2)]^2+[Im(\Phi_1^+\Phi_2)]^2)+\lambda_5\ |\Phi_1|^2|\Phi_2|^2\ . \end{aligned} \tag{69}$$

$\bar{\ell}_{iL}^0$ and E_{jR}^0 are the left-handed doublet and right-handed singlet of leptons, respectively. η is a non-diagonal 3x3 matrix. Not being involved in $W^\pm$ and $H^\pm$ decays in this section, quarks are not discussed. Notice FCNC's would occur if $\xi_{ij}^{E,0}\ \bar{\ell}_{iL}^0\Phi_2 E_{jR}^0$ was added to $\mathscr{L}_Y$ since η and ξ may not be simultaneously diagonalized [88][6].

The potential above, V, is CP conserving. Unlike the standard model case, there is freedom in choosing the potential. Having invariance under Z_2 symmetry ($\Phi_1,\Phi_2 \rightarrow \Phi_1,-\Phi_2$) or global symmetry ($\Phi_2 \rightarrow e^{i\phi}\Phi_2$) allows for the minimum potential to be CP invariant [98].

The full Lagrangian is $\mathscr{L} = \mathscr{L}^{leptons}+\mathscr{L}^{bosons}+\mathscr{L}^{\Phi}$. Under electroweak symmetry breaking two charge-neutral vacuum expectation values (υ_1,υ_2) occur.

$$<\Phi_1>=\begin{pmatrix}0\\ \frac{\upsilon_1}{\sqrt{2}}\end{pmatrix};<\Phi_2>=\begin{pmatrix}0\\ \frac{\upsilon_2}{\sqrt{2}}\end{pmatrix}. \tag{70}$$

The vevs are constrained by the standard model expectation $\upsilon^2\equiv\upsilon_1^2+\upsilon_2^2=246\ \mathrm{GeV}^2$. After SSB, masses for the Higgs bosons are generated and all the vertices for the interactions can be written down [89, 99]. The physical mass eigenstates are related to the gauge eigenstates as follows where

[6] Alternate mechanism to avoid FCNC in 2HDM is discussed in Ref. [97].

α is the mixing angle between the light and heavy CP-even Higgs and $\tan\beta \equiv \frac{\upsilon_2}{\upsilon_1}$.

$$\begin{pmatrix} \cos\beta & \sin\beta \\ -\sin\beta & \cos\beta \end{pmatrix} \begin{pmatrix} \phi_1^+ \\ \phi_2^+ \end{pmatrix} = \begin{pmatrix} G^+ \\ H^+ \end{pmatrix}.$$

$$\begin{pmatrix} \cos\alpha & \sin\alpha \\ -\sin\alpha & \cos\alpha \end{pmatrix} \begin{pmatrix} h_1 \\ h_2 \end{pmatrix} = \begin{pmatrix} H^0 \\ h^0 \end{pmatrix}.$$

$$\begin{pmatrix} \cos\beta & \sin\beta \\ -\sin\beta & \cos\beta \end{pmatrix} \begin{pmatrix} g_1 \\ g_2 \end{pmatrix} = \begin{pmatrix} G^0 \\ A^0 \end{pmatrix}. \tag{71}$$

$H^{\pm}, H^0, h^0, A^0$ are the five physical Higgs particles. The light CP even Higgs h^0 is labeled H. In the R-gauge, the Goldstone bosons, $G^{\pm}$ and G^0, would be useful in processes involving highly energetic longitudinal vector bosons [100].

In Ref. [88] the relations amongst the various parameters of Type II 2HDM can be found. The following notation for the relevant vertices[7] of type II are from Ref. [89].

$$\underline{\text{Interaction}} \quad : \quad \underline{\text{Vertex}}$$

$$W^+W^-H \quad : \quad ig\, m_W \sin(\beta-\alpha)\, g^{\mu\nu}$$

$$W^{\pm}H^{\mp}H \quad : \quad \frac{\mp ig}{2}\cos(\beta-\alpha)(p+p')^{\mu}$$

[7] See Appendix A.1.3 in Ref. [88] for conversion of parameters to the usage in Ref. [89].

$$H^+H^-H \quad : \quad -ig[m_W\sin(\beta-\alpha)+\frac{m_Z}{2\cos\theta_W}\cos 2\beta\sin(\beta+\alpha)]$$

$$\tau^+\nu_\tau H^+ \quad : \quad \frac{ig\;m_\tau\;\tan\beta}{2\sqrt{2}M_W}[1+\gamma_5]=\frac{i\sqrt{2}m_\tau}{\upsilon}\tan\beta\;P_R$$

$$\tau^-\bar{\nu}_\tau H^- \quad : \quad \frac{ig\;m_\tau\;\tan\beta}{2\sqrt{2}M_W}[1-\gamma_5]=\frac{i\sqrt{2}m_\tau}{\upsilon}\tan\beta\;P_L$$

For example the amplitude for $W^\pm H^\mp H$ is $\frac{\mp ig}{2}\cos(\beta-\alpha)\;\varepsilon_2^{\mu *}(p_H+p_{H^+})_\mu$ where p_H and p_{H^+} are the 4-momenta of H and $H^\mp$, respectively. All the interactions are specified in terms of the mixing angles β and α. For the W^+W^-H vertex, $\sin(\beta-\alpha)$ can be constrained from experiment [80]. The H^+H^-H interaction will contribute to the $H\to\gamma\gamma$ rate though the charged Higgs loop [101]. Hence the measured $H\to\gamma\gamma$ rate puts constraints on the mixing angles α and β.

5.3.2 L2HDM

Treatments of L2HDM have already been given in the literature [102, 103]. The charged Higgs leptonic interaction in L2HDM is the same as in Type II since one doublet couples to leptons in both models. However, unlike in the Type II case, L2HDM has the other Higgs doublet coupling exclusively to up-type and down-type quarks. After EWSB,

$$\mathscr{L}_Y=-\frac{\sqrt{2}V_{ud}}{\tan\beta\;\upsilon}\bar{d}(m_uP_L-m_dP_R)\;u\;H^- -\frac{\sqrt{2}\tan\beta}{\upsilon}\bar{\nu}(m_\ell P_R)\;e\;H^+ + \text{neutral Higgs + h.c.}$$

$\mathscr{L}_Y$ above implies L2HDM becomes truly leptophilic in the charged Higgs as $\tan\beta$ grows [102].

In comparison to Eq. (69), the potential in L2HDM [8] has an additional term. This only trivially changes the parametrization of the Higgs masses relative to Type II. Hence the other charged Higgs vertices are the same as in Type II 2HDM except when quarks are involved. By using $\mathscr{L}^\Phi$,

[8] See Buckley et al. [102], Eq. (2). Eq. (69) above has a common parameter for $[Re(\Phi_1^\dagger\Phi_2)]^2$ and $[Im(\Phi_1^\dagger\Phi_2)]$ unlike Buckley et al.

Eqs. (68) and (71), and the unitary gauge, the derivation of interactions in L2HDM easily follow. Recently L2HDM has been discussed for the resolution of the $(g-2)_\mu$ anomaly and the galactic center γ-ray excess from a light pseudoscalar and large $\tan\beta$ [102].

5.3.3 Type II 2HDM and L2HDM Distributions for $H \to W^- W^{+*}$(or H^{+*}) $\to \tau^- \bar{\nu}_\tau \tau^+ \nu_\tau$

Now add new physics channels H^+ via 2HDM (see Figure 11). The four-fold angular distribution is

$$\frac{d\Gamma(H \to W^- W^{+*}(\text{or } H^{+*}) \to \tau^- \bar{\nu}_\tau \tau^+ \nu_\tau)}{dq^2 d(\cos\theta_q) d(\cos\theta_p) d\chi} \tag{72}$$

$$= \frac{Br_{W\tau\nu_\tau}}{(2\pi)^4} \frac{(1-\frac{m^2}{q^2})|\vec{q}|}{2^5 M_H^2} \sum_{\lambda_{\tau^-},\lambda_{\tau^+}} \Big| \sum_{s_{W^+},\lambda_{W^\pm},\lambda_{H^+}} \mathscr{A} \Big|^2,$$

where

$$\begin{aligned} \mathscr{A} &= \sin(\beta-\alpha)(-F_s)^{1-s_{W^+}} A_{\lambda_{W^-},\lambda_{W^+}} B^{\lambda_{W^-}}_{\lambda_{\tau^-},\lambda_{\bar{\nu}_\tau}} C^{\lambda_{W^+}}_{\lambda_{\tau^+},\lambda_{\nu_\tau}} + \\ & D_{\lambda_{W^-},\lambda_{H^+}} B^{\lambda_{W^-}}_{\lambda_{\tau^-},\lambda_{\bar{\nu}_\tau}} E^{\lambda_{H^+}}_{\lambda_{\tau^+},\lambda_{\nu_\tau}}. \end{aligned} \tag{73}$$

Apart from coupling constants, the NP amplitudes are

$$
\begin{aligned}
D_{00} &= \varepsilon_2^{\mu^*}(0)(p_H + p_{H^+})_\mu = \frac{2M_H|\vec{q}|}{M_W} \\
E^0 &= \bar{u}(1+\gamma_5)v. \qquad (74)
\end{aligned}
$$

Here the contribution from the H^+H^- intermediate states has been neglected. This is justified as the H^+H^-H coupling is small and both the charged Higgs are off-shell for $m_{H^\pm}$ greater than m_H. Both the SM and 2HDM leptonic amplitudes are written in Appendix 2.1.

Suppressing λ_ℓ subscripts,

$$
|\sum_{\lambda_{W^-},\lambda_{W^+},\lambda_{H^+}} \mathscr{A}\ |^2 =
$$

$$
\sin^2(\beta-\alpha)\mid A^{+,+}B^+C^+ + A^{-,-}B^-C^- + A^{0,0}B^0C^0 + (-F_s)A^{0,t}B^0C^t\mid^2
$$

$$
+
$$

$$
\mid D^{0,0}B^0E^0\mid^2 +
$$

$$
\sin(\beta-\alpha)\ 2\mathrm{Re}\Big[(\mathrm{A}^{+,+}\mathrm{B}^+\mathrm{C}^+ + \mathrm{A}^{-,-}\mathrm{B}^-\mathrm{C}^- + \mathrm{A}^{0,0}\mathrm{B}^0\mathrm{C}^0 + (-\mathrm{F_s})\mathrm{A}^{0,t}\mathrm{B}^0\mathrm{C}^t)(\mathrm{D}^{0,0}\mathrm{B}^0\mathrm{E}^0)^*\Big].
$$

Expanding the latter equation yields 25 terms. The last term in brackets is the interference between the standard model and NP. For massless leptons, the distribution is the same as Eq. (105) apart from an overall factor $\sin^2(\beta-\alpha)$. The interference terms are expected to be more sizable than the purely NP term, i.e. $\cos(\beta-\alpha) > \cos^2(\beta-\alpha)$.

The momentum of the mediators is again

$$
|\vec{q}| = \frac{\sqrt{((q^2-M_W^2)^2 + M_H^4 - 2M_H^2M_W^2 - 2M_H^2q^2)}}{2M_H}, \text{ if } m_\tau^2 < q^2 < (M_H - M_W)^2. \qquad (75)
$$

From Eqs. (72), (73), (64), (74), and appendices 2.1, 2.2, and 2.3, the total distribution with respect to q^2 and χ can now be written as

$$\frac{d^2\Gamma^{2HDM}}{dq^2\,d\chi} = \sin^2(\beta-\alpha)\frac{d^2\Gamma^{SM}}{dq^2\,d\chi} + \frac{d^2\Gamma^{NP}}{dq^2\,d\chi}, \tag{76}$$

$$\begin{aligned}\frac{d^2\Gamma^{NP}}{dq^2\,d\chi} &= -\frac{12}{\sqrt{q^2}}\, mF_s\, B_{W\tau\nu}D_1^{H^+}(q^2)\,(A_{t0}D_{00})\Big(1+\frac{\varepsilon_p}{2}\Big)+ \\ &\quad 6\, B_{W\tau\nu}D_2^{H^+}(q^2)|D_{00}|^2\Big(1+\frac{\varepsilon}{2}\Big),\end{aligned} \tag{77}$$

where $\frac{d^2\Gamma^{SM}}{dq^2\,d\chi}$ is given in Eq. (66a).

See Appendix 2.3 for $D_1^{H^+}(q^2)$ and $D_2^{H^+}(q^2)$. The total decay width Γ_{H^+} is within the latter two kinematic variables and is defined as the partial width $\Gamma(H^+ \to \tau^+\nu_\tau)$ (see appendix in [89]), which is on the order of one tenth of the standard model Higgs total decay width for 90 GeV$<$ $M_{H^+} < 200$ GeV. The first and second terms of Eq. (77) represent SM-NP interference and pure NP, respectively. No resonance will occur in Eq. (77) since $\sqrt{q^2} < M_{H^\pm}$.

After integrating with respect to χ, the total distribution with respect to q^2 is

$$\frac{d\Gamma^{2HDM}}{dq^2} = \sin^2(\beta-\alpha)\frac{d\Gamma^{SM}}{dq^2} + \frac{d\Gamma^{NP}}{dq^2}, \tag{78}$$

where

$$\begin{aligned}\frac{d\Gamma^{NP}}{dq^2} &= -\frac{24\pi}{\sqrt{q^2}}\, mF_s\, B_{W\tau\nu}D_1^{H^+}(q^2)(A_{t0}D_{00})(1+\frac{\varepsilon}{2}) \\ &\quad +12\pi\, B_{W\tau\nu}D_2^{H^+}(q^2)|D_{00}|^2(1+\frac{\varepsilon}{2}),\end{aligned} \tag{79}$$

and $\frac{d\Gamma^{SM}}{dq^2}$ is in Eq. (67a). There is both SM-NP and pure NP interference for $\frac{d\Gamma}{dq^2}$.

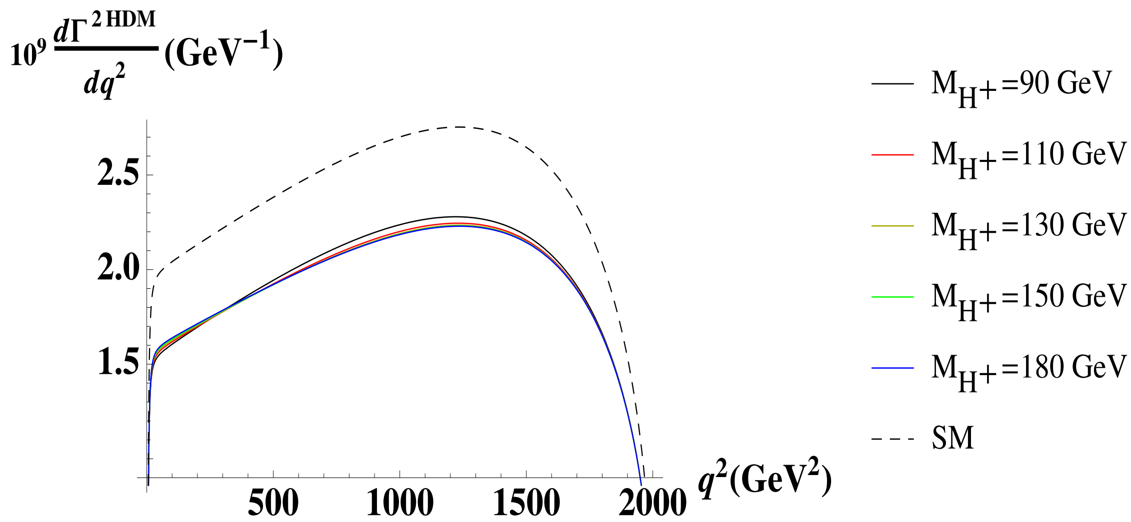

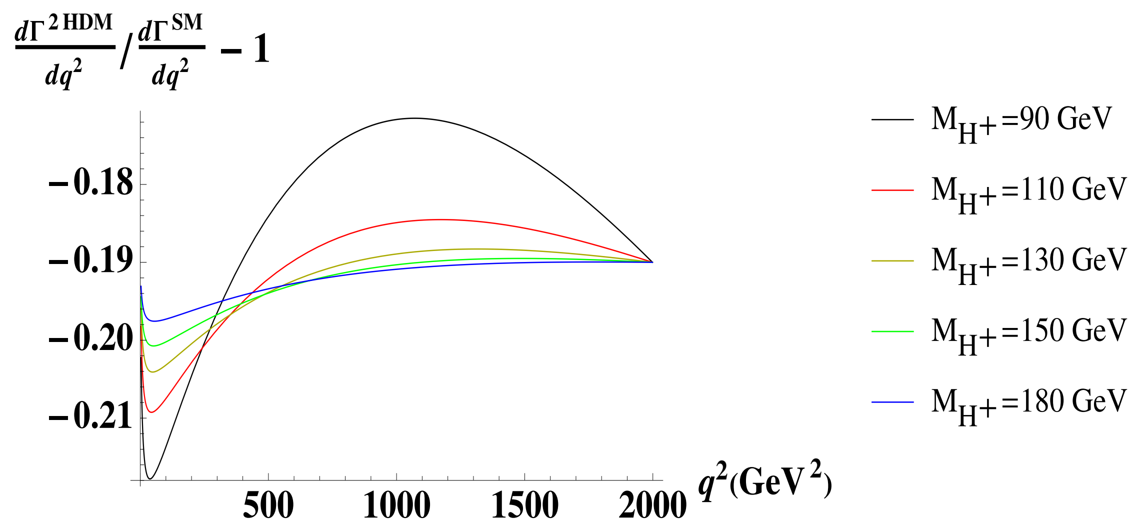

Figure 13: The above two plots depict the kinematic distribution and relative contribution of NP to the SM for various masses of M_{H^+}. Only channels W^-W^+ and W^-H^+ are relevant since W^- is taken as on-shell.

5.4 Plots

Only channels W^-W^{+*} and W^-H^{+*} have been considered since W^- is taken as on-shell. Let the charged Higgs mass range from 90 GeV to 180 GeV. This mass range is chosen since $H^\pm \to \tau\nu$ is a dominant decay mode over $H^\pm \to tb$ when $m_{H^\pm} < m_t + m_b \approx 180$ GeV and $\tan\beta > 2$ [83, 104]. The relevant standard model input parameters are listed in Table 4 [80].

Table 4: Standard Model Parameters

G	$Br_{W\tau\nu_\tau}$	Γ_W	M_W	M_H
1.1663787×10^{-5} GeV^{-2}	0.1138	2.085 GeV	80.385 GeV	125.09 GeV

Table 5: New Physics Parameters

$\tan\beta$	$\sin(\beta-\alpha)$	$\cos(\beta-\alpha)$	$\lvert g_{HW^-H^+}\rvert = \frac{g}{2}\cos(\beta-\alpha)$	$\lvert g_{H^+\tau\nu_\tau}\rvert = \frac{g\ m_\tau}{2\sqrt{2}\ M_W}\tan\beta$
80	0.90	0.44	0.14	0.41

Table 5 lists the new physics parameters. The mixing angles, α and β, are chosen as follows. The normalized coupling of HW^-W^+ in the standard model is expected to be unity. ATLAS and CMS have found the normalized coupling of HW^-W^+ at 68% confidence interval to have ranges (1.05, 1.22) and (0.81, 0.97), respectively [105]. With vertex HW^-W^+ being $ig\ m_W \sin(\beta-\alpha)$ and considering the latter CMS confidence interval, let $\sin(\beta-\alpha) = 0.9$. To have an appreciable effect from the charged Higgs states a large $\tan\beta$ is required and so the type II 2HDM will not be considered since it disfavors large $\tan\beta$ [106]. The type II 2HDM may also be ruled out from measurements in semileptonic B decays of $R_{D^{(*)}} \equiv \mathscr{B}(\bar{B} \to D^{(*)}\tau^-\bar{\nu}_\tau)/\mathscr{B}(\bar{B} \to D^{(*)}\ell^-\bar{\nu}_\ell)$ $(\ell = e, \mu)$ which are difficult to understand in the SM and in Type II 2HDM [50, 51].

Focus on the L2HDM and choose $\tan\beta = 80$ which is allowed by present measurements [102] since a large $\tan\beta$ can help explain the $(g-2)_\mu$ anomaly and the galactic center γ-ray excess in the L2HDM. This then gives $\beta = 89.3^\circ$, $\alpha = 25.1^\circ$, and $\cos(\beta-\alpha) = 0.44$. For the choices of the mixing angles, the H^+H^-H coupling from Eq. (72) is around $\frac{g_{H^+H^-H}}{v} \sim -0.06$ and the correction to the $H \to \gamma\gamma$ signal strength is small and within the measured experimental error [80].

Plots of $\frac{d\Gamma^{2HDM}}{dq^2}$ and $(\frac{d\Gamma^{2HDM}}{dq^2}/\frac{d\Gamma^{SM}}{dq^2} - 1)$ (see Eqs. 78 and 79) are shown in Figure 13 for 90 GeV$< M_{H^\pm} <$ 180 GeV. Essentially, $\frac{d\Gamma^{2HDM}}{dq^2}$ is a scaled down version of $\frac{d\Gamma^{SM}}{dq^2}$ owing to the factor $\sin^2(\beta - \alpha)$. The maximum relative contribution of NP to the SM in magnitude, i.e. $|\frac{d\Gamma^{2HDM}}{dq^2}/\frac{d\Gamma^{SM}}{dq^2} - 1|$x100%, is over 21%. For the specified charged Higgs mass range, this latter relative contribution is dominantly from $\sin^2(\alpha - \beta) - 1 \approx -0.19$.

Plots of $\frac{d\Gamma^{2HDM}}{d\chi}$ and $(\frac{d\Gamma^{2HDM}}{d\chi}/\frac{d\Gamma^{SM}}{d\chi} - 1)$ are shown in Figure 14. The deviation between 2HDM and SM is conspicuous at $\chi = \pm\pi$. The maximum relative contribution of NP to the SM in magnitude, i.e. $|\frac{d\Gamma^{2HDM}}{d\chi}/\frac{d\Gamma^{SM}}{d\chi} - 1|$x100%, is over 19%.

A MadGraph 5 analysis is performed for a Higgs decay from rest, namely $H \to W^- \ W^{+*}$ (or $H^{+*}) \to \tau^-\tau^+\bar{\nu}_\tau\nu_\tau$. Figure 15 shows a MadGraph distribution for the dihedral angle χ. Mass of the charged Higgs is taken as $M_{H^+} = 150$ GeV. Only events where W^- is on-shell are included. Figure 15 shows a deviation between the SM and the 2HDM at $\chi = \pi$. This plot is invariant to a boost along the $W^\pm$ momenta, hence also the same in the Higgs rest frame. A boost along one of the W bosons would only change the directions of the leptons within their respective decay planes. See Figure 11. One might also consider looking in the channel $H \to ZZ^* \to \ell_1\ell_2\ell_3\ell_4$. Therein, leptonic mass effects are not as pronounced as in $H \to W^{+*}(\to \tau^+\nu_\tau)W^-(\to \tau^-\bar{\nu}_\tau)$ [93]. Note that at the LHC, gluon-gluon fusion is the dominant mode for Higgs production. Relative to a normalized coupling in the standard model, the Hgg vertex in the models L2HDM and Type II have the common factor $\frac{\cos\alpha}{\sin\beta} = .91$ for a light CP-even Higgs.

5.5 Conclusion of Searching for a Charged Higgs

2HDM's are a simple extension of the standard model which have an extended Higgs sector including charged Higgs. In particular, ATLAS and CMS have been recently constraining scenarios with a charged Higgs, $H^\pm$. The charged Higgs might also be seen at lepton colliders [107] in the channel $\ell^+\ell^- \to W^\pm H^\mp$.

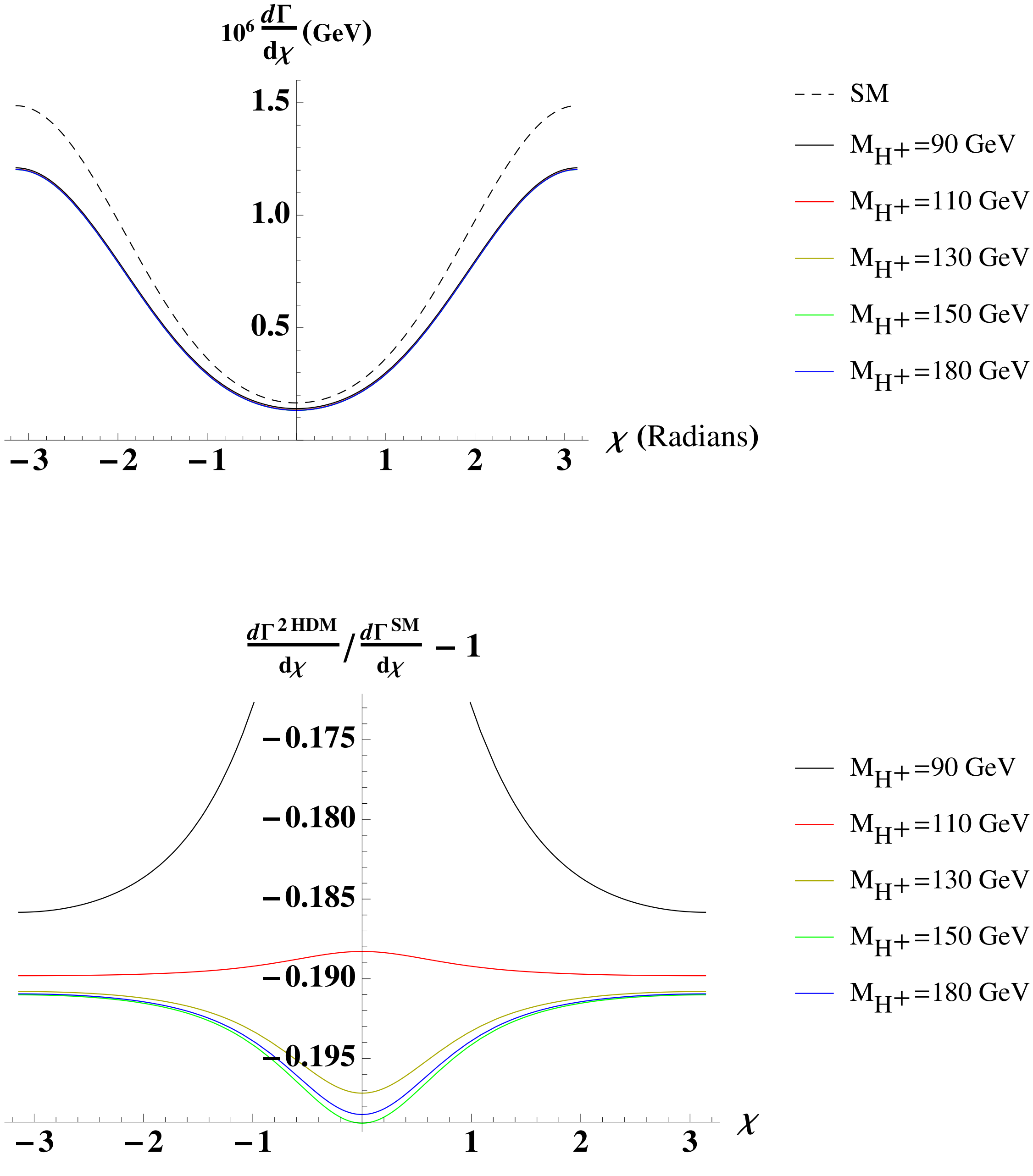

Figure 14: The above two plots depict the dihedral distribution and relative contribution of NP to the SM for various masses of M_{H^+}. Only channels W^-W^+ and W^-H^+ are relevant since W^- is on-shell. The top plot shows the curves for different values of M_{H^+}, i.e. 90 GeV$< M_{H^+} <$ 180 GeV, as bunched together.

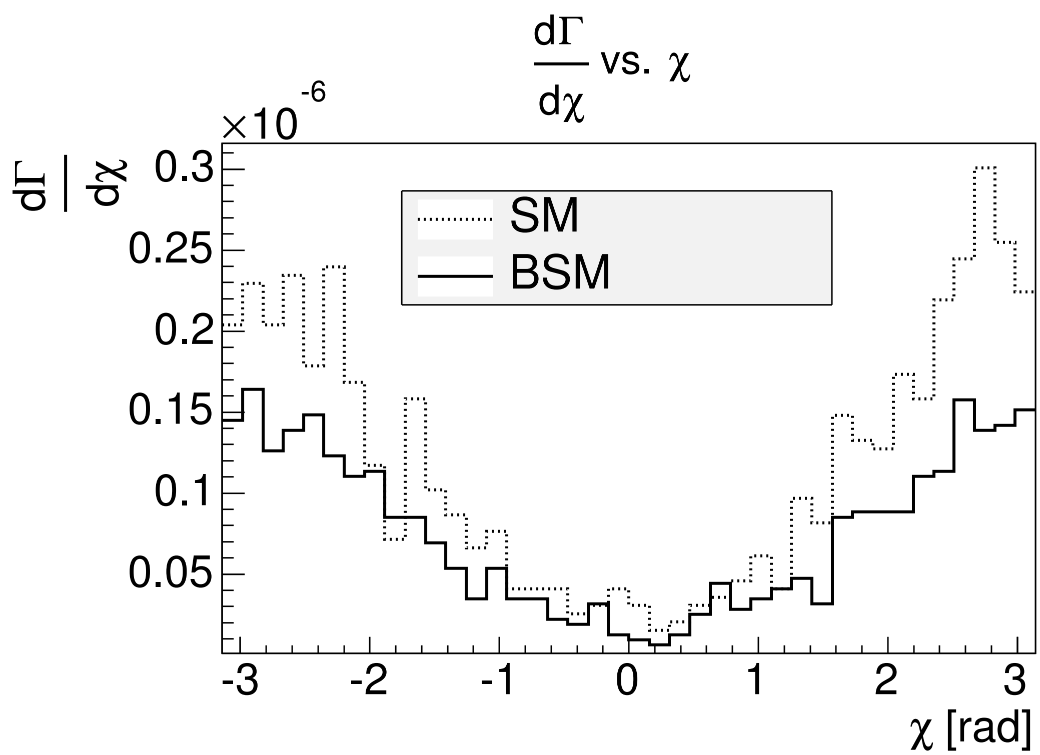

Figure 15: The above depicts the dihedral distribution versus dihedral angle, χ. The dihedral angle is the angle between the decay planes of W^{+*} (or H^{+*}) and W^- with $M_{H^+} = 150$ GeV. See Figure 11. The full process is $H \to W^- W^{+*}(\text{or } H^{+*}) \to \tau^- \bar{\nu}_\tau \tau^+ \nu_\tau$.
The vertical scale is in arbitrary units.

Given the uncertainty in the standard model Higgs couplings, there may exist a charged Higgs. A discovery can aid in resolving many problems in physics, one possibly being the hierarchy problem by suggesting supersymmetry. A venue that should be considered is the Higgs decay $H \to W^-W^{+*}(\text{or } H^{+*}) \to \tau^-\bar{\nu}_\tau\tau^+\nu_\tau$.

The four-fold distribution for the latter process has been calculated via helicity amplitudes. It is written in a general manner allowing for new physics, e.g. an admixture of CP even and CP odd terms in the Higgs coupling to two standard model vector bosons. A charged Higgs is considered in the context of Type II 2HDM and L2HDM models. Recent experimental results suggest the L2HDM is somewhat less constrained over Type II. Differential decay distribution plots of the new physics and the standard model are provided. Kinematic and dihedral distributions show deviations from the standard model when a charged Higgs is present in L2HDM. At tree level, the NP decay amplitude, $H \to W^-H^+$, becomes more pronounced if the dihedral angle, or angle between decay planes of the leptons, approaches $\pm\pi$. A MadGraph 5 simulation confirms the latter.

CHAPTER 6: CONCLUSION

There are signs that lepton flavor universality within the standard model may be violated. Recently, the LHCb Collaboration measurement of $R_K \equiv \mathscr{B}(B^+ \to K^+\mu^+\mu^-)/\mathscr{B}(B^+ \to K^+e^+e^-)$ differs from the SM prediction of $R_K = 1$ by 2.6σ [3]. Also, the Heavy-Flavor Averaging Group has averaged the BaBar, Belle, and LHCb ratios $R(D^{(*)}) \equiv \mathscr{B}(\bar{B} \to D^{(*)+}\tau^-\bar{\nu}_\tau)/\ \mathscr{B}(\bar{B} \to D^{(*)+}\ell^-\bar{\nu}_\ell)$ ($\ell = e, \mu$), finding discrepancies with respect to the SM by 1.9σ ($R(D)$) and 3.3σ ($R(D^*)$) [1]. These R_K and $R(D^{(*)})$ puzzles suggest lepton flavor non-universality, and therefore may signal physics beyond the standard model. In light of the measured R_{K^*} anomaly by the LHCb this year, this topic of lepton flavor universality takes on added importance [12].

Glashow, Guadagnoli and Lane (GGL) [22] propose an explanation for the R_K puzzle. They assume that the NP couples preferentially to the third generation, generating a neutral-current operator $(\bar{b}'_L\gamma_\mu b'_L)(\bar{\tau}'_L\gamma^\mu\tau'_L)$, wherein the primed fields denote states in the gauge basis. When transforming to the mass basis, operators arise giving decays that violate lepton flavor universality (and lepton flavor conservation). Futhermore, assuming the scale of NP is much larger than the weak scale, all NP operators must be made invariant under the full $SU(3)_C \times SU(2)_L \times U(1)_Y$ gauge group. When the latter is applied to the GGL operator, there are two types of fully gauge-invariant NP operators that may occur. One of these contains both neutral-current and charged-current interactions. While GGL has shown that the neutral-current piece of this NP operator can explain the R_K puzzle, another possibility is that the charged-current piece can simultaneously explain the $R(D^{(*)})$ puzzle. This model in section 3.4 makes a prediction for the double ratio $R(D)/R(D^*)$, thus this very model can be ruled out with a more precise measurement of this quantity. From current measurements, the model also implies bounds on the new physics parameters that are associated with these new physics operators.

Since the decays $\bar{B} \to D^{(*)+}\tau^-\bar{\nu}_\tau$ and $\Lambda_b \to \Lambda_c\tau\bar{\nu}_\tau$ share the same quark-level transition $b \to c$ and given the recent hints of lepton flavor non-universality observed in $R(D^{(*)})$, this dissertation studies the decay process $\Lambda_b \to \Lambda_c\tau\bar{\nu}_\tau$. SM and NP predictions are derived for this decay. The general parametrization of the NP operators has been made to include scalar, pseudoscalar, vector, and axial vector interactions while the new physics couplings are fixed from the experimental measurements of $R(D)$ and $R(D^*)$. The general formulas for the various angular distributions in the presence of NP operators has been calculated via the helicity formalism technique. Predictions follow in terms of $R_{\Lambda_b} \equiv \dfrac{\mathscr{B}(\Lambda_b \to \Lambda_c\tau\bar{\nu}_\tau)}{\mathscr{B}(\Lambda_b \to \Lambda_c\ell\bar{\nu}_\ell)}$ $(\ell = e,\mu)$, $\dfrac{d\Gamma}{dq^2}$, and $B_{\Lambda_b}(q^2) \equiv \dfrac{\frac{d\Gamma[\Lambda_b \to \Lambda_c\tau\bar{\nu}_\tau]}{dq^2}}{\frac{d\Gamma[\Lambda_b \to \Lambda_c\ell\bar{\nu}_\ell]}{dq^2}}$ $(\ell = e,\mu)$ for the various NP couplings taken one at a time. It has been found that $g_{L,R}$ couplings gave predictions larger than the SM values for all the three observables. Also, the g_P couplings produce larger effects than the g_S couplings. Future confirmation of anomalies in these observables such as at the LHCb would make new physics even more compelling.

Lastly, distributions are applied in the Higgs sector. 2HDM's are a simple extension of the standard model which have an extended Higgs sector including the charged Higgs. Notwithstanding that ATLAS and CMS have been recently constraining scenarios of a charged Higgs, $H^\pm$, the charged Higgs might also be seen at lepton colliders [107] in the channel $\ell^+\ell^- \to W^\pm H^\mp$. The uncertainty in the standard model Higgs couplings allows for a charged Higgs. A discovery can aid in resolving many problems in physics, one possibly being the hierarchy problem by suggesting supersymmetry. In this dissertation, the Higgs decay $H \to W^-W^{+*}(\text{or } H^{+*}) \to \tau^-\bar{\nu}_\tau\tau^+\nu_\tau$ is explored.

The four-fold distribution for the latter process has been calculated via the density matrix method. It is written in a general manner allowing for new physics, e.g. an admixture of CP even and CP odd terms in the Higgs coupling to two standard model vector bosons. A charged Higgs is considered in the context of Type II 2HDM and L2HDM models. Recent experimental results suggest that L2HDM is somewhat less constrained with respect to Type II [50, 51, 102, 106]. Plots of differential decay distributions are provided. Kinematic and dihedral distributions show deviations from the standard model when a charged Higgs is present in L2HDM. At tree level, the NP decay amplitude, $H \to W^- H^+$, becomes more pronounced if the dihedral angle, or angle between decay planes of the leptons, approaches $\pm\pi$. A MadGraph 5 simulation is performed confirming the latter theoretical result.

LIST OF REFERENCES

References

[1] Y. Amhis et al., Averages of b-hadron, c-hadron, and τ-lepton properties as of winter 2016. `http://www.slac.stanford.edu/xorg/hfag/semi/winter16/winter16_dtaunu.html`, 2016.

[2] G. Ricciardi, Mod. Phys. Lett. A **32**, no. 05, 1730005 (2017) doi:10.1142/S0217732317300051 [arXiv:1610.04387 [hep-ph]].

[3] G. Hiller and F. Kruger, Phys. Rev. D **69**, 074020 (2004) [arXiv:hep-ph/0310219]; C. Bobeth, G. Hiller and G. Piranishvili, JHEP **0712**, 040 (2007) [arXiv:0709.4174 [hep-ph]]; C. Bouchard *et al.* [HPQCD Collaboration], Phys. Rev. Lett. **111**, no. 16, 162002 (2013) [Erratum-ibid. **112**, no. 14, 149902 (2014)] [arXiv:1306.0434 [hep-ph]].

[4] B. Bhattacharya, A. Datta, D. London and S. Shivashankara, Phys. Lett. B **742**, 370 (2015) [arXiv:1412.7164 [hep-ph]].

[5] S. Shivashankara, W. Wu and A. Datta, Phys. Rev. D **91**, no. 11, 115003 (2015) [arXiv:1502.07230 [hep-ph]].

[6] S. Shivashankara, J. Acosta and A. Datta. Searching for a Charged Higgs in $H \to W^- W^{+*}(\text{or } H^{+*}) \to \tau^- \bar{\nu}_\tau \tau^+ \nu_\tau$. Work in Progess.

[7] J. G. Korner and G. A. Schuler, Z. Phys. C **46**, 93 (1990).

[8] R. Aaij *et al.* [LHCb Collaboration], Phys. Rev. Lett. **113**, 151601 (2014) [arXiv:1406.6482 [hep-ex]].

[9] W. Altmannshofer and D. M. Straub, arXiv:1503.06199 [hep-ph]; S. Descotes-Genon, L. Hofer, J. Matias and J. Virto, JHEP **1606**, 092 (2016) doi:10.1007/JHEP06(2016)092 [arXiv:1510.04239 [hep-ph]]; T. Hurth, F. Mahmoudi and S. Neshatpour, Nucl. Phys. B **909**, 737 (2016) doi:10.1016/j.nuclphysb.2016.05.022 [arXiv:1603.00865 [hep-ph]].

[10] Y. Sakaki, M. Tanaka, A. Tayduganov and R. Watanabe, Phys. Rev. D **88**, no. 9, 094012 (2013) doi:10.1103/PhysRevD.88.094012 [arXiv:1309.0301 [hep-ph]].

[11] A. Crivellin, arXiv:1605.02934 [hep-ph]; Z. Ligeti, PoS LeptonPhoton **2015**, 031 (2016) [arXiv:1606.02756 [hep-ph]]; G. Ricciardi, arXiv:1610.04387 [hep-ph].

[12] R. Aaij *et al.* [LHCb Collaboration], arXiv:1705.05802 [hep-ex].

[13] A. Datta, J. Kumar, J. Liao and D. Marfatia, arXiv:1705.08423 [hep-ph].

[14] A. K. Alok, B. Bhattacharya, A. Datta, D. Kumar, J. Kumar and D. London, arXiv:1704.07397 [hep-ph].

[15] W. Altmannshofer, P. Ball, A. Bharucha, A. J. Buras, D. M. Straub and M. Wick, JHEP **0901**, 019 (2009) [arXiv:0811.1214 [hep-ph]]; A. K. Alok, A. Dighe, D. Ghosh, D. London, J. Matias, M. Nagashima and A. Szynkman, JHEP **1002**, 053 (2010) [arXiv:0912.1382 [hep-ph]]; A. K. Alok, A. Datta, A. Dighe, M. Duraisamy, D. Ghosh and D. London, JHEP **1111**, 121 (2011) [arXiv:1008.2367 [hep-ph]], JHEP **1111**, 122 (2011) [arXiv:1103.5344 [hep-ph]]; D. Becirevic and E. Schneider, Nucl. Phys. B **854**, 321 (2012) [arXiv:1106.3283 [hep-ph]]; J. Matias, F. Mescia, M. Ramon and J. Virto, JHEP **1204**, 104 (2012) [arXiv:1202.4266 [hep-ph]]; S. Descotes-Genon, J. Matias, M. Ramon and J. Virto, JHEP **1301**, 048 (2013) [arXiv:1207.2753 [hep-ph]]; C. Bobeth, G. Hiller and D. van Dyk, Phys. Rev. D **87**, 034016 (2013) [arXiv:1212.2321 [hep-ph]]; S. Descotes-Genon, T. Hurth, J. Matias and J. Virto, JHEP **1305**, 137 (2013) [arXiv:1303.5794 [hep-ph]].

[16] R. Aaij *et al.* [LHCb Collaboration], Phys. Rev. Lett. **111** (2013) 191801 [arXiv:1308.1707 [hep-ex]].

[17] S. Jäger and J. Martin Camalich, JHEP **1305** (2013) 043 [arXiv:1212.2263 [hep-ph]]; S. Descotes-Genon, J. Matias and J. Virto, Phys. Rev. D **88** (2013) 074002 [arXiv:1307.5683 [hep-ph]]; W. Altmannshofer and D. M. Straub, Eur. Phys. J. C **73** (2013) 2646 [arXiv:1308.1501 [hep-ph]]; R. Gauld, F. Goertz and U. Haisch, Phys. Rev. D **89** (2014) 015005

[arXiv:1308.1959 [hep-ph]]; C. Hambrock, G. Hiller, S. Schacht and R. Zwicky, Phys. Rev. D **89** (2014) 074014 [arXiv:1308.4379 [hep-ph]]; A. J. Buras and J. Girrbach, JHEP **1312** (2013) 009 [arXiv:1309.2466 [hep-ph]]; R. Gauld, F. Goertz and U. Haisch, JHEP **1401** (2014) 069 [arXiv:1310.1082 [hep-ph]]; A. Datta, M. Duraisamy and D. Ghosh, Phys. Rev. D **89** (2014) 071501 [arXiv:1310.1937 [hep-ph]]; F. Beaujean, C. Bobeth and D. van Dyk, Eur. Phys. J. C **74** (2014) 2897 [arXiv:1310.2478 [hep-ph]]; R. R. Horgan, Z. Liu, S. Meinel and M. Wingate, Phys. Rev. Lett. **112** (2014) 212003 [arXiv:1310.3887 [hep-ph]]; A. J. Buras, F. De Fazio and J. Girrbach, JHEP **1402** (2014) 112 [arXiv:1311.6729 [hep-ph]]; W. Altmannshofer, S. Gori, M. Pospelov and I. Yavin, Phys. Rev. D **89**, 095033 (2014) [arXiv:1403.1269 [hep-ph]]; T. Hurth and F. Mahmoudi, JHEP **1404** (2014) 097 [arXiv:1312.5267 [hep-ph]]; S. Descotes-Genon, L. Hofer, J. Matias and J. Virto, [arXiv:1407.8526 [hep-ph]]; A. Khodjamirian, T. Mannel, A. A. Pivovarov and Y. -M. Wang, JHEP **1009** (2010) 089 [arXiv:1006.4945 [hep-ph]]; J. Lyon and R. Zwicky, [arXiv:1406.0566 [hep-ph]]; S. Descotes-Genon, L. Hofer, J. Matias and J. Virto, [arXiv:1411.0922 [hep-ph]].

[18] T. Hurth, F. Mahmoudi and S. Neshatpour, [arXiv:1410.4545 [hep-ph]]. W. Altmannshofer and D. M. Straub, [arXiv:1411.3161 [hep-ph]].

[19] A. J. Buras, J. Girrbach-Noe, C. Niehoff and D. M. Straub, [arXiv:1409.4557 [hep-ph]].

[20] G. Hiller and M. Schmaltz, Phys. Rev. D **90** (2014) 054014 [arXiv:1408.1627 [hep-ph]].

[21] A. Celis, J. Fuentes-Martin, M. Jung and H. Serodio, Phys. Rev. D **92**, no. 1, 015007 (2015) doi:10.1103/PhysRevD.92.015007 [arXiv:1505.03079 [hep-ph]]; R. Alonso, B. Grinstein and J. Martin Camalich, JHEP **1510**, 184 (2015) doi:10.1007/JHEP10(2015)184 [arXiv:1505.05164 [hep-ph]].

[22] S. L. Glashow, D. Guadagnoli and K. Lane, Phys. Rev. Lett. **114**, 091801 (2015) doi:10.1103/PhysRevLett.114.091801 [arXiv:1411.0565 [hep-ph]].

[23] S. L. Glashow, J. Iliopoulos and L. Maiani, Phys. Rev. D **2**, 1285 (1970).

[24] R. Alonso, B. Grinstein and J. M. Camalich, [arXiv:1407.7044 [hep-ph]].

[25] W. Altmannshofer, S. Gori, M. Pospelov and I. Yavin, Ref. [17].

[26] D. Ghosh, M. Nardecchia and S. A. Renner, [arXiv:1408.4097 [hep-ph]]; G. Hiller and M. Schmaltz, [arXiv:1411.4773 [hep-ph]].

[27] B. Gripaios, M. Nardecchia and S. A. Renner, [arXiv:1412.1791 [hep-ph]].

[28] S. Biswas, D. Chowdhury, S. Han and S. J. Lee, [arXiv:1409.0882 [hep-ph]];

[29] S. M. Boucenna, J. W. F. Valle and A. Vicente, Phys. Lett. B **750**, 367 (2015) doi:10.1016/j.physletb.2015.09.040 [arXiv:1503.07099 [hep-ph]].

[30] D. M. Lindemann, arXiv:1212.5578 [hep-ex].

[31] D. Boubaa, A. Datta, M. Duraisamy and S. Khalil, Int. J. Mod. Phys. A **28**, 1350153 (2013) [arXiv:1211.5168 [hep-ph]].

[32] S. M. Boucenna, J. W. F. Valle and A. Vicente, Phys. Lett. B **750**, 367 (2015) doi:10.1016/j.physletb.2015.09.040 [arXiv:1503.07099 [hep-ph]].

[33] J. Alwall, M. Herquet, F. Maltoni, O. Mattelaer and T. Stelzer, JHEP **1106**, 128 (2011) [arXiv:1106.0522 [hep-ph]].

[34] T. Han, Int. J. Mod. Phys. A **23**, 4107 (2008) [arXiv:0804.3178 [hep-ph]].

[35] S. Fajfer, J. F. Kamenik, I. Nisandzic and J. Zupan, Phys. Rev. Lett. **109**, 161801 (2012) [arXiv:1206.1872 [hep-ph]]; A. Crivellin, C. Greub and A. Kokulu, Phys. Rev. D **86**, 054014 (2012) [arXiv:1206.2634 [hep-ph]]; A. Datta, M. Duraisamy and D. Ghosh, Phys. Rev. D **86**, 034027 (2012) [arXiv:1206.3760 [hep-ph]]; D. Becirevic, N. Kosnik and A. Tayduganov, Phys. Lett. B **716**, 208 (2012) [arXiv:1206.4977 [hep-ph]]; N. G. Deshpande and A. Menon, [arXiv:1208.4134 [hep-ph]]; A. Celis, M. Jung, X. -Q. Li and A. Pich, JHEP **1301**, 054 (2013) [arXiv:1210.8443 [hep-ph]]; D. Choudhury, D. K. Ghosh and A. Kundu, Phys. Rev. D **86**,

114037 (2012) [arXiv:1210.5076 [hep-ph]]; M. Tanaka and R. Watanabe, [arXiv:1212.1878 [hep-ph]]; P. Ko, Y. Omura and C. Yu, [arXiv:1212.4607 [hep-ph]]; Y. -Y. Fan, W. -F. Wang and Z. -J. Xiao, [arXiv:1301.6246 [hep-ph]]; P. Biancofiore, P. Colangelo and F. De Fazio, [arXiv:1302.1042 [hep-ph]]; A. Celis, M. Jung, X. -Q. Li and A. Pich, [arXiv:1302.5992 [hep-ph]]; M. Duraisamy and A. Datta, JHEP **1309**, 059 (2013) [arXiv:1302.7031 [hep-ph]]; I. Dorsner, S. Fajfer, N. Kosnik and I. Nisandzic, JHEP **1311**, 084 (2013) [arXiv:1306.6493 [hep-ph]]; Y. Sakaki, M. Tanaka, A. Tayduganov and R. Watanabe, Phys. Rev. D **88**, 094012 (2013) [arXiv:1309.0301 [hep-ph]], [arXiv:1412.3761 [hep-ph]]; M. Duraisamy, P. Sharma and A. Datta, Phys. Rev. D **90**, 074013 (2014) [arXiv:1405.3719 [hep-ph]]; Y. Sakaki, M. Tanaka, A. Tayduganov and R. Watanabe, [arXiv:1412.3761 [hep-ph]].

[36] S. Fajfer, J. F. Kamenik and I. Nisandzic, [arXiv:1203.2654 [hep-ph]]; Y. Sakaki and H. Tanaka, [arXiv:1205.4908 [hep-ph]].

[37] R. Feger, T. Mannel, V. Klose, H. Lacker and T. Luck, Phys. Rev. D **82**, 073002 (2010) [arXiv:1003.4022 [hep-ph]]; B. Dassinger, R. Feger and T. Mannel, Phys. Rev. D **79**, 075015 (2009) [arXiv:0803.3561 [hep-ph]], Phys. Rev. D **75**, 095007 (2007) [arXiv:hep-ph/0701054].

[38] M. Jung, arXiv:1606.09191 [hep-ph];C. W. Chiang, X. G. He and G. Valencia, Phys. Rev. D **93**, no. 7, 074003 (2016) doi:10.1103/PhysRevD.93.074003 [arXiv:1601.07328 [hep-ph]]; A. Celis, J. Fuentes-Martin, M. Jung and H. Serodio, Phys. Rev. D **92**, no. 1, 015007 (2015) doi:10.1103/PhysRevD.92.015007 [arXiv:1505.03079 [hep-ph]]; D. Aristizabal Sierra, F. Staub and A. Vicente, Phys. Rev. D **92**, no. 1, 015001 (2015) doi:10.1103/PhysRevD.92.015001 [arXiv:1503.06077 [hep-ph]]; A. Crivellin, G. D'Ambrosio and J. Heeck, Phys. Rev. D **91**, no. 7, 075006 (2015) doi:10.1103/PhysRevD.91.075006 [arXiv:1503.03477 [hep-ph]].

[39] F. Feruglio, P. Paradisi and A. Pattori, arXiv:1606.00524 [hep-ph].

[40] M. Bordone, G. Isidori and A. Pattori, Eur. Phys. J. C **76**, no. 8, 440 (2016) doi:10.1140/epjc/s10052-016-4274-7 [arXiv:1605.07633 [hep-ph]]; B. Capdevila, S. Descotes-Genon, J. Matias and J. Virto, JHEP **1610**, 075 (2016) doi:10.1007/JHEP10(2016)075

[arXiv:1605.03156 [hep-ph]]; J. Aebischer, A. Crivellin, M. Fael and C. Greub, JHEP **1605**, 037 (2016) doi:10.1007/JHEP05(2016)037 [arXiv:1512.02830 [hep-ph]]; T. Huber, T. Hurth and E. Lunghi, JHEP **1506**, 176 (2015) doi:10.1007/JHEP06(2015)176 [arXiv:1503.04849 [hep-ph]].

[41] J. Zhu, H. M. Gan, R. M. Wang, Y. Y. Fan, Q. Chang and Y. G. Xu, Phys. Rev. D **93**, no. 9, 094023 (2016) doi:10.1103/PhysRevD.93.094023 [arXiv:1602.06491 [hep-ph]].

[42] A. Greljo, G. Isidori and D. Marzocca, JHEP **1507**, 142 (2015) doi:10.1007/JHEP07(2015)142 [arXiv:1506.01705 [hep-ph]].

[43] P. Stangl, PoS EPS **-HEP2015**, 555 (2015) [arXiv:1510.04596 [hep-ph]]; C. Niehoff, P. Stangl and D. M. Straub, Phys. Lett. B **747**, 182 (2015) doi:10.1016/j.physletb.2015.05.063 [arXiv:1503.03865 [hep-ph]].

[44] L. Calibbi, A. Crivellin and T. Ota, Phys. Rev. Lett. **115**, 181801 (2015) doi:10.1103/PhysRevLett.115.181801 [arXiv:1506.02661 [hep-ph]].

[45] N. Kosnik, arXiv:1610.00447 [hep-ph]; R. Barbieri, C. W. Murphy and F. Senia, arXiv:1611.04930 [hep-ph]; B. Bhattacharya, A. Datta, J. P. Guvin, D. London and R. Watanabe, arXiv:1609.09078 [hep-ph]; G. Hiller, D. Loose and K. Schnwald, JHEP **1612**, 027 (2016) doi:10.1007/JHEP12(2016)027 [arXiv:1609.08895 [hep-ph]]; S. Sahoo, R. Mohanta and A. K. Giri, arXiv:1609.04367 [hep-ph]; D. Bečirević, S. Fajfer, N. Košnik and O. Sumensari, Phys. Rev. D **94**, no. 11, 115021 (2016) doi:10.1103/PhysRevD.94.115021 [arXiv:1608.08501 [hep-ph]]; D. Bečirević, N. Košnik, O. Sumensari and R. Zukanovich Funchal, JHEP **1611**, 035 (2016) doi:10.1007/JHEP11(2016)035 [arXiv:1608.07583 [hep-ph]]; N. G. Deshpande and X. G. He, arXiv:1608.04817 [hep-ph]; X. Q. Li, Y. D. Yang and X. Zhang, JHEP **1608**, 054 (2016) doi:10.1007/JHEP08(2016)054 [arXiv:1605.09308 [hep-ph]]; D. Das, C. Hati, G. Kumar and N. Mahajan, Phys. Rev. D **94**, 055034 (2016) doi:10.1103/PhysRevD.94.055034 [arXiv:1605.06313 [hep-ph]]; B. Dumont, K. Nishiwaki and R. Watanabe, Phys. Rev. D **94**, no.

3, 034001 (2016) doi:10.1103/PhysRevD.94.034001 [arXiv:1603.05248 [hep-ph]]; C. W. Murphy, Phys. Lett. B **757**, 192 (2016) doi:10.1016/j.physletb.2016.03.076 [arXiv:1512.06976 [hep-ph]]; R. Barbieri, G. Isidori, A. Pattori and F. Senia, Eur. Phys. J. C **76**, no. 2, 67 (2016) doi:10.1140/epjc/s10052-016-3905-3 [arXiv:1512.01560 [hep-ph]]; S. Fajfer and N. Košnik, Phys. Lett. B **755**, 270 (2016) doi:10.1016/j.physletb.2016.02.018 [arXiv:1511.06024 [hep-ph]]; A. Crivellin, EPJ Web Conf. **118**, 01007 (2016) doi:10.1051/epjconf/201611801007 [arXiv:1511.04015 [hep-ph]]; M. Bauer and M. Neubert, Phys. Rev. Lett. **116**, no. 14, 141802 (2016) doi:10.1103/PhysRevLett.116.141802 [arXiv:1511.01900 [hep-ph]]; M. Freytsis, Z. Ligeti and J. T. Ruderman, Phys. Rev. D **92**, no. 5, 054018 (2015) doi:10.1103/PhysRevD.92.054018 [arXiv:1506.08896 [hep-ph]]; D. Bečirević, S. Fajfer and N. Košnik, Phys. Rev. D **92**, no. 1, 014016 (2015) doi:10.1103/PhysRevD.92.014016 [arXiv:1503.09024 [hep-ph]].

[46] S. M. Boucenna, A. Celis, J. Fuentes-Martin, A. Vicente and J. Virto, Phys. Lett. B **760**, 214 (2016) doi:10.1016/j.physletb.2016.06.067 [arXiv:1604.03088 [hep-ph]]; W. Huang and Y. L. Tang, Phys. Rev. D **92**, no. 9, 094015 (2015) doi:10.1103/PhysRevD.92.094015 [arXiv:1509.08599 [hep-ph]].

[47] D. Bečirević, O. Sumensari and R. Zukanovich Funchal, Eur. Phys. J. C **76**, no. 3, 134 (2016) doi:10.1140/epjc/s10052-016-3985-0 [arXiv:1602.00881 [hep-ph]].

[48] W. Wu, arXiv:1505.03418 [hep-ph].

[49] D. Guadagnoli and K. Lane, Phys. Lett. B **751**, 54 (2015) doi:10.1016/j.physletb.2015.10.010 [arXiv:1507.01412 [hep-ph]].

[50] J. P. Lees *et al.* [BaBar Collaboration], Phys. Rev. Lett. **109**, 101802 (2012) [arXiv:1205.5442 [hep-ex]].

[51] J. P. Lees *et al.* [BaBar Collaboration], Phys. Rev. D **88**, 072012 (2013) [arXiv:1303.0571 [hep-ex]].

[52] M. Huschle *et al.* [Belle Collaboration], Phys. Rev. D **92**, no. 7, 072014 (2015) doi:10.1103/PhysRevD.92.072014 [arXiv:1507.03233 [hep-ex]]; A. Abdesselam *et al.* [Belle Collaboration], arXiv:1603.06711 [hep-ex].

[53] R. Aaij *et al.* [LHCb Collaboration], Phys. Rev. Lett. **115**, no. 11, 111803 (2015) Erratum: [Phys. Rev. Lett. **115**, no. 15, 159901 (2015)] doi:10.1103/PhysRevLett.115.159901, 10.1103/PhysRevLett.115.111803 [arXiv:1506.08614 [hep-ex]].

[54] A. Datta, M. Duraisamy and D. Ghosh, Phys. Rev. D **86**, 034027 (2012) [arXiv:1206.3760 [hep-ph]]; M. Duraisamy and A. Datta, JHEP **1309**, 059 (2013) [arXiv:1302.7031 [hep-ph]]; M. Duraisamy, P. Sharma and A. Datta, Phys. Rev. D **90**, 074013 (2014) [arXiv:1405.3719 [hep-ph]].

[55] R. Aaij *et al.* [LHCb Collaboration], Phys. Rev. D **85**, 032008 (2012) doi:10.1103/PhysRevD.85.032008 [arXiv:1111.2357 [hep-ex]]; S. Meinel, PoS LATTICE **2013**, 024 (2014) [arXiv:1401.2685 [hep-lat]].

[56] T. Gutsche, M. A. Ivanov, J. G. Korner, V. E. Lyubovitskij, P. Santorelli and N. Habyl, arXiv:1502.04864 [hep-ph].

[57] R. M. Woloshyn, PoS Hadron **2013**, 203 (2013).

[58] D. Santel *et al.* (Belle Collaboration), Phys. Rev. D **93**, 011101 (2016).

[59] B. Aubert *et al.* (BaBar Collaboration), Phys. Rev. Lett. **102**, 012001 (2009).

[60] See for e.g. M. Neubert, ”Heavy-quark symmetry.”, Phy. Rep. **245**, 259 (1994) [arXiv:hep-ph/9306320]; A. Datta, Phys. Lett. B **349**, 348 (1995) [hep-ph/9411306].

[61] T. Bhattacharya, V. Cirigliano, S. D. Cohen, A. Filipuzzi, M. Gonzalez-Alonso, M. L. Graesser, R. Gupta and H. -W. Lin, Phys. Rev. D **85**, 054512 (2012) [arXiv:1110.6448 [hep-ph]]; C. -H. Chen and C. -Q. Geng, Phys. Rev. D **71**, 077501 (2005) [hep-ph/0503123].

[62] A. Datta, S. Kamali, S. Meinel and A. Rashed, arXiv:1702.02243 [hep-ph].

[63] J. G. Korner and M. Kramer, Phys. Lett. B **275**, 495 (1992).

[64] A. Datta and D. London, Int. J. Mod. Phys. A **19**, 2505 (2004) [hep-ph/0303159]; W. Bensalem, A. Datta and D. London, Phys. Rev. D **66**, 094004 (2002) [hep-ph/0208054]; W. Bensalem, A. Datta and D. London, Phys. Lett. B **538**, 309 (2002) [hep-ph/0205009].

[65] E. Di Salvo and Z. J. Ajaltouni, arXiv:1610.01469 [hep-ph].

[66] A. Celis, M. Jung, X. Q. Li and A. Pich, arXiv:1612.07757 [hep-ph].

[67] A. K. Alok, D. Kumar, S. Kumbhakar and S. U. Sankar, arXiv:1606.03164 [hep-ph].

[68] M.A.Shifman, A.I. Vainshtein and V.I. Zakharov, Nucl. Phys. **B147**, 385(1979); 448

[69] De Carvalho, RS Marques, et al. "Form factors and decay rates for heavy Λ semileptonic decays from QCD sum rules." Phys. Rev. D **60**, 034009 (1999) [arXiv:hep-ph/9903326v1]

[70] W. Detmold, C. Lehner and S. Meinel, Phys. Rev. D **92**, no. 3, 034503 (2015) doi:10.1103/PhysRevD.92.034503 [arXiv:1503.01421 [hep-lat]].

[71] M. Pervin, W. Roberts and S. Capstick, Phys. Rev. C **72**, 035201 (2005) [nucl-th/0503030].

[72] L. Wang, J. M. Yang and Y. Zhang, arXiv:1610.05681 [hep-ph].

[73] M. Bauer and M. Neubert, Phys. Rev. Lett. **116**, no. 14, 141802 (2016) doi:10.1103/PhysRevLett.116.141802 [arXiv:1511.01900 [hep-ph]].

[74] S. Fajfer and N. Košnik, Phys. Lett. B **755**, 270 (2016) doi:10.1016/j.physletb.2016.02.018 [arXiv:1511.06024 [hep-ph]].

[75] X. Q. Li, Y. D. Yang and X. Zhang, arXiv:1611.01635 [hep-ph].

[76] S. Nandi, S. K. Patra and A. Soni, arXiv:1605.07191 [hep-ph].

[77] R. Dutta and A. Bhol, arXiv:1611.00231 [hep-ph].

[78] R. Dutta, Phys. Rev. D **93**, no. 5, 054003 (2016) doi:10.1103/PhysRevD.93.054003 [arXiv:1512.04034 [hep-ph]].

[79] G. Aad *et al.* [ATLAS Collaboration], Phys. Lett. B **716**, 1 (2012) [arXiv:1207.7214 [hep-ex]]; S. Chatrchyan *et al.* [CMS Collaboration], Phys. Lett. B **716**, 30 (2012) [arXiv:1207.7235 [hep-ex]]; G. Aad *et al.* [ATLAS Collaboration], Phys. Lett. B **726**, 88 (2013) [Phys. Lett. B **734**, 406 (2014)] [arXiv:1307.1427 [hep-ex]]; G. Aad *et al.* [ATLAS Collaboration], Phys. Lett. B **726**, 120 (2013) [arXiv:1307.1432 [hep-ex]]; S. Chatrchyan *et al.* [CMS Collaboration], JHEP **1401**, 096 (2014) [arXiv:1312.1129 [hep-ex]]; V. Khachatryan *et al.* [CMS Collaboration], Eur. Phys. J. C **74**, no. 10, 3076 (2014) [arXiv:1407.0558 [hep-ex]]; S. Chatrchyan *et al.* [CMS Collaboration], Phys. Rev. D **89** (2014) 9, 092007 [arXiv:1312.5353 [hep-ex]].

[80] K.A. Olive et al. (Particle Data Group), Chin. Phys. C, 38, 090001 (2014).

[81] G. Abbiendi *et al.* [OPAL Collaboration], Eur. Phys. J. C **32**, 453 (2004) [hep-ex/0309014]; J. Beringer *et al.* [Particle Data Group], Phys. Rev. Lett. **86**, 010001 (2012)

[82] M. Misiak *et al.*, Phys. Rev. Lett. **114**, no. 22, 221801 (2015) doi:10.1103/PhysRevLett.114.221801 [arXiv:1503.01789 [hep-ph]].

[83] G. Aad *et al.* [ATLAS Collaboration], JHEP **1503**, 088 (2015) [arXiv:1412.6663 [hep-ex]].

[84] G. Aad *et al.* [ATLAS Collaboration], Phys. Rev. Lett. **114**, no. 23, 231801 (2015) [arXiv:1503.04233 [hep-ex]].

[85] G. Aad *et al.* [ATLAS Collaboration], JHEP **1603**, 127 (2016) doi:10.1007/JHEP03(2016)127 [arXiv:1512.03704 [hep-ex]]; M. Aaboud *et al.* [ATLAS Collaboration], arXiv:1603.09203 [hep-ex].

[86] V. Khachatryan *et al.* [CMS Collaboration], JHEP **1512**, 178 (2015) doi:10.1007/JHEP12(2015)178 [arXiv:1510.04252 [hep-ex]]; V. Khachatryan *et al.* [CMS Collaboration], arXiv:1508.07774 [hep-ex]; CMS Collaboration [CMS Collaboration], CMS-PAS-HIG-13-026; CMS Collaboration [CMS Collaboration], CMS-PAS-HIG-14-020.

[87] G. Aad *et al.* [ATLAS Collaboration], arXiv:1509.06047 [hep-ex]; G. Aad *et al.* [ATLAS Collaboration], JHEP **1406**, 008 (2014) [arXiv:1403.6293 [hep-ex]].

[88] R. A. Diaz, hep-ph/0212237.

[89] J. F. Gunion, H. E. Haber, G. L. Kane and S. Dawson, Front. Phys. **80**, 1 (2000).

[90] G. C. Branco, P. M. Ferreira, L. Lavoura, M. N. Rebelo, M. Sher and J. P. Silva, Phys. Rept. **516**, 1 (2012) [arXiv:1106.0034 [hep-ph]].

[91] A. Menon, T. Modak, D. Sahoo, R. Sinha, and H. Cheng Phys. Rev. D **89**, 095021 (2014) [arXiv:1301.5404 [hep-ph]];

[92] B. Bhattacherjee, T. Modak, S. Patra, and R. Sinha [arXiv:1503.08924 [hep-ph]].

[93] S. Berge, S. Groote, J.G. Körner, and L. Kaldamäe Phys. Rev. D **92**, 033001 (2015) [arXiv:1505.06568]

[94] B. Bhattacharya, A. Datta, M. Duraisamy and D. London, Phys. Rev. D **88**, no. 1, 016007 (2013) doi:10.1103/PhysRevD.88.016007 [arXiv:1306.1911 [hep-ph]]; A. Datta, M. Duraisamy and D. London, Phys. Rev. D **86**, 076011 (2012) doi:10.1103/PhysRevD.86.076011 [arXiv:1207.4495 [hep-ph]].

[95] See for example, A. Datta, M. Duraisamy and D. London, Phys. Lett. B **701**, 357 (2011) doi:10.1016/j.physletb.2011.06.002 [arXiv:1103.2442 [hep-ph]]; A. Datta and D. London, Int. J. Mod. Phys. A **19**, 2505 (2004) doi:10.1142/S0217751X04018300 [hep-ph/0303159];

[96] S. Chatrchyan *et al.* [CMS Collaboration], Phys. Rev. Lett. **110**, 081803 (2013) [arXiv:1212.6639 [hep-ex]].

[97] A. Datta and P. J. O'Donnell, Phys. Rev. D **72**, 113002 (2005) doi:10.1103/PhysRevD.72.113002 [hep-ph/0508314]; A. Datta, Phys. Rev. D **74**, 014022 (2006) doi:10.1103/PhysRevD.74.014022 [hep-ph/0605039]; A. Datta, Phys. Rev. D **78**, 095004 (2008) doi:10.1103/PhysRevD.78.095004 [arXiv:0807.0795 [hep-ph]].

[98] J. Velhinho, R. Santos and A. Barroso, Phys. Lett. B **322**, 213 (1994).

[99] M. E. Peskin and D. V. Schroeder. An Introduction to Quantum Field Theory. 1995. ed., Boulder, CO: Westview.

[100] Goldstone Boson Equivalence Theorem, `http://www.slac.stanford.edu/~mpeskin/GBET.pdf`, 15 10 2015

[101] M. Carena, I. Low and C. E. M. Wagner, JHEP **1208**, 060 (2012) doi:10.1007/JHEP08(2012)060 [arXiv:1206.1082 [hep-ph]].

[102] M. R. Buckley and D. Feld, Phys. Rev. D **92**, no. 7, 075024 (2015) doi:10.1103/PhysRevD.92.075024 [arXiv:1508.00908 [hep-ph]].

[103] S. Su and B. Thomas, Phys. Rev. D **79**, 095014 (2009) [arXiv:0903.0667 [hep-ph]].

[104] R. Enberg, W. Klemm, S. Moretti, S. Munir and G. Wouda, Nucl. Phys. B **893**, 420 (2015) [arXiv:1412.5814 [hep-ph]].

[105] Status of Higgs boson physics, `http://pdg.lbl.gov/2015/reviews/rpp2015-rev-higgs-boson.pdf`, 16 10 2015.

[106] B. Coleppa, F. Kling and S. Su, JHEP **1401**, 161 (2014) doi:10.1007/JHEP01(2014)161 [arXiv:1305.0002 [hep-ph]].

[107] W. Aicheler *et al.,* SLAC-R-985 (2012); P. Raimondi and A. Seryi, Phys. Rev.Lett. **86**, 3779 (2001; V. Balakin *et al.,* Phys. Rev. Lett. **74**, 2479 (1995); J. Gallardo *et al.,* Snowmass 1996, BNL-52503; D. Stratakis *et al.,* Phys. Rev. ST Accel. Beams **16**, 091001 (2013); D. Stratakis and R. Palmer, Phys. Rev. ST Accel. Beams **18**, 031003 (2015).

[108] T. Gutsche, M. A. Ivanov, J. G. Korner, V. E. Lyubovitskij, P. Santorelli and N. Habyl, Phys. Rev. D **91**, no. 7, 074001 (2015) [Phys. Rev. D **91**, no. 11, 119907 (2015)] doi:10.1103/PhysRevD.91.074001, 10.1103/PhysRevD.91.119907 [arXiv:1502.04864 [hep-ph]].

[109] M. Tanaka and R. Watanabe, Phys. Rev. D **87**, no. 3, 034028 (2013) doi:10.1103/PhysRevD.87.034028 [arXiv:1212.1878 [hep-ph]].

[110] H. Liu, A. Rashed and A. Datta, Phys. Rev. D **92**, no. 7, 073016 (2015) Erratum: [Phys. Rev. D **93**, no. 3, 039902 (2016)] doi:10.1103/PhysRevD.93.039902, 10.1103/PhysRevD.92.073016 [arXiv:1505.04594 [hep-ph]].

LIST OF APPENDICES

APPENDIX 1: $\Lambda_b \to \Lambda_c\, \ell^- \bar{\nu}_\ell$

1.1 Introduction

The general Hamiltonian for the decay process $\Lambda_b \to \Lambda_c\ \ell^- \bar{\nu}_\ell$ (see Figure 16) containing all four-Fermi operators may be written as

$$\begin{aligned}\mathscr{H}_{eff} &= \frac{G_F V_{cb}}{\sqrt{2}} \Big\{ \Big[\bar{c}\gamma_\mu(1-\gamma_5)b + g_L \bar{c}\gamma_\mu(1-\gamma_5)b + g_R \bar{c}\gamma_\mu(1+\gamma_5)b \Big]\ \bar{l}\gamma^\mu(1-\gamma_5)\nu_l \\ &\quad + \Big[g_S \bar{c}b + g_P \bar{c}\gamma_5 b \Big]\ \bar{l}(1-\gamma_5)\nu_l \\ &\quad + \Big[\bar{c}\ \sigma^{\mu\nu}(1-\gamma_5)b \Big]\ \bar{l}\sigma_{\mu\nu}(1-\gamma_5)\nu_l + h.c. \Big\}. \end{aligned} \tag{80}$$

where $G_F = 1.1663787 \times 10^{-5}$ GeV^{-2} is the Fermi coupling constant, V_{cb} is the Cabibbo-Koboyashi-Maskawa (CKM) matrix element, and $\sigma_{\mu\nu} = i[\gamma_\mu, \gamma_\nu]/2$. ℓ represents the charged leptons $\tau,\ \mu$, or e. Vector, scalar, and pseudo-tensor interactions make up the first, second, and third lines of Eq. (80), respectively. The NP coefficients g_L, g_R, g_S, g_P, and g_T, represent pure left, pure right, scalar, pseudo-scalar, and tensor interactions, respectively. When these NP couplings are set to zero, the SM effective Hamiltonian occurs. For the tensor interaction, notice opposite quark chiralities, namely $(\bar{c}_L\ \sigma^{\mu\nu} b_R)\ (\bar{l}_R\ \sigma_{\mu\nu}\nu_{lL})$, has not been included since it is zero[9].

It is assumed that the neutrinos are always left chiral and to introduce non-universality, the NP couplings are in general different for different lepton flavors. The NP effect by assumption occurs mainly through the third generation or the τ lepton. Further, no relation between $b \to u l^- \bar{\nu}_l$ and $b \to c l^- \bar{\nu}_l$ transitions is assumed and hence constraints from $B \to \tau\nu_\tau$ are not included.

The two-fold angular distribution is

$$\frac{d\Gamma\Big(\Lambda_b \to \Lambda_c\ \ell^- \bar{\nu}_\ell\Big)}{dq^2 d(\cos\theta_\ell)} = \frac{G_F^2}{(2\pi)^3} |V_{bc}|^2 \frac{(1-\dfrac{m^2}{q^2})|\vec{q}|}{2^6 M_1^2} \Big[\frac{1}{2} \sum_{\lambda_{\Lambda_b}, \lambda_{\Lambda_c}, \lambda_\ell} |M|^2 \Big]. \tag{81}$$

In the latter sum, final state particles' helicities are summed while the initial state is averaged,

[9] Since $\gamma_5 = i\gamma^0\gamma^1\gamma^2\gamma^3$, then $\sigma^{13} = -i\sigma^{02}\gamma_5$. Therefore, $(\bar{c}_L\sigma^{13}b_R)\ (\bar{l}_R\sigma_{13}\nu_{lL}) = -(\bar{c}_L\sigma^{02}b_R)\ (\bar{l}_R\sigma_{02}\nu_{lL})$. The others follow similarly.

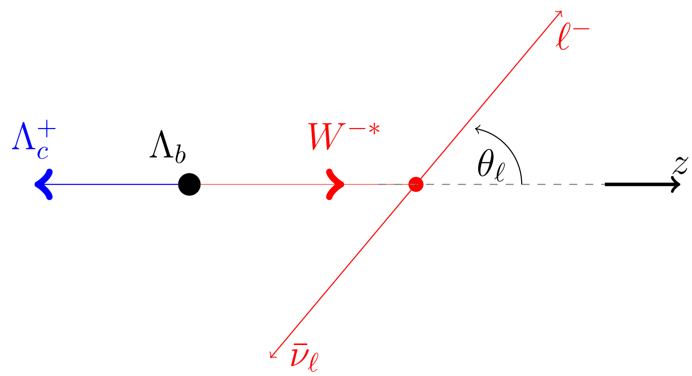

Figure 16: Three body decay of Λ_b: $\Lambda_b \to \Lambda_c\ \ell^- \bar{\nu}_\ell$. The positive z-axis coincides with the momentum of the off-shell boson W^-. θ_ℓ is the decay angle in the dilepton center of momentum frame.

hence the factor of $\frac{1}{2}$. M is the amplitude and written as follows wherein the helicities and momenta have been suppressed.

$$\begin{aligned}
M \;=\; & <\Lambda_c|\bar{c}\gamma_\mu(1-\gamma_5)b|\Lambda_b><\bar{l}\bar{\nu}_l|\bar{l}\gamma^\mu(1-\gamma_5)\nu_l|0> \\
& +\Big[\, g_L <\Lambda_c|\bar{c}\gamma_\mu(1-\gamma_5)b|\Lambda_b> + g_R <\Lambda_c|\bar{c}\gamma_\mu(1+\gamma_5)b|\Lambda_b> \Big] <\bar{l}\bar{\nu}_l|\bar{l}\gamma^\mu(1-\gamma_5)\nu_l|0> \\
& +\Big[\, g_S <\Lambda_c|\bar{c}b|\Lambda_b> + g_P <\Lambda_c|\bar{c}\gamma_5 b|\Lambda_b> \Big] <\bar{l}\bar{\nu}_l|\bar{l}(1-\gamma_5)\nu_l|0> \\
& + g_T <\Lambda_c|\bar{c}\,\sigma^{\mu\nu}(1-\gamma_5)b|\Lambda_b><\bar{l}\bar{\nu}_l|\bar{l}\sigma_{\mu\nu}(1-\gamma_5)\nu_l|0>\,.
\end{aligned}$$

The W^- boson polarization vectors, $\varepsilon_\mu(\cdot)$, can be included in the vector, axial vector, and pseudotensor interactions via the identity

$$\sum_{\lambda,\lambda'} \varepsilon_\mu(\lambda)\varepsilon^*_\nu(\lambda')g_{\lambda\lambda'} = g_{\mu\nu},$$

where $g_{\mu\nu} = diag(+1,-1-1-1)$ and λ is the W^- boson helicity. For example, given a hadronic-leptonic contraction $H^{\mu}L_{\mu}$,

$$
\begin{aligned}
H^{\mu}L_{\mu} &= g^{\mu\alpha}H_{\alpha}L_{\mu} = \sum_{\lambda,\lambda'} g_{\lambda\lambda'}(\varepsilon^{*\alpha}(\lambda)H_{\alpha})(\varepsilon^{\mu}(\lambda')L_{\mu}) \\
&= \sum_{\lambda}\eta_{\lambda}(\varepsilon^{*\alpha}(\lambda)H_{\alpha})(\varepsilon^{\mu}(\lambda)L_{\mu}),
\end{aligned}
$$

where η_{λ} = 1 for $\lambda = t$ and $\eta_{\lambda} = -1$ for $\lambda = 0, \pm 1$.

In terms of these polarization vectors, M becomes

$$
\begin{aligned}
M &= \sum_{\lambda}\eta_{\lambda}\left(1+g_L+g_R\right)\left[\varepsilon^{*\mu}(\lambda) < \Lambda_c|\bar{c}\gamma_{\mu}b|\Lambda_b > \right]\left[\varepsilon^{\nu}(\lambda) < \bar{l}\bar{\nu}_l|\bar{l}\gamma_{\nu}(1-\gamma_5)\nu_l|0 > \right] \\
&\quad -\sum_{\lambda}\eta_{\lambda}\left(1+g_L-g_R\right)\left[\varepsilon^{*\mu}(\lambda) < \Lambda_c|\bar{c}\gamma_{\mu}\gamma_5)b|\Lambda_b > \right]\left[\varepsilon^{\nu}(\lambda) < \bar{l}\bar{\nu}_l|\bar{l}\gamma_{\nu}(1-\gamma_5)\nu_l|0 > \right] \\
&\quad +\left[\, g_S < \Lambda_c|\bar{c}b|\Lambda_b > + g_P < \Lambda_c|\bar{c}\gamma_5 b|\Lambda_b > \right] < \bar{l}\bar{\nu}_l|\bar{l}(1-\gamma_5)\nu_l|0 > \\
&\quad +\sum_{\lambda,\lambda'}\eta_{\lambda}\ \eta_{\lambda'}g_T\left[\varepsilon^{*\alpha}(\lambda)\varepsilon^{*\beta}(\lambda') < \Lambda_c|\bar{c}\ i\sigma_{\alpha\beta}(1-\gamma_5)b|\Lambda_b > \right] * \\
&\quad \left[\varepsilon^{\mu}(\lambda)\varepsilon^{\nu}(\lambda') < \bar{l}\bar{\nu}_l|\bar{l}\ (-i)\sigma_{\mu\nu}(1-\gamma_5)\nu_l|0 > \right].
\end{aligned}
$$

Note that $-i^2$ has been inserted into the previous tensor interaction.

Define the helicity form factors as

$$
\begin{aligned}
H_{\lambda_{\Lambda_c},\lambda} &= H^{V}_{\lambda_{\Lambda_c},\lambda} - H^{A}_{\lambda_{\Lambda_c},\lambda} \\
& H^{V}_{\lambda_{\Lambda_c},\lambda} = \left(1+g_L+g_R\right)\left[\ \varepsilon^{*\mu}(\lambda) < \Lambda_c|\bar{c}\gamma_{\mu}b|\Lambda_b > \right] \\
& H^{A}_{\lambda_{\Lambda_c},\lambda} = \left(1+g_L-g_R\right)\left[\ \varepsilon^{*\mu}(\lambda) < \Lambda_c|\bar{c}\gamma_{\mu}\gamma_5)b|\Lambda_b > \right],
\end{aligned}
$$

$$
H^{SP}_{\lambda_{\Lambda_c},\lambda=0} = H^{S}_{\lambda_{\Lambda_c},\lambda=0} + H^{P}_{\lambda_{\Lambda_c},\lambda=0}
$$

$$H^S_{\lambda_{\Lambda_c},\lambda=0} = g_S < \Lambda_c|\bar{c}b|\Lambda_b >$$
$$H^P_{\lambda_{\Lambda_c},\lambda=0} = g_P < \Lambda_c|\bar{c}\gamma_5 b|\Lambda_b >,$$

and

$$\begin{aligned} H^{T(\lambda_{\Lambda_b})}_{\lambda_{\Lambda_c},\lambda,\lambda'} &= H^{T1(\lambda_{\Lambda_b})}_{\lambda_{\Lambda_c},\lambda,\lambda'} - H^{T2(\lambda_{\Lambda_b})}_{\lambda_{\Lambda_c},\lambda,\lambda'} \\ &\quad H^{T1(\lambda_{\Lambda_b})}_{\lambda_{\Lambda_c},\lambda,\lambda'} = \varepsilon^{*\alpha}(\lambda)\varepsilon^{*\beta}(\lambda') < \Lambda_c|\bar{c}\; i\sigma_{\alpha\beta} b|\Lambda_b > \\ &\quad H^{T2(\lambda_{\Lambda_b})}_{\lambda_{\Lambda_c},\lambda,\lambda'} = \varepsilon^{*\alpha}(\lambda)\varepsilon^{*\beta}(\lambda') < \Lambda_c|\bar{c}\; i\sigma_{\alpha\beta}\gamma_5 b|\Lambda_b > . \end{aligned} \tag{82}$$

Define the leptonic amplitudes as

$$\begin{aligned} L^{\lambda_\ell}_{\lambda} &= \varepsilon^{\mu} < \bar{l}\bar{\nu}_l|\bar{l}\gamma_\mu(1-\gamma_5)\nu_l|0 >, \\ L^{\lambda_\ell} &= < \bar{l}\bar{\nu}_l|\bar{l}(1-\gamma_5)\nu_l|0 >, \\ L^{\lambda_\ell}_{\lambda,\lambda'} &= \varepsilon^{\mu}(\lambda)\varepsilon^{\nu}(\lambda') < \bar{l}\bar{\nu}_l|\bar{l}\;(-i)\sigma_{\mu\nu}(1-\gamma_5)\nu_l|0 > . \end{aligned}$$

Therefore, M can be written succinctly as

$$M = \sum_{\lambda} \eta_\lambda H_{\lambda_{\Lambda_c},\lambda} L^{\lambda_\ell}_{\lambda} + H^{SP}_{\lambda_{\Lambda_c},\lambda=0} L^{\lambda_\ell} + \sum_{\lambda,\lambda'} \eta_\lambda\; \eta_{\lambda'} H^{T(\lambda_{\Lambda_b})}_{\lambda_{\Lambda_c},\lambda,\lambda'} L^{\lambda_\ell}_{\lambda,\lambda'} \tag{83}$$

for a given λ_{Λ_b}. Note that for $H_{\lambda_{\Lambda_c},\lambda}$ and $H^{SP}_{\lambda_{\Lambda_c},\lambda=0}$, helicity is conserved, namely $\lambda_{\Lambda_b} = \lambda - \lambda_{\Lambda_c}$ with $\lambda_{\Lambda_b}, \lambda_{\Lambda_c} = \pm\frac{1}{2}$ and $\lambda = t, 0, \pm 1$. In appendices 1.2-1.3, the helicity form factors $H_{\lambda_{\Lambda_c},\lambda}$, $H^{SP}_{\lambda_{\Lambda_c},\lambda=0}$, and $H^{T(\lambda_{\Lambda_b})}_{\lambda_{\Lambda_c},\lambda,\lambda'}$ are listed. In Appendix 1.4, the leptonic amplitudes are listed.

Finally, the two-fold distribution for $\Lambda_b \to \Lambda_c\, \ell^- \bar{\nu}_\ell$ may be written:

$$\frac{d\Gamma\Big(\Lambda_b \to \Lambda_c \tau^- \bar{\nu}_\tau\Big)}{dq^2 d(\cos\theta_\ell)} = \mathscr{A}_1 + \mathscr{A}_2, \tag{84a}$$

with

$$\mathscr{A}_1 = \text{eqn. (51)} \tag{84b}$$

and

$$\begin{aligned}
\mathscr{A}_2 = \; & \frac{G_F^2}{(2\pi)^3}|V_{bc}|^2 \frac{(1-\frac{m^2}{q^2})|\vec{q}|}{2^6 M_1^2} * \\
& \Big[\frac{1}{2}\sum_{\lambda_{\Lambda_b},\lambda_{\Lambda_c},\lambda_\ell} \Big(2Re[(\sum_\lambda \eta_\lambda H_{\lambda_{\Lambda_c},\lambda} L_\lambda^{\lambda_\ell})^* (\sum_{\lambda,\lambda'} \eta_\lambda\ \eta_{\lambda'} H^{T(\lambda_{\Lambda_b})}_{\lambda_{\Lambda_c},\lambda,\lambda'} L^{\lambda_\ell}_{\lambda,\lambda'})] \\
& + 2Re[(H^{SP}_{\lambda_{\Lambda_c},\lambda=0} L^{\lambda_\ell})^* (\sum_{\lambda,\lambda'} \eta_\lambda\ \eta_{\lambda'} H^{T(\lambda_{\Lambda_b})}_{\lambda_{\Lambda_c},\lambda,\lambda'} L^{\lambda_\ell}_{\lambda,\lambda'})] \\
& + |\sum_{\lambda,\lambda'} \eta_\lambda\ \eta_{\lambda'} H^{T(\lambda_{\Lambda_b})}_{\lambda_{\Lambda_c},\lambda,\lambda'} L^{\lambda_\ell}_{\lambda,\lambda'}|^2\Big)\Big].
\end{aligned} \tag{84c}$$

$\mathscr{A}_1$ is derived in [108]. $\mathscr{A}_2$ is rather long and not written herein. The tensor helicity form factors for $\mathscr{A}_2$ are given below in section 1.3.

1.2 Scalar and Vector Helicity Form Factors

The scalar and vector helicity form factors are taken from [5] (on page 4). The decay $\Lambda_b \to \Lambda_c\, \ell^- \bar{\nu}_\ell$ proceeds via $\Lambda_b \to \Lambda_c W^*$(off-shell W) followed by $W^* \to \ell^- \bar{\nu}_\ell$. Following [63] one can analyze the decay in terms of helicity amplitudes which are given by

$$H_{\lambda_c \lambda_W} = M_\mu(\lambda_2)\varepsilon^{*\mu}(\lambda_W), \tag{85}$$

where λ_c, λ_W are the polarizations of the daughter baryon and the W-boson respectively and M_μ is the hadronic current for $\Lambda_b \to \Lambda_c$ transition. The helicity amplitudes can be expressed in terms of form factors and the NP couplings.

$$
\begin{aligned}
H_{\lambda_{\Lambda_c},\lambda_w} &= H^V_{\lambda_{\Lambda_c},\lambda_w} - H^A_{\lambda_{\Lambda_c},\lambda_w}, \\
H^V_{\frac{1}{2}0} &= (1+g_L+g_R)\frac{\sqrt{Q_-}}{\sqrt{q^2}}\Big((M_1+M_2)f_1 - q^2 f_2\Big), \\
H^A_{\frac{1}{2}0} &= (1+g_L-g_R)\frac{\sqrt{Q_+}}{\sqrt{q^2}}\Big((M_1-M_2)g_1 + q^2 g_2\Big), \\
H^V_{\frac{1}{2}1} &= (1+g_L+g_R)\sqrt{2Q_-}\Big(f_1 - (M_1+M_2)f_2\Big), \\
H^A_{\frac{1}{2}1} &= (1+g_L-g_R)\sqrt{2Q_+}\Big(g_1 + (M_1-M_2)g_2\Big), \\
H^V_{\frac{1}{2}t} &= (1+g_L+g_R)\frac{\sqrt{Q_+}}{\sqrt{q^2}}\Big((M_1-M_2)f_1 + q^2 f_3\Big), \\
H^A_{\frac{1}{2}t} &= (1+g_L-g_R)\frac{\sqrt{Q_-}}{\sqrt{q^2}}\Big((M_1+M_2)g_1 - q^2 g_3\Big), \qquad (86)
\end{aligned}
$$

where $Q_\pm = (M_1 \pm M_2)^2 - q^2$.

Also,

$$
\begin{aligned}
H^V_{\lambda_{\Lambda_c},\lambda_w} &= H^V_{-\lambda_{\Lambda_c},-\lambda_w}, \\
H^A_{\lambda_{\Lambda_c},\lambda_w} &= -H^A_{-\lambda_{\Lambda_c},-\lambda_w}. \qquad (87)
\end{aligned}
$$

The scalar and pseudo-scalar helicities associated with the new physics scalar and pseudo-scalar interactions are

$$
\begin{aligned}
H^{SP}{}_{1/2,0} &= H^P{}_{1/2,0} + H^S{}_{1/2,0}, \\
H^S{}_{1/2,0} &= g_S\frac{\sqrt{Q_+}}{m_b - m_c}\Big((M_1-M_2)f_1 + q^2 f_3\Big), \\
H^P{}_{1/2,0} &= -g_P\frac{\sqrt{Q_-}}{m_b + m_c}\Big((M_1+M_2)g_1 - q^2 g_3\Big). \qquad (88)
\end{aligned}
$$

The parity related amplitudes are,

$$
H^S{}_{\lambda_{\Lambda_c},\lambda_{NP}} = H^S{}_{-\lambda_{\Lambda_c},-\lambda_{NP}},
$$

$$H^{P}{}_{\lambda_{\Lambda_c},\lambda_{NP}} = -H^{P}{}_{-\lambda_{\Lambda_c},-\lambda_{NP}}. \qquad (89)$$

1.3 Tensor Helicity Form Factors

Before listing the tensor helicity form factors (see Eq. (82)), note the following relations.

$$\begin{aligned}
H^{T(\lambda_{\Lambda_b})}_{\lambda_{\Lambda_c},\lambda,\lambda'} &= -H^{T(\lambda_{\Lambda_b})}_{\lambda_{\Lambda_c},\lambda',\lambda}, \\
&= H^{T1(\lambda_{\Lambda_b})}_{\lambda_{\Lambda_c},\lambda,\lambda'} - H^{T2(\lambda_{\Lambda_b})}_{\lambda_{\Lambda_c},\lambda,\lambda'},
\end{aligned}$$

$$\begin{aligned}
q^{\mu} &= p^{\mu}_{\Lambda_b} - p^{\mu}_{\Lambda_c}, \\
<\Lambda_c|\bar{c}\, i\sigma^{\mu\nu} b|\Lambda_b> &= \bar{u}_{\lambda_{\Lambda_c}}\Big[2h_+(q^2)\frac{p^{\mu}_{\Lambda_b}p^{\nu}_{\Lambda_c} - p^{\nu}_{\Lambda_b}p^{\mu}_{\Lambda_c}}{Q_+} \\
&+h_\perp(q^2)\Big(\frac{M_1+M_2}{q^2}(q^{\mu}\gamma^{\nu} - q^{\nu}\gamma^{\mu}) - 2(\frac{1}{q^2}+\frac{1}{Q_+})(p^{\mu}_{\Lambda_b}p^{\nu}_{\Lambda_c} - p^{\nu}_{\Lambda_b}p^{\mu}_{\Lambda_c})\Big) \\
&+\tilde{h}_+(q^2)\Big(i\sigma^{\mu\nu} - \frac{2}{Q_-}(M_1(p^{\mu}_{\Lambda_c}\gamma^{\nu} - p^{\nu}_{\Lambda_c}\gamma^{\mu}) \\
&-M_2(p^{\mu}_{\Lambda_b}\gamma^{\nu} - p^{\nu}_{\Lambda_b}\gamma^{\mu}) + p^{\mu}_{\Lambda_b}p^{\nu}_{\Lambda_c} - p^{\nu}_{\Lambda_b}p^{\mu}_{\Lambda_c})\Big) \\
&+\tilde{h}_\perp(q^2)\frac{M_1-M_2}{q^2 Q_-}\Big((M_1^2 - M_2^2 - q^2)(\gamma^{\mu}p^{\nu}_{\Lambda_b} - \gamma^{\nu}p^{\mu}_{\Lambda_b}) \\
&-(M_1^2 - M_2^2 + q^2)(\gamma^{\mu}p^{\nu}_{\Lambda_c} - \gamma^{\nu}p^{\mu}_{\Lambda_c}) + 2(M_1-M_2)(p^{\mu}_{\Lambda_b}p^{\nu}_{\Lambda_c} - p^{\nu}_{\Lambda_b}p^{\mu}_{\Lambda_c})\Big) \\
&\Big]u_{\Lambda_b} \text{ (See eqn. (2.14) in Ref.[62].)},
\end{aligned}$$

$$\sigma^{\mu\nu}\gamma_5 = -\frac{i}{2}\varepsilon^{\mu\nu\alpha\beta}\sigma_{\alpha\beta},$$

$$p = \frac{\sqrt{Q_-Q_+}}{2M_1} \text{ (momentum of } W^- \text{ in } \Lambda_b\text{'s rest frame)},$$

$$E_{\Lambda_c} = \frac{M_1^2 + M_2^2 - q^2}{2M_1} \text{ (energy of } \Lambda_c \text{ in } \Lambda_b\text{'s rest frame)},$$

$$a = \sqrt{E_{\Lambda_c} + M_2},\ b = \frac{1}{E_{\Lambda_c} + M_2},$$

$$Q_{\pm} \;=\; (M_1 \pm M_2)^2 - q^2$$

There are 64 possibilities in listing the tensor helicities $H^{T(\lambda_{\Lambda_b})}_{\lambda_{\Lambda_c},\lambda,\lambda'}$ since $\lambda,\lambda' \in (t,0,\pm)$ and $\lambda_{\Lambda_b},\lambda_{\Lambda_c} \in (\pm\frac{1}{2})$. However, only 24 possibilities require calculation since $H^{T(\lambda_{\Lambda_b})}_{\lambda_{\Lambda_c},\lambda,\lambda'}$ is asymmetric under $(\lambda,\lambda') \to (\lambda',\lambda)$. 12 of these 24 are non-zero.

$\underline{\lambda = t, \lambda' = 0}$

$$\begin{aligned}
H^{T(-1/2)}_{-1/2,t,0} \;=\; & -\frac{1}{q^2 Q_- Q_+} 2aM_1 p(bp+1)\Big[Q_+\Big(q^2\tilde{h}_1 - \tilde{h}_2(M_1-M_2)^2\Big) \\
& +Q_-\Big(h_2({M_1}^2+{M_2}^2) - h_1 q^2\Big)\Big]
\end{aligned}$$

$$\begin{aligned}
H^{T(-1/2)}_{+1/2,t,0} \;=\; & -\frac{1}{2M_1 q^2 Q_- Q_+} ap\Big[Q_+\Big(2bM_1 q^2\tilde{h}_1({M_1}^2 - 2M_1M_2 - 2M_1 p + {M_2}^2 - q^2) \\
& +\tilde{h}_2(M_1-M_2)(b{M_1}^4 + {M_1}^3(-2+4bp) - 2{M_1}^2(b{M_2}^2 - M_2(2-2bp) + bq^2) \\
& +b({M_2}^2-q^2)^2 - 2M_1({M_2}^2-q^2))\Big) \\
& +Q_-\Big(4{M_1}^2 q^2(bp-1)(h_1-h_2) - h_2 Q_+(b{M_1}^3 + {M_1}^2(bM_2+4bp-2) \\
& +M_1(-b{M_2}^2 + bq^2 + 2M_2) + bM_2(q^2 - {M_2}^2))\Big)\Big]
\end{aligned}$$

$$\begin{aligned}
H^{T(+1/2)}_{-1/2,t,0} \;=\; & \frac{1}{2M_1 q^2 Q_- Q_+} ap\Big[Q_+\Big(-2bM_1 q^2\tilde{h}_1({M_1}^2 - 2M_1(M_2-p) + {M_2}^2 - q^2) \\
& -\tilde{h}_2(M_1-M_2)(b{M_1}^4 - {M_1}^3(4bp+2) - 2{M_1}^2(b{M_2}^2 - 2M_2(bp+1) + bq^2) \\
& +b({M_2}^2-q^2)^2 - 2M_1({M_2}^2-q^2))\Big) \\
& +Q_-\Big(4{M_1}^2 q^2(bp+1)(h_1-h_2) + h_2 Q_+(b{M_1}^3 + {M_1}^2(bM_2-4bp-2) \\
& +M_1(-b{M_2}^2 + bq^2 + 2M_2) + bM_2(q^2 - {M_2}^2))\Big)\Big]
\end{aligned}$$

$$H^{T(+1/2)}_{+1/2,t,0} \;=\; \frac{1}{q^2 Q_- Q_+} 2aM_1 p(bp-1)\Big[Q_+\Big(q^2\tilde{h}_1 - \tilde{h}_2(M_1-M_2)^2\Big)$$

$$+Q_-\Big(h_2({M_1}^2+{M_2}^2)-h_1q^2\Big)\Big]$$

$\underline{\lambda = t, \lambda' = +}$

$$
\begin{aligned}
H^{T(-1/2)}_{-1/2,t,+} &= 0 \\
H^{T(-1/2)}_{+1/2,t,+} &= 0 \\
H^{T(+1/2)}_{-1/2,t,+} &= 0 \\
H^{T(+1/2)}_{+1/2,t,+} &= \frac{\sqrt{2}abp(M_1+M_2)(h_2-\tilde{h_1})}{\sqrt{q^2}}+\frac{2\sqrt{2}abM_1p^2(M_1-M_2)(\tilde{h_1}-\tilde{h_2})}{\sqrt{q^2}Q_-}
\end{aligned}
$$

$\underline{\lambda = t, \lambda' = -}$

$$
\begin{aligned}
H^{T(-1/2)}_{-1/2,t,-} &= +\frac{\sqrt{2}abp(M_1+M_2)(h_2-\tilde{h_1})}{\sqrt{q^2}}-\frac{2\sqrt{2}abM_1p^2(M_1-M_2)(\tilde{h_1}-\tilde{h_2})}{\sqrt{q^2}Q_-} \\
H^{T(-1/2)}_{+1/2,t,-} &= 0 \\
H^{T(+1/2)}_{-1/2,t,-} &= 0
\end{aligned}
$$

$$H^{T(+1/2)}_{+1/2,t,-} = 0$$

$\underline{\lambda = 0, \lambda' = +}$

$$H^{T(-1/2)}_{-1/2,0,+} = 0$$

$$H^{T(-1/2)}_{+1/2,0,+} = 0$$

$$H^{T(+1/2)}_{-1/2,0,+} = 0$$

$$H^{T(+1/2)}_{+1/2,0,+} = -\frac{2\sqrt{2}abM_1p^2(M_1-M_2)(\tilde{h_1}-\tilde{h_2})}{\sqrt{q^2}Q_-} - \frac{\sqrt{2}abp(M_1+M_2)(h_2-\tilde{h_1})}{\sqrt{q^2}}$$

$\underline{\lambda = 0, \lambda' = -}$

$$H^{T(-1/2)}_{-1/2,0,-} = -\frac{2\sqrt{2}abM_1p^2(M_1-M_2)(\tilde{h_1}-\tilde{h_2})}{\sqrt{q^2}Q_-} + \frac{\sqrt{2}abp(M_1+M_2)(h_2-\tilde{h_1})}{\sqrt{q^2}}$$

$$H^{T(-1/2)}_{+1/2,0,-} = 0$$

$$H^{T(+1/2)}_{-1/2,0,-} = 0$$

$$H^{T(+1/2)}_{+1/2,0,-} = 0$$

$\underline{\lambda = +, \lambda' = -}$

$$\begin{aligned}
H^{T(-1/2)}_{-1/2,t,+,-} &= -\frac{1}{q^2 Q_- Q_+} 2aM_1 p(bp+1)\Big[Q_+\Big(q^2\tilde{h_1} - \tilde{h_2}(M_1-M_2)^2\Big) \\
&\quad + Q_-\Big(h_2(M_1^2+M_2^2) - h_1 q^2\Big)\Big]
\end{aligned}$$

$$\begin{aligned}
H^{T(-1/2)}_{+1/2,+,-} &= -\frac{1}{2M_1 q^2 Q_- Q_+} ap\Big[Q_+\Big(2bM_1 q^2 \tilde{h_1}(M_1^2 - 2M_1M_2 - 2M_1 p + M_2^2 - q^2) \\
&\quad - \tilde{h_2}(M_1-M_2)(bM_1^4 - M_1^3(2-4bp) - 2M_1^2(bM_2^2 - M_2(2-2bp) + bq^2) \\
&\quad + b(M_2^2-q^2)^2 - 2M_1(M_2^2-q^2))\Big) \\
&\quad + Q_-\Big(4M_1^2 q^2(bp-1)(h_1-h_2) - h_2 Q_+(bM_1^3 + M_1^2(bM_2 + 4bp - 2) \\
&\quad + M_1(-bM_2^2 + bq^2 + 2M_2) + bM_2(q^2 - M_2^2))\Big)\Big]
\end{aligned}$$

$$\begin{aligned}
H^{T(+1/2)}_{-1/2,+,-} &= \frac{1}{2M_1 q^2 Q_- Q_+} ap\Big[Q_+\Big(-2bM_1 q^2 \tilde{h_1}(M_1^2 - 2M_1(M_2-p) + M_2^2 - q^2) \\
&\quad - \tilde{h_2}(M_1-M_2)(bM_1^4 - M_1^3(4bp+2) - 2M_1^2(bM_2^2 - 2M_2(bp+1) + bq^2) \\
&\quad + b(M_2^2-q^2)^2 - 2M_1(M_2^2-q^2))\Big) \\
&\quad + Q_-\Big(4M_1^2 q^2(bp+1)(h_1-h_2) + h_2 Q_+(bM_1^3 + M_1^2(bM_2 - 4bp - 2) \\
&\quad + M_1(-bM_2^2 + bq^2 + 2M_2) + bM_2(q^2 - M_2^2))\Big)\Big]
\end{aligned}$$

$$\begin{aligned}
H^{T(+1/2)}_{+1/2,+,-} &= \frac{1}{q^2 Q_- Q_+} 2aM_1 p(bp-1)\Big[Q_+\Big(q^2\tilde{h_1} - \tilde{h_2}(M_1-M_2)^2\Big) \\
&\quad + Q_-\Big(h_2(M_1^2+M_2^2) - h_1 q^2\Big)\Big]
\end{aligned}$$

1.4 Leptonic Amplitudes

The vector type leptonic amplitudes are given by

$$
\begin{aligned}
L^{+}_{\pm} &= \mp\sqrt{2}m_\ell v \sin\theta_\ell \,, && (90)\\
L^{+}_{0} &= -2m_\ell v \cos\theta_\ell \,, && (91)\\
L^{+}_{s} &= -2m_\ell v \,, && (92)\\
L^{-}_{\pm} &= -\sqrt{2}\sqrt{q^2}v(1\mp\cos\theta_\ell) \,, && (93)\\
L^{-}_{0} &= -2\sqrt{q^2}v \sin\theta_\ell \,, && (94)\\
L^{-}_{s} &= 0 \,, && (95)
\end{aligned}
$$

where $v = \sqrt{1-m_\ell^2/q^2}$.

The scalar type leptonic amplitudes are written as

$$
\begin{aligned}
L^{+} &= -2\sqrt{q^2}v \,, && (96)\\
L^{-} &= 0 \,. && (97)
\end{aligned}
$$

The tensor type leptonic amplitudes are

$$
\begin{aligned}
L^{\pm}_{\lambda\lambda} &= 0 \,, && (98)\\
L^{+}_{0\pm} &= -L^{+}_{\pm 0} = \sqrt{2}\sqrt{q^2}v \sin\theta_\ell \,, && (99)\\
L^{+}_{+-} &= -L^{+}_{-+} = L^{+}_{s0} = -L^{+}_{0s} = 2\sqrt{q^2}v\cos\theta_\ell \,, && (100)\\
L^{+}_{\pm s} &= -L^{+}_{s\pm} = \pm\sqrt{2}\sqrt{q^2}v\sin\theta_\ell \,, && (101)\\
L^{-}_{0\pm} &= -L^{-}_{\pm 0} = \pm\sqrt{2}m_\ell v(1\mp\cos\theta_\ell) \,, && (102)\\
L^{-}_{+-} &= -L^{-}_{-+} = L^{-}_{s0} = -L^{-}_{0s} = -2m_\ell v\sin\theta_\ell \,, && (103)\\
L^{-}_{\pm s} &= -L^{-}_{s\pm} = \sqrt{2}m_\ell v(1\mp\cos\theta_\ell) \,. && (104)
\end{aligned}
$$

The above are confirmed in Ref. [109], Appendix A. Therein, the W boson moves in the -z direction with the leptonic angle defined with respect to the +z axis, hence our θ would become $\pi - \theta$. Also, there is a minus sign difference between our transverse leptonic amplitudes and those of Ref. [109]. However, the partial amplitudes HL would be the same since the transverse polarization vector occurs in both H and L.

APPENDIX 2: $H \to W^-W^{+*}(\textbf{or } H^{+*}) \to \tau^-\bar{\nu}_\tau\tau^+\nu_\tau$

2.1 Leptonic Amplitudes for $H \to W^{+*}(\to \tau^+ \nu_\tau) W^-(\to \tau^- \bar{\nu}_\tau)$

The leptonic amplitudes (see Eqs. (64b) and (64c)) are written below, normalizing with respect to the coupling and propagator denominator. Note $v_q = 1 - \dfrac{m^2}{q^2}$ and $v_p = 1 - \dfrac{m^2}{M_W^2}$.

$$B^{\lambda_{W^+}}_{\lambda_{\tau^+},\lambda_{\nu_\tau}} = \bar{u}(p_1,\lambda_{\nu_\tau}) \not{\epsilon}_1(\lambda_{W^+})(1-\gamma_5) v(p_2,\lambda_{\tau^+})$$

$$C^{\lambda_{W^-}}_{\lambda_{\tau^-},\lambda_{\bar{\nu}_\tau}} = \bar{u}(p_3,\lambda_{\tau^-}) \not{\epsilon}_2(\lambda_{W^-})(1-\gamma_5) v(p_4,\lambda_{\bar{\nu}_\tau})$$

$$E^{\lambda_{H^+}}_{\lambda_{\tau^-},\lambda_{\bar{\nu}_\tau}} = \bar{u}(1+\gamma_5) v$$

$\underline{B^{\lambda_{W^+}}_{\lambda_{\tau^+},\lambda_{\nu_\tau}}}$	$\underline{C^{\lambda_{W^-}}_{\lambda_{\tau^-},\lambda_{\bar{\nu}_\tau}}}$	$\underline{E^{\lambda_{H^+}}_{\lambda_{\tau^+},\lambda_{\nu_\tau}}}$
$B^{\pm}_{+,-} = \sqrt{2q^2 v_q}(1 \pm \cos\theta_q)\, e^{\pm i\chi}$	$C^{\pm}_{-,+} = \sqrt{2M_W^2 v_p}(1 \mp \cos\theta_p)$	$E^{0}_{-,-} = 2\sqrt{q^2 v_q}$
$B^{0}_{+,-} = -\sqrt{2q^2 v_q}\sin\theta_q$	$C^{0}_{-,+} = \sqrt{2M_W^2 v_p}\sin\theta_p$	
$B^{t}_{-,-} = -2m\sqrt{v_q}$	$C^{\pm}_{+,+} = \mp m\sqrt{2v_p}\sin\theta_p$	
$B^{\pm}_{-,-} = \mp m\sqrt{2v_q}\sin\theta_q\, e^{\pm i\chi}$	$C^{0}_{+,+} = -2m\sqrt{v_p}\cos\theta_p$	
$B^{0}_{-,-} = -2m\sqrt{v_q}\cos\theta_q$		

2.2 Standard Model Distribution: $H \to W^{+*}(\to \tau^+ \nu_\tau) W^-(\to \tau^- \bar{\nu}_\tau)$

The full four-fold distribution is written below for $H \to W^{+*}(\to \tau^+ \nu_\tau) W^-(\to \tau^- \bar{\nu}_\tau)$ without dropping NP terms, such as parity violating terms $(, |A_{++}|^2 - |A_{--}|^2, (A_{++} - A_{--})A^*_{t0}$, $(A_{++} -$

$A_{--})A^*_{00}$) or triple product terms ($\sin\chi$ or $\sin 2\chi$)[10]. By writing the angular distribution in terms of $P_2(\cos\theta) = \dfrac{3\cos^2\theta - 1}{2}$, which is the Legendre polynomial, it simplifies the integration over the polar angles.

$$\frac{d\Gamma^{SM}\Big(H \to W^{+*}(\to \tau^+ \nu_\tau) W^-(\to \tau^- \bar{\nu}_\tau)\Big)}{dq^2 d(\cos\theta_q) d(\cos\theta_p) d\phi} = f(q^2)\ (\alpha_1 + \alpha_2 + \alpha_3), \tag{105}$$

where

$$\begin{aligned}
f(q^2) &= B_{W\tau\nu}\, C^W(q^2) \frac{1}{2\pi} \frac{M_W^2 q^2}{1 + \varepsilon_p/2}, \qquad (106) \\
C^W(q^2) &= \frac{g^4 |\vec{q}| v_q^2}{1536\pi^3\, M_H^2} \frac{1}{(q^2 - M_W^2)^2 + M_W^2 \Gamma_W^2}, \\
|\vec{q}| &= \frac{\sqrt{((q^2 - M_W^2)^2 + M_H^4 - 2M_H^2 M_W^2 - 2M_H^2 q^2)}}{2M_H}, \\
v_q &= 1 - \frac{m^2}{q^2}, \\
\varepsilon_q &= \frac{m^2}{q^2},\ \ \varepsilon_p = \frac{m^2}{M_W^2}, \\
F_s &= 1 - \frac{q^2}{M_W^2}, \\
\alpha_1 &= \frac{3}{2} |A_{t0}|^2\, F_s^2\, \varepsilon_q \Big(P_2(\cos\theta_p)(\varepsilon_p - 1) + \frac{\varepsilon_p}{2} + 1 \Big), \qquad (107)
\end{aligned}$$

$$\begin{aligned}
\alpha_2 = {} & 2F_s\, \varepsilon_q\, \mathrm{Re}\Big[\\
& \frac{3}{2} A_{00} A^*_{t0} \left((P_2(\cos\theta_p) - 1)\cos\theta_q - (P_2(\cos\theta_p) + \frac{1}{2})\varepsilon_p \cos\theta_q \right) \qquad (108) \\
& + \frac{9}{16} A_{--} A^*_{t0}\, e^{-i\chi} \Big(2\sin\theta_p \sin\theta_q \\
& \qquad + \sin 2\theta_p \sin\theta_q - \varepsilon_p \sin 2\theta_p \sin\theta_q \Big)
\end{aligned}$$

[10]See [93] for SM derivation. In this latter paper, NP terms and $\dfrac{m^2}{M_W^2}$ terms are dropped

$$
\begin{aligned}
&+\frac{9}{16}A_{++}A_{t0}^{*}\,e^{i\chi}\Big(-2\sin\theta_p\sin\theta_q+\sin 2\theta_p\sin\theta_q\\
&\qquad\qquad -\varepsilon_p\sin 2\theta_p\sin\theta_q\Big)\\
&\qquad \Big],
\end{aligned}
$$

$$
\begin{aligned}
\alpha_3 \;=\;& |A_{00}|^2\Big(P_2(\cos\theta_q)P_2(\cos\theta_p)-P_2(\cos\theta_q)\varepsilon_pP_2(\cos\theta_p)\\
&\quad+\varepsilon_pP_2(\cos\theta_p)-P_2(\cos\theta_q)\varepsilon_qP_2(\cos\theta_p)+P_2(\cos\theta_q)\varepsilon_p\varepsilon_qP_2(\cos\theta_p)\\
&\quad+\frac{1}{2}\varepsilon_p\varepsilon_qP_2(\cos\theta_p)-\frac{\varepsilon_qP_2(\cos\theta_p)}{2}-P_2(\cos\theta_p)-P_2(\cos\theta_q)\\
&\quad-\frac{P_2(\cos\theta_q)\varepsilon_p}{2}+\frac{\varepsilon_p}{2}+P_2(\cos\theta_q)\varepsilon_q+\frac{1}{2}P_2(\cos\theta_q)\varepsilon_p\varepsilon_q\\
&\quad+\frac{\varepsilon_p\varepsilon_q}{4}+\frac{\varepsilon_q}{2}+1\Big)\\
&+|A_{--}|^2\Big(-\frac{9}{4}\cos\theta_q\cos\theta_p+\frac{3}{4}P_2(\cos\theta_q)\cos\theta_p-\frac{3}{4}P_2(\cos\theta_q)\varepsilon_q\cos\theta_p\\
&\quad+\frac{3}{4}\varepsilon_q\cos\theta_p+\frac{3\cos\theta_p}{2}-\frac{3\cos\theta_q}{2}-\frac{3}{4}\cos\theta_qP_2(\cos\theta_p)\\
&\quad+\frac{P_2(\cos\theta_p)}{2}+\frac{P_2(\cos\theta_p)P_2(\cos\theta_q)}{4}+\frac{P_2(\cos\theta_q)}{2}-\frac{3}{4}\cos\theta_q\varepsilon_p\\
&\quad+\frac{3}{4}\cos\theta_qP_2(\cos\theta_p)\varepsilon_p-\frac{P_2(\cos\theta_p)\varepsilon_p}{2}\\
&\quad-\frac{1}{4}P_2(\cos\theta_p)P_2(\cos\theta_q)\varepsilon_p+\frac{P_2(\cos\theta_q)\varepsilon_p}{4}+\frac{\varepsilon_p}{2}+\frac{P_2(\cos\theta_p)\varepsilon_q}{4}\\
&\quad-\frac{1}{4}P_2(\cos\theta_p)P_2(\cos\theta_q)\varepsilon_q-\frac{P_2(\cos\theta_q)\varepsilon_q}{2}-\frac{1}{4}P_2(\cos\theta_p)\varepsilon_p\varepsilon_q\\
&\quad+\frac{1}{4}P_2(\cos\theta_p)P_2(\cos\theta_q)\varepsilon_p\varepsilon_q-\frac{1}{4}P_2(\cos\theta_q)\varepsilon_p\varepsilon_q+\frac{\varepsilon_p\varepsilon_q}{4}+\frac{\varepsilon_q}{2}+1\Big)\\
&+|A_{++}|^2\Big(-\frac{9}{4}\cos\theta_q\cos\theta_p-\frac{3}{4}P_2(\cos\theta_q)\cos(\theta_p)+\frac{3}{4}P_2(\cos\theta_q)\varepsilon_q\cos\theta_p\\
&\quad-\frac{3}{4}\varepsilon_q\cos\theta_p-\frac{3\cos\theta_p}{2}+\frac{3\cos(\theta_q)}{2}+\frac{3}{4}\cos\theta_qP_2(\cos\theta_p)+\frac{P_2(\cos\theta_p)}{2}\\
&\quad+\frac{P_2(\cos\theta_p)P_2(\cos\theta_q)}{4}+\frac{P_2(\cos\theta_q)}{2}+\frac{3}{4}\cos\theta_q\varepsilon_p\\
&\quad-\frac{3}{4}\cos(\theta_q)P_2(\cos\theta_p)\varepsilon_p-\frac{P_2(\cos\theta_p)\varepsilon_p}{2}\\
&\quad-\frac{1}{4}P_2(\cos\theta_p)P_2(\cos\theta_q)\varepsilon_p+\frac{P_2(\cos\theta_q)\varepsilon_p}{4}+\frac{\varepsilon_p}{2}+\frac{P_2(\cos\theta_p)\varepsilon_q}{4}\\
&\quad-\frac{1}{4}P_2(\cos\theta_p)P_2(\cos\theta_q)\varepsilon_q-\frac{P_2(\cos\theta_q)\varepsilon_q}{2}-\frac{1}{4}P_2(\cos\theta_p)\varepsilon_p\varepsilon_q\\
&\quad+\frac{1}{4}P_2(\cos\theta_p)P_2(\cos\theta_q)\varepsilon_p\varepsilon_q-\frac{1}{4}P_2(\cos\theta_q)\varepsilon_p\varepsilon_q+\frac{\varepsilon_p\varepsilon_q}{4}+\frac{\varepsilon_q}{2}+1\Big)
\end{aligned}
$$

$$
\begin{aligned}
&+2\mathrm{Re}\Big[\frac{9}{8}\mathrm{A}_{--}\mathrm{A}^*_{00}\,\mathrm{e}^{-\mathrm{i}\chi}\Big]*\\
&\qquad\Big(-\sin\theta_p\sin\theta_q-\frac{1}{2}\sin2\theta_p\sin(\theta_q)+\frac{1}{2}\sin2\theta_p\varepsilon_p\sin\theta_q\\
&\qquad+\frac{1}{2}\sin\theta_p\sin2\theta_q+\frac{1}{4}\sin2\theta_p\sin2\theta_q-\frac{1}{4}\sin2\theta_p\sin2\theta_q\varepsilon_p\\
&\qquad-\frac{1}{2}\sin\theta_p\sin2\theta_q\varepsilon_q-\frac{1}{4}\sin2\theta_p\sin2\theta_q\varepsilon_q+\frac{1}{4}\sin2\theta_p\sin2\theta_q\varepsilon_p\varepsilon_q\Big)\\
&+2\mathrm{Re}\Big[\frac{9}{8}\mathrm{A}_{++}\mathrm{A}^*_{00}\,\mathrm{e}^{\mathrm{i}\chi}\Big]*\\
&\qquad\Big(-\sin\theta_p\sin\theta_q+\frac{1}{2}\sin2\theta_p\sin\theta_q-\frac{1}{2}\sin2\theta_p\varepsilon_p\sin\theta_q\\
&\qquad-\frac{1}{2}\sin\theta_p\sin2\theta_q+\frac{1}{4}\sin2\theta_p\sin2\theta_q-\frac{1}{4}\sin2\theta_p\sin2\theta_q\varepsilon_p\\
&\qquad+\frac{1}{2}\sin\theta_p\sin2\theta_q\varepsilon_q-\frac{1}{4}\sin2\theta_p\sin2\theta_q\varepsilon_q+\frac{1}{4}\sin2\theta_p\sin2\theta_q\varepsilon_p\varepsilon_q\Big)\\
&+2\mathrm{Re}\Big[\frac{1}{4}\mathrm{A}_{++}\mathrm{A}^*_{--}\,\mathrm{e}^{2\mathrm{i}\chi}\Big]*\\
&\qquad\Big(-P_2(\cos\theta_p)+P_2(\cos\theta_q)P_2(\cos\theta_p)+\varepsilon_pP_2(\cos\theta_p)\\
&\qquad-P_2(\cos\theta_q)\varepsilon_pP_2(\cos\theta_p)+\varepsilon_qP_2(\cos\theta_p)\\
&\qquad-P_2(\cos\theta_q)\varepsilon_qP_2(\cos\theta_p)-\varepsilon_p\varepsilon_qP_2(\cos\theta_p)\\
&\qquad+P_2(\cos\theta_q)\varepsilon_p\varepsilon_qP_2(\cos\theta_p)+1-P_2(\cos\theta_q)-\varepsilon_p\\
&\qquad+P_2(\cos\theta_q)\varepsilon_p-\varepsilon_q+P_2(\cos\theta_q)\varepsilon_q+\varepsilon_p\varepsilon_q\\
&\qquad-P_2(\cos\theta_q)\varepsilon_p\varepsilon_q\Big).
\end{aligned}
$$

2.3 2HDM Distribution:

$H\to W^-W^{+*}$(**or** H^{+*}) $\to\tau^-\bar{\nu}_\tau\tau^+\nu_\tau$

$$
\frac{d\Gamma^{2HDM}\Big(H\to W^-W^{+*}(\text{or }H^{+*})\to\tau^-\bar{\nu}_\tau\tau^+\nu_\tau\Big)}{dq^2d(\cos\theta_q)d(\cos\theta_p)d\phi}= \tag{109a}
$$

$$
\mathscr{A}_1-B_{W\tau\nu}D_1^{H^+}(q^2)\mathscr{A}_2+B_{W\tau\nu}D_2^{H^+}(q^2)\mathscr{A}_3, \tag{109b}
$$

where

$$
\begin{aligned}
D_1^{H^+}(q^2) &= -\frac{1}{2^{11}\pi^4\cdot 3}\frac{m\, v_q^2|\vec{q}|}{M_H^2}\frac{g^4\sin(\beta-\alpha)\cos(\beta-\alpha)\tan\beta}{(q^2-M_{W^+}^2)(q^2-M_{H^+}^2)+\Gamma_{W^+}\Gamma_{H^+}M_{W^+}M_{H^+}}\frac{q^2}{1+\frac{\varepsilon}{2}},\\
D_2^{H^+}(q^2) &= \frac{1}{2^{12}\pi^4\cdot 3}\frac{m^2\, v_q^2|\vec{q}|}{M_W^2 M_H^2}\frac{g^4\cos^2(\beta-\alpha)\tan^2\beta}{(q^2-M_{H^+}^2)^2+(\Gamma_{H^+}M_{H^+})^2}\frac{q^2}{1+\frac{\varepsilon}{2}},\\
\Gamma_{H^+} &= \Gamma(H^+\to\tau^+\nu_\tau) = \frac{g^2\ (M_{H^+}^2-m_\tau^2)^2}{32\pi M_W^2 M_{H^+}^3}(m_\tau\tan\beta)^2,\\
\mathscr{A}_1 &= \text{equation}(105)\cdot\sin^2(\alpha-\beta),\\
\mathscr{A}_2 &= \frac{3m}{\sqrt{q^2}}\mathrm{Re}(\mathrm{A}_{00}\mathrm{D}_{00}^*)\Big(-\mathrm{p_p}\cos\theta_\mathrm{q}+\mathrm{p_p}\varepsilon_\mathrm{p}\cos\theta_\mathrm{q}+\frac{\varepsilon_\mathrm{p}\cos\theta_\mathrm{q}}{2}\\
&\qquad\qquad +\cos\theta_q\Big)\\
&\quad +\frac{9}{8\sqrt{q^2}}m\,\mathrm{Re}\Big(\mathrm{A}_{--}\mathrm{D}_{00}^*\,\mathrm{e}^{-\mathrm{i}\chi})(2\sin\theta_\mathrm{p}\sin\theta_\mathrm{q}+\sin(2\theta_\mathrm{p})\sin\theta_\mathrm{q}\\
&\qquad\qquad -\varepsilon_p\sin(2\theta_p)\sin\theta_q\Big)\\
&\quad +\frac{9}{8\sqrt{q^2}}m\,\mathrm{Re}(\mathrm{A}_{++}\mathrm{D}_{00}^*\,\mathrm{e}^{\mathrm{i}\chi})\Big(-2\sin\theta_\mathrm{p}\sin\theta_\mathrm{q}+\sin(2\theta_\mathrm{p})\sin\theta_\mathrm{q}\\
&\qquad\qquad -\varepsilon_p\sin(2\theta_p)\sin\theta_q\Big)\\
&\quad +\frac{3}{\sqrt{q^2}}mF_s\,\mathrm{Re}(\mathrm{A}_{\mathrm{t}0}\mathrm{D}_{00}^*)\Big(\mathrm{p_p}\varepsilon_\mathrm{p}+\frac{\varepsilon_\mathrm{p}}{2}-\mathrm{p_p}+1\Big),\\
\mathscr{A}_3 &= \frac{3}{2}|D_{00}|^2\Big((p_p+\frac{1}{2})\varepsilon_p-(p_p-1)\Big).
\end{aligned}
$$

VITA

Shanmuka Shivashankara

U.S. Veteran (156th Army Band)

sshivash@go.olemiss.edu

August 11, 2017

Teaching Experience

Spring 2017 (Mississippi Gulf Coast Community College)	Instructor in Algebra-based General Physics II Textbook: Serway, R. A. & Vuille, C. *College Physics*, 9th Edition. Instructor in Calculus-based General Physics II Textbook: Serway, R. A. & Jewett, J. W. *Physics for Scientists and Engineers*, 8th Edition. Instructor in Physical Science (online and traditional) Textbook: Shipman, J., *et. al*. *An Introduction to Physical Science*, 14th Edition. (Duties: Lecturing; Recitation; Grading; Writing quizzes, homework, and exams; Designing, setting up, and teaching laboratories; Performing demonstrations; Ordering and repairing equipment)

Fall 2016 (University of Wisconsin-Marathon County)	Instructor in Algebra-based General Physics I Textbook: Giancoli, D. C. *Physics: Principles with Applications*, 7th Edition. Instructor in Calculus-based General Physics I Textbook: Halliday, D., *et. al*. *Fundamentals of Physics*, 10th Edition. (Duties: Lecturing; Recitation; Grading; Writing quizzes, homework, and exams; Designing, setting up, and teaching laboratories; Performing demonstrations; Ordering and repairing equipment)
2015 - 2016 (Ole Miss)	Instructor in Thermodynamics (Junior Level Undergraduate Course) Textbook: Schroeder, D. V. *An Introduction to Thermal Physics*. Instructor in Mechanics (Junior Level Undergraduate Course) Textbook: Fowles, G. R. and Cassiday, G. L. *Analytical Mechanics*, 7th edition. (Duties: Lecturing; Recitation; Grading; Writing quizzes, homework, and exams)
2011-2014 (Ole Miss)	Laboratory Instructor in General Physics, Optics, Physical Science (Duties: Designing labs; Editing lab manual; Prepping Experiments; Teaching; Writing quizzes; Grading)

Skills

OS	Linux, Mac, Windows
Platforms	Blackboard, Canvas, D2L
Software	LaTeX, MatLab, Mathematica, Microsoft, Python
Electronics	Current Balance, Digital Multimeter, Oscilloscope, etc.

Education

2013	MA in Physics, University of Mississippi
2007	MS in Economics, University of Texas at Dallas

Publications

[1] S. Shivashankara, A. Datta. Searching for a charged Higgs in $H \to W^-(\to \tau^-\bar{\nu}_\tau)\, W^+(\to \tau^+\nu_\tau)$. In the process of submission for publication.

[2] S. Shivashankara, W. Wu, and A. Datta. $\Lambda_b \to \Lambda_c \tau\bar{\nu}_\tau$ decay in the standard model and with new physics. Phys. Rev. D, 91 (2015) 115003. (click on)http://arxiv.org/abs/1502.07230

[3] B. Bhattacharya, A. Datta, D. London, and S. Shivashankara. Simultaneous explanation of the R_K and $R(D^{(*)})$ puzzles. Phys. Lett. B, 742 (2015) 370-374. (click on)http://arxiv.org/abs/1412.7164

Talks

2016 Mississippi Academy of Sciences (February 18-19) in Hattiesburg, MS
Searching for a charged Higgs in $H \to W^-(\to \tau^-\bar{\nu}_\tau)\, W^+(\to \tau^+\nu_\tau)$.

2015 Phenomenology Symposium (May 4-6) in Pittsburgh, PA
Simultaneous explanation of the R_K and $R(D^{(*)})$ puzzles

Summer Schools

2016 Theoretical Advanced Study Institute (June 5 -July 2) in Boulder, CO
Anticipating the Next Discoveries in Particle Physics

2015 National Nuclear Physics Summer School (June 15-25) in Lake Tahoe, CA

2013 Prospects in Theoretical Physics (July 15-26) at IAS in Princeton, NJ
LHCPhysics

Volunteering

2016 Middle School Science Fair Judging in February at the University of Mississippi

2015 Science Fair Judging in February at Oxford Elementary School in Oxford, MS

References

Dr. Lucien Cremaldi
Professor
Department of Physics
and Astronomy
University of Mississippi
(662) 915-5311
cremaldi@phy.olemiss.edu

Dr. James Dunn
Chairman
Science Department
Mississippi Gulf Coast
Community College
(228) 497-7765
james.dunn@mgccc.edu

Dr. Jayant Anand
Regional Associate Dean
for Academic Affairs
University of Wisconsin -
Marathon County
(715) 600-0350
jayant.anand@uwc.edu